AFSC PROCESSED REPORT 2022-08

NOAA FISHERIES

Alaska Fisheries Science Center
Resource Assessment and Conservation Engineering Division
Groundfish Assessment Program

# Results of the Acoustic-Trawl Surveys of Walleye Pollock (*Gadus chalcogrammus*) in the Shumagin Islands and Shelikof Strait, February and March 2020 (DY-202001 and DY-202003)

DECEMBER 2022



U.S. Department of Commerce | National Oceanic and Atmospheric Administration | National Marine Fisheries Service

Cooper, P. Watson, and M. W. Sandahl

AFSC Processed Report

This document should be cited as follows:

McCarthy, A. L., M. Levine, and D. T. Jones. 2022. Results of the acoustic-trawl surveys of walleye pollock (*Gadus chalcogrammus*) in the Shumagin Islands and Shelikof Strait, February and March 2020 (DY-202001 and DY-202003). AFSC Processed Rep. 2022-08, 80 p. Alaska Fish. Sci. Cent., NOAA, Natl. Mar. Fish. Serv., 7600 Sand Point Way NE, Seattle WA 98115.

This document is available online at: https://repository.library.noaa.gov/

# Results of the Acoustic-Trawl Surveys of Walleye Pollock (*Gadus chalcogrammus*) in the Shumagin Islands and Shelikof Strait, February and March 2020 (DY-202001 and DY-202003)

by A.L. McCarthy, M. Levine, and D.T. Jones

Resource Assessment and Conservation Engineering Division
Alaska Fisheries Science Center
National Marine Fisheries Service
National Oceanic and Atmospheric Administration
7600 Sand Point Way, NE
Seattle, WA 98115

December 2022

## ABSTRACT

Scientists from the Alaska Fisheries Science Center conducted acoustic-trawl surveys in the Gulf of Alaska during late winter and early spring 2020 to estimate the distribution and abundance of walleye pollock (*Gadus chalcogrammus*) at several of their main spawning grounds. These pre-spawning pollock surveys covered the Shumagin Islands (DY-202001; 11-18) Feb. and Shelikof Strait (202003; 2-16 March) areas. The Shelikof Strait area has been surveyed annually in winter since 1981 (except in 1982, 1999, and 2011). The Shumagin Islands area has been surveyed annually in winter since 2001 (except in 2004, 2011, and 2019), as well as in 1994, 1995, and 1996.

The quantity of walleye pollock for the winter 2020 Shumagin Islands survey was estimated to be 31 million fish weighing 4,889 metric tons (t). The estimated quantity of walleye pollock for the winter 2020 Shelikof Strait survey was 985 million fish weighing 459,399 t. Walleye pollock between 40 and 55 cm fork length (FL) (primarily the 2012 year class) and pollock between 25 and 40 cm FL (primarily the 2017 year class) contributed the majority of the biomass in all areas. Some age-1 fish were also seen in the Shumagin Islands area.

These estimates were based on a primary analysis where backscatter was attributed to walleye pollock and other species using the biological data from the nearest haul locations to assign length-frequency distributions of all species to the backscatter. It also included a correction for escapement of fishes and other catch from the survey trawl (i.e., net selectivity). These results were compared with two alternate analyses: one considering the effects of not incorporating corrections for net selectivity in the primary analysis (‘no-selectivity analysis’) and the other applying historical methods used for earlier surveys (‘historic-mimic analysis’) where backscatter was allocated only to pollock and no selectivity correction was used. In general, the no-selectivity analysis estimated slightly more biomass (23.1% higher in the Shumagins and 2.9% higher in Shelikof) as compared to the primary analysis. The historic-mimic analysis produced biomass estimates of 34.5 % and 2.7% more than the primary estimates for the Shumagins and Shelikof, respectively.

## CONTENTS

## INTRODUCTION

The Midwater Assessment and Conservation Engineering (MACE) Program of the Alaska Fisheries Science Center's (AFSC) Resource Assessment and Conservation Engineering (RACE) Division conducts annual acoustic-trawl (AT) surveys in the Gulf of Alaska (GOA) during late winter and early spring. The goal of these surveys is to estimate the distribution and abundance of pre-spawning walleye pollock (*Gadus chalcogrammus*; hereafter pollock) at several of their main spawning grounds (i.e., pre-spawning surveys) in the Shumagin Islands and Shelikof Strait. The Shumagin Islands area has been surveyed annually since 2001 (except in 2004, 2011, and 2019) with prior surveys in 1994, 1995 and 1996. Shelikof Strait has been surveyed annually since 1981 except in 1982, 1999, and 2011. Historical surveys also frequently included Sanak Trough, Morzhovoi Bay, and Pavlof Bay since 2002 as part of the Shumagins survey, and the continental shelf break near Chirikof Island and Marmot Bay as part of the Shelikof Survey. None of these ancillary areas were surveyed in 2020 due to 1) time constraints in February because vessel departure from winter repairs was delayed and 2) the necessity of ending the March survey early due to increased concerns about the growing global COVID-19 pandemic. This report presents the results from AT surveys conducted in the aforementioned areas of the GOA during February and March of 2020.

## METHODS

Two GOA pollock spawning areas were surveyed in 2020 including the Shumagin Islands (11-18 February) and the Shelikof Strait (2-16 March). Shelikof Strait was surveyed a few days earlier in 2020 than in 2019, and earlier than other years back to 1986. Since relatively higher percentages of fish in spawning and spent stages of development were seen in the 2017, 2018, and 2019 Shelikof surveys, an earlier start date was intended to increase the chances of surveying when more pollock were in the mature (or pre-spawning) stage, a timing consistent with most prior surveys. The surveys were conducted with the NOAA ship *Oscar Dyson*, a 64-m stern trawler equipped for fisheries and oceanographic research. Survey procedures followed established AT methods as specified in NOAA protocols for fisheries acoustics surveys and related sampling (NMFS, 2014). The acoustic units used here are defined in MacLennan et al. (2002). Survey itineraries are listed in Appendix I and scientific personnel in Appendix II.

## Acoustic Equipment, Calibration, and Data Collection

Acoustic measurements were collected with a Simrad EK80 scientific echosounder (Simrad 2018, Bodholt and Solli 1992). System electronics were housed inside the vessel in a permanent laboratory space dedicated to acoustics. Six split-beam transducers (18, 38, 70, 120, 200, and 333 kHz) were mounted on the bottom of the vessel's retractable centerboard, which extended 9.15 m below the water surface.

Two standard sphere acoustic system calibrations were conducted to measure acoustic system performance during the winter cruises (Table 1). The vessel's dynamic positioning system was used to maintain the vessel location during calibrations. Local water temperature and salinity were measured and used to estimate absorption and sound speed. A tungsten carbide sphere (38.1 mm diameter) suspended below the centerboard-mounted transducers was used to calibrate the 38, 70, 120, and 200 kHz systems. Due to unexplained, excessive noise that obscured the majority of the water column on the 333 kHz frequency, no calibration of that transducer was conducted. Acoustic measurements made using the 333 kHz frequency were strictly experimental, and noise did not affect acoustic measurements at other (18 kHz – 200 kHz) frequencies. The tungsten carbide sphere was then replaced with a 64 mm diameter copper sphere to calibrate the 18 kHz system. A two-stage calibration approach was followed for each frequency. On-axis sensitivity (i.e., transducer gain and $s_A$ correction) was estimated from measurements with the sphere placed in the center of the beam following the calibration procedure described in Foote et al. (1987). Transducer beam characteristics (i.e., beam angles and angle offsets) were estimated by moving the sphere in a horizontal plane using the EK80's calibration utility (Simrad 2018, Jech et al. 2005). The equivalent beam angle (for characterizing the volume sampled by the beam) and angle sensitivities (for conversion of electrical to mechanical angles) cannot be estimated from the calibration approach used because knowledge is required of the absolute position of the sphere (see Demer et al. 2015). Therefore, the factory-measured equivalent beam angle and angle sensitivities for each transducer were used during calibration.

Raw acoustic data were recorded at six frequencies using EK80 software (version 1.12.4) at a nominal ping interval of 1 second, and analyzed from 16 m below the sea surface to within 0.5 m of the sounder-detected bottom to a maximum depth of 500 m. The raw acoustic data were analyzed using Echoview post-processing software (version 10.0.298, Echoview Software Pty Ltd).

## Trawl Gear and Oceanographic Equipment

Midwater and near-bottom acoustic backscatter was sampled using an LFS1421 trawl (LFS Marine, NOAA, 1421 Research Trawl, designed and built in 2018/2019 to MACE specifications; hereafter LFS1421) and an Aleutian Wing 30/26 Trawl (AWT). This is the first winter survey where the LFS1421 replaced the AWT as the primary sampling trawl. To determine if the species and size composition varied between nets, which would affect survey results, back-to-back paired hauls with the LFS1421 and AWT trawl were conducted throughout the survey area. The order in which the trawls were fished at a given site was determined at random.

The headrope and footrope of the LFS1421 each measure 76.8 m (252 ft), with meshes tapering from 650 cm (256 in.) in the forward sections to 8.9 cm (3.5 in.) in the codend (mesh sizes are stretched measurements unless otherwise noted). To increase retention of small organisms, the LFS1421 coded is fitted with a knotless nylon 7.9 mm (5/16 in.) stretched mesh, 3.2 mm (1/8 in.) square opening codend liner. The AWT headrope and footrope each measure 81.7 m (268 ft) and mesh sizes taper from 325.1 cm (128 in.) in the forward section of the net to 8.9 cm (3.5 in.) in the codend, which is fitted with a heavy delta nylon 12.7 mm (1/2 in.) stretched mesh, 6.4 mm (1/4 in.) square opening codend liner. A poly Nor'eastern (PNE) bottom trawl, which is a 4-panel high-opening trawl equipped with roller gear and constructed with stretch mesh sizes that range from 13 cm (5 in.) in the forward portion of the net to 8.9 cm (3.5 in.) in the codend, was available for sampling near-bottom organisms, but was not utilized on this survey. The PNE codend was also fitted with a heavy delta nylon 12.7 mm (1/2 in.) stretched mesh, 6.4 mm (1/4 in.) square opening codend liner. The AWT and PNE are described in detail by Guttormsen et al. (2010).

The LFS1421 was fished with four 45.7 m (150 ft) bridles and the AWT was fished with four 82.3 m (270 ft) bridles (1.9 cm (0.75 in.) dia.). Both were fished with two 5 $m^2$ Fishbuster trawl doors (1,247 kg (2,750 lb) each). The LFS1421 was fished with 226.8 kg (500 lb) tom weights attached to each wingtip, while the AWT was fished with 113.4 kg (250 lb) tom weights. Average trawling speed was approximately 1.6 m/sec (3.2 knots) for both the LFS1421 and AWT. Vertical net openings and headrope depths were monitored with a Simrad FS70, third-wire netsonde attached to the headrope. The vertical net opening of the LFS1421 ranged from 16.8 to 24.5 m (55 to 80 ft) and averaged 19.9 m (65 ft) while fishing. The vertical mouth opening of the AWT ranged from 21 to 29.6 m (69 to 97 ft) and averaged 25.6 m (84 ft) while fishing.

To gauge escapement of smaller fishes from the net, recapture (or pocket) nets were placed at several locations along both the LFS1421 and AWT nets (Williams et al. 2011). The LFS1421 trawl was fitted with a total of nine recapture nets placed on forward (813 mm stretch mesh), mid (102 mm stretch mesh), and aft (102 mm stretch mesh) sections of the trawl, with one recapture net on the top, bottom, and port panel of each section. The recapture nets were constructed from knotless nylon 7.9 mm (5/16 in.) stretched mesh, 3.2 mm (1/8 in.) square opening mesh material (matching the codend liner). The AWT was fitted with a total of eight recapture nets constructed from heavy delta nylon 12.7 mm (1/2 in.) stretched mesh, 6.4 mm (1/4 in.) square opening mesh (matching the codend liner), with one placed on the top, bottom, port, and starboard panels of the mid (406 mm stretch mesh) and aft (102 mm stretch mesh) sections of the net. These data are being used in ongoing work to estimate the trawl selectivity of the nets and to gauge escapement of juvenile pollock and other small fishes (see Appendix IV).

A stereo camera system (CamTrawl; Williams et al. 2010, Appendix V) was also attached to the starboard panel forward of the codend on both the LFS1421 and AWT nets. The CamTrawl was used to capture stereo images for species identification and length measurement of individual fish as they pass through the net toward the codend. The CamTrawl data are useful in determining size and species composition of fish when distinct and separate backscatter layers are sampled by a trawl haul but could not be differentiated in the trawl catch. Images are viewed and annotated using procedures described in Williams et al. (2010).

Physical oceanographic data collected during the cruise included temperature profiles obtained with a temperature-depth probe (SBE 39, Sea-Bird Scientific) attached to the headrope of the LFS1421 and AWT trawls. Additional temperature-depth measurements were taken from conductivity-temperature-depth (CTD) observations collected with a Sea-Bird CTD (SBE 911plus) system at calibration sites. Sea surface temperature data were collected using the ship's sea surface temperature system (SBE 38, Sea-Bird Scientific, accuracy $\pm$ 0.002°C) located near the ship's bow, approximately 1.4 m below the surface. At times when the SBE 38 was not operating, sea surface temperatures were taken from the Furuno T-2000 temperature probe (accuracy $\pm$ 0.2°C) located amidships 1.4 m below the surface. During these surveys, the SBE 38 was used 94.7% of the time in the Shumagins and 95.2% of the time in Shelikof, and the Furuno was used 5.3% and 4.8% of the time, in these areas respectively. These and other environmental data were recorded using the ship's Scientific Computing Systems (SCS).

## Survey Design

The survey consisted of a series of predetermined parallel transects in each survey area, except in areas where it was necessary to reorient transects to maintain a perpendicular alignment to the isobaths or navigate around landmasses. Spatial coverage and transect spacing were chosen to be consistent with previous surveys in each area. Transect start and end locations matched those from 2018 in the Shumagin Islands and those from 2019 in Shelikof Strait, although at the end of the Shelikof survey transects were modified to save time and return the ship and the science team to their home ports in the early stages of the Covid pandemic. The surveys were conducted 24 hours/day.

Trawl hauls were conducted to identify the species and size composition of acoustically-observed fish aggregations and to determine biological characteristics of pollock and other specimens. Catches were sorted to species and weighed. When large numbers of juvenile and adult pollock were encountered, the predominant size groups in the catch were sampled separately (e.g., age-1 vs. larger sizes). Sex (for FL > 20 cm), length, body weight, maturity, age (otoliths), and gonad measurements were taken for a random subset of pollock within each size group. Pollock and other fishes were measured to the nearest 1 mm fork length (FL), or standard

length (SL) for small specimens, with an electronic measuring board (Towler and Williams 2010). All lengths are reported as FLs in this report. Lengths were converted to FL using SL to FL regressions if necessary. Gonad maturity was determined by visual inspection and categorized as immature, developing, mature (hereafter, "pre-spawning"), spawning, or spent[1]. The ovary weight was determined for pre-spawning females. An electronic motion-compensating scale (Marel M60) was used to weigh individual pollock and selected ovaries to the nearest 2 g. Otoliths collected were stored in a 50% glycerin/thymol/water solution and interpreted by AFSC Age and Growth Program researchers to determine ages. Trawl station information and biological measurements were electronically recorded using the MACE Program's custom Catch Logger for Acoustic Midwater Surveys (CLAMS) software. Each pocket net catch was logged separately, in a manner similar to the codend catch.

Additional biological samples were collected for special projects. Pollock ovaries were collected from pre-spawning walleye pollock to investigate interannual variation in fecundity of mature females (Sandi Neidetcher, Sandi.Neidetcher@noaa.gov), and from female walleye pollock of all maturity stages for a histological study (Martin Dorn, Martin.Dorn@noaa.gov). Fin clips were taken from pollock to investigate the genetic population structure within spawning stocks (Ingrid Spies, Ingrid.Spies@noaa.gov), and gill tissues from pollock and cod were collected for an evolutionary marker analysis (Einar Arnason, einararn@hi.is). In Shelikof, egg and liver tissue samples were collected from 60 adult female pollock for a parasite study (Paul Hershberger, phershberger@usgs.gov). Results from these special projects will be reported elsewhere.

## Data Analysis

Processing of acoustic data

Although acoustic data were recorded at six frequencies, the results of this report and the survey time series are based on the 38 kHz data. The sounder-detected bottom was calculated by averaging the bottom detections for the five frequencies from 18-200 kHz (Jones et al. 2011) and

[1] Groundfish survey species code manual. 2021. RACE Division, AFSC, NMFS, NOAA; 7600 Sand Point Way NE, Seattle, WA 98115. Available online https://repository.library.noaa.gov/view/noaa/31571 .

then carefully examined to remove bottom integrations. A minimum $S_v$ threshold of –70 dB re 1 $m^{-1}$ was applied to the 38 kHz acoustic data, which were then echo-integrated from 16 m below the surface to 0.5 m above the sounder-detected bottom; 16 m is the minimum range at which the transmit pulse is not above the integration threshold at any frequency. Data were averaged at 0.5 nmi horizontal by 10 m vertical resolution intervals and exported to a database.

Associating size and species composition with acoustic backscatter

Pollock abundance was estimated by combining acoustic and trawl catch information. The analysis method employed here had three principal steps. First, backscatter was associated with the trawl catches from nearest geographic haul locations within a stratum. Second, a correction estimate was made for net selectivity (escapement from the midwater net, based on relationships derived from the recapture nets; Williams et al. 2011). Third, backscatter was converted to estimates of abundance from the nearest-haul catch association (step 1) and sample corrections (step 2). Biomass was computed from abundance using the mean weight-at-length from all specimens in a survey.

More specifically, acoustic backscatter was assigned to strata based on the appearance and vertical distribution of the aggregations in the echogram. Strata containing backscatter not considered to be from pollock (e.g., the near-surface mixture of unidentifiable backscatter, backscatter with frequency response indicative of euphausiids or myctophiids [De Robertis et al. 2010], or near-bottom backscatter "haystack" morphology indicative of some rockfishes that could not be sampled) were excluded from further analyses. Each trawl was associated with a stratum, and the backscatter at a given location was associated with the species and size composition of the geographically-nearest haul within that stratum (see De Robertis et al. 2017b for details). For example, juvenile pollock can be found in shallow, dense schools with a diffuse layer of adult pollock at deeper depths in that same area. In this case, the backscatter dominated by aggregations of juveniles would be assigned to a shallow stratum (A) and the backscatter dominated by adult layers would be assigned to a deep stratum (B). Hauls that sampled the shallow layer would be assigned to stratum A, and hauls that sampled the deeper layer would be assigned to stratum B. Backscatter would be converted to abundance by species and size within a stratum using the selectivity-corrected catch composition from the geographically-nearest trawl

in that stratum as described below (see Appendix III for detailed description of this method). Abundance was then converted to biomass using mean weight at length from all specimens included in the "length-weight key," which, for all winter surveys, is the entirety of the survey.

Selectivity Correction

Previous research has found that smaller fish are less likely to be retained in large midwater trawls than larger fish (Williams et al. 2011). To correct for this difference in retention, trawl selectivity was estimated using recapture nets mounted on both the AWT and LFS1421 trawls (Appendix IV). The counts and weights of animals caught in the recapture nets were expanded to provide an estimate of escapement from the entire trawl. The catch of all species was corrected for the estimated probability of escapement by dividing the abundance of a given species and size class by the estimated probability of retention of that species and size class. To generate trawl selectivity correction functions for all organisms in the catch, the species and size selectivity of the survey trawl was accounted for in the acoustic-trawl abundance estimate (e.g., De Robertis et al. 2017a). Species-specific selectivity functions were estimated for the most abundant species. More generic selectivity functions obtained by pooling species were applied to less abundant species (Appendix IV; De Robertis et al. 2017b). Thus the 2020 estimates reflect adjustments to the trawl-derived estimates of species and size composition which incorporate the estimated probability of retention of all organisms in the catch.

In this report, estimates for 2008-2018 surveys reflect selectivity corrections for juvenile pollock escapement, but not for escapement of other species, in all areas. The 2019 estimates also reflect corrections for eulachon (*Thaleichthys pacificus*) escapement in all areas. The 2020 survey is the first winter survey in which explicit selectivity corrections have been applied to all species, including pollock and eulachon, in the analysis. A mean selectivity correction was applied to winter survey data from 2008 to 2017, calculated using the years when recapture net data were collected (2008, 2013, and 2018). In surveys 2018-2019, corrections were applied based on recapture net data from each year's survey only. In 2020, the curves in Appendix IV were used.

Abundance Calculations

Fish abundance was calculated by combining species and size compositions from the hauls with acoustic backscatter data following the approach described in De Robertis et al. (2017a) and in Appendix III. A series of target strength (TS) to length relationships from the literature (Table 2) were used along with size and species distributions from trawl catches to estimate the proportion of the observed acoustic scattering attributable to each of the species captured in the trawls. For species for which the TS relationship was derived using a different length measurement type than the one used for measuring the trawl catch specimens, an appropriate length-length conversion was applied. For abundant species (e.g., contributing > 5% of the numbers or weight of the total catch), the most appropriate TS to length relationship available in the literature was used for that species. Other less abundant taxa were assigned to one of five generic categories: fishes with swim bladders, fishes without swim bladders, jellyfish, squid, and pelagic crustaceans (Table 2).

Pollock, eulachon, and Pacific herring contributed more than 5% of the catch in DY202001 by weight or numbers, and pollock, eulachon, and Northern smoothtongue (*Leuroglossus schmidti*) contributed to > 5% of the catch in DY202003. Therefore, a more specific TS relationship was used for pollock, eulachon, and herring in the analysis (Table 2). As a more specific TS relationship is not available for Northern smoothtongue, the relationship for generic fish without swim bladders was used (Table 2).

Pollock mean weight-at-length was estimated using data from all trawl catches. When < 5 pollock occurred per 1 cm length interval, weight at a that length interval was estimated from a linear regression of the natural logs of the length and weight data and corrected for a small bias due to back-transformation (Miller 1984, De Robertis and Williams 2008; Appendix IV).

An age-length key and a proportion-at-age matrix, were applied to the population numbers-at-length and biomass-at-length to estimate numbers and biomass at age (Appendix III in Jones et al. 2019; Appendix IV in this report). For population estimates at lengths where no otolith specimens were collected, the proportion-at-age was estimated using a Gaussian-model approach based on historical age-at-length data (2000-2014).

Processing of maturity data

Maturity data by haul were weighted by the local abundance of adult pollock (number of individuals > 30 cm FL), and all maturity data presented in this report are weighted. The 30 cm size criterion was selected as it represents the minimum size at which 5% of pollock are mature. The sum of the local abundance, $A_h$, assigned to the geographically-nearest haul, was computed. A weight, $W_h$, was then assigned to each haul by dividing the local haul abundance $A_h$ by the average abundance per haul $\bar{A}$,

$$W_h = {A_h}/{\bar{A}} \quad \text{(Eqn 1)}$$

where

$$\bar{A} = {\sum_h A_h}/{N_h}, \quad \text{(Eqn 2)}$$

and $N_h$ is the total number of hauls.

The percent of pollock, $PP_{sex,mat}$ greater than 40 cm FL by sex and maturity stage (immature, developing, pre-spawning, spawning, or spent) was computed for each haul and combined by survey area using a weighted average with $W_h$,

$$PP_{sex,mat} = {\sum_h (N_{sex,mat,h} \cdot W_h)}\Big/{\sum_h W_h}, \quad \text{(Eqn 3)}$$

where $N_{sex,mat,h}$ is the number of pollock greater than 40 cm by sex and maturity for each haul. The > 40 cm cutoff is used for consistency with reporting from past surveys; 40 cm FL is a common *L50* for pollock and the proportion of fish above 40 cm that are pre-spawning versus spawning has historically been used as a qualitative measure of survey timing.

For each haul, the number of female pollock considered mature (pre-spawning, spawning, or spent) and immature (immature or developing) were determined for each cm length bin. The length at 50% maturity (*L50*) was estimated for female pollock as a logistic regression using a weighted generalized linear model following Williams (2007) with the inclusion of the haul weights, $W_h$, into the model (function glm, R Core Team 2019).

The gonadosomatic index, $GSI_h$, (GSI: ovary weight/(ovary weight + body weight)) was calculated for pre-spawning females in each haul and then a weighted average was computed for each survey area with $W_h$,

$$GSI = \sum_h (GSI_h \cdot W_h) \Big/ \sum_h W_h. \quad \text{(Eqn 4)}$$

Relative estimation error

In all areas, transects were parallel and relative estimation errors for the acoustic-based estimates were derived using a one-dimensional (1-D) geostatistical method (Petitgas 1993, Williamson and Traynor 1996, Walline 2007). "Relative estimation error" is defined as the ratio of the square root of the 1-D estimation variance ($variance_{sum}$) to the biomass estimate (i.e., the sum of biomass over all transects, $biomass_{sum}$, kg):

$$Relative\ estimation\ error_{1\text{-}D} = \frac{\sqrt{variance_{sum}}}{biomass_{sum}}. \quad \text{(Eqn 5)}$$

Because sampling resolution affects the variance estimate, and the 1-D method assumes equal transect spacing, estimation variance was determined separately in each area with unique transect spacing. Relative estimation error for an entire survey area (among *n* survey areas with different transect spacings) was computed by summing the estimation variance for each area *j*, taking the square root, and then dividing by the sum of the biomass over all areas, assuming independence among estimation errors for each survey area (Rivoirard et al. 2000):

$$Relative\ estimation\ error_{1\text{-}D\ survey} = \frac{\sqrt{\sum_{j=1}^{n} variance_{sum_j}}}{\sum_{j=1}^{n} biomass_{sum_j}}. \quad \text{(Eqn 6)}$$

Geostatistical methods were used to compute estimation error to account for uncertainty arising from the observed spatial structure in the fish distribution. These errors, however, quantify only transect sampling variability of the acoustic data (Rivoirard et al. 2000). Other sources of error (e.g., target strength, trawl sampling) were not evaluated.

Additional Analyses

A primary analysis and two alternate analyses were conducted to estimate the effect of selectivity corrections on the numbers and biomass of pollock and other target species. The primary analysis described above relies on the fewest assumptions to generate abundance estimates and is thus considered the most appropriate approach. The secondary (no-selectivity) analysis was the same as the primary analysis except that it did not include a selectivity correction for escapement. That is, the selectivity ($S_{s,l}$) was set to 1 (see Eqn. x, Appendix IV) for all species and size classes. An analysis similar to historic methods used through 2017 was also conducted (see Honkalehto et al. 2018 for details). This historic-mimic analysis: 1) did not incorporate species mixtures: in general all backscatter in a stratum assigned to pollock was assumed to be exclusively pollock, 2) used nearest haul to assign length-frequency distributions of pollock to the backscatter, and 3) did not include a selectivity correction for age 1+ pollock trawl escapement or for any other species escapement (see McCarthy et al. 2018).

To examine pollock vertical distribution in terms of distance above the seafloor, a bottom-referenced analysis was conducted, where all data were exported using Echoview in 10 m vertical bins referenced to a scrutinized line 0.5 m above the sounder-detected seafloor echo. The bottom-referenced analysis was generated for previous years (2015-2019) to allow for inter-annual comparison of vertical distribution. All other parts of this analysis are the same as the primary analysis.

## RESULTS and DISCUSSION

Calibration

Pre- and post-survey calibration measurements of the 38 kHz echosounder showed no significant differences in gain parameters or beam pattern characteristics for either the swing or the on-axis results, confirming that the acoustic system was stable throughout the survey (Table 1). The on-axis results were used to calculate gain, while the swing results are used to verify that the beam pattern matched expectations. At 38 kHz, the integration gain differed by < 0.05 dB across the two measurements. Acoustic system gain and beam pattern parameters measured during the first and second calibrations were averaged (averages calculated in the linear domain for dB

quantities), nominal soundspeed and absorption values appropriate for the survey areas were used in the final parameter set for survey data analysis, and the equivalent beam angle initially measured by the manufacturer in a test tank was adjusted (Bodholt 2002) using the *in situ* sound speed during survey conditions (Table 1).

## Shumagin Islands

Acoustic backscatter was measured along 882.8 km (476.7 nmi) of transects spaced an average of 4.3 km (2.3 nmi) apart, with spacing varying from 1.85 to 9.26 km (1 to 5 nmi) in the survey area (Fig. 1). Bottom depths in the survey area ranged from 52 m to 231 m.

Surface water temperatures in the Shumagin Islands averaged 3.5 °C overall (Fig. 2), and ranged from 3.1 °C to 4.0 °C as measured by the ship's flow-through instrumentation. Surface water temperatures at haul locations averaged 3.4 °C (Table 3), which was 0.8 degrees cooler than the average of 4.2 °C observed during 2018 and 0.3 °C lower than the historic mean of the prior 19 surveys conducted in this area since 1994 (3.7 °C). Mean temperature between the surface and deepest trawl depth at haul locations varied by around 1 °C across all hauls (Fig. 3). The mean water temperature at fishing depths was 4.4 °C (Table 3).

### Trawl Samples

Biological data and specimens were collected in the Shumagin Islands area from 5 LFS1421 hauls (Tables 3, 4, and 5; Fig. 1) that targeted backscatter attributed to pollock. The lengths of an average of 216 randomly selected pollock were measured for each haul in the Shumagins, with an average of 43 individuals more extensively sampled for at least one of the following: Body weight, maturity, or age (Table 5). A total of 215 otoliths to estimate pollock ages were collected from the Shumagin Islands (Table 5).

In the Shumagin Islands area, pollock and eulachon were the most abundant species in the LFS1421 hauls, contributing 94.5% and 3.1% of the total catch by weight, respectively. Pollock and eulachon were also the most abundant species by numbers with 62% and 25.6%, respectively (Table 4).

Both male and female pollock observed in the Shumagin Islands area were predominately in the pre-spawning maturity stage. The maturity composition of males > 40 cm FL (n = 40) was 0% immature, 1% developing, 55% pre-spawning, 44% spawning, and 0% spent (Fig. 4a). The maturity composition of females > 40 cm FL (n = 30) was 0% immature, 36% developing, 52% pre-spawning, 0% spawning, and 12% spent (Fig. 4a). The length at which 50% of female pollock > 22 cm FL were determined to be reproductively mature (i.e., pre-spawning, spawning, or spent) is 45 cm FL (Fig. 4b). The average GSI from 25 pre-spawning females was 0.1 ± 0.02 (Fig. 4c, mean ± standard deviation), which was the same as the 2019 estimate and the historical mean (0.10 ± 0.02). Most females were in the pre-spawning stage of maturity and substantially fewer were spawning or spent, which suggests that the 2020 Shumagins survey was well-timed relative to the spawning period.

Distribution and Abundance

Pollock were observed throughout the surveyed area and were most abundant to the northwest and southwest of Korovin Island (Fig. 5). Adult pollock were detected in both of these regions, but not in the Shumagin Trough. Juveniles (≤ 30 cm FL) were concentrated in the areas directly north and south of Korovin Island and were rare elsewhere in the survey area. Adult pollock were detected at an average depth of 100 m, and 50 m above the seafloor, and juvenile pollock were similarly distributed, but had a slightly greater average height above bottom (Fig. 6).

Pollock with lengths 10-16 cm FL, considered to be indicative of age-1 pollock, accounted for 51.4 % of the numbers and 3.6% of the biomass of all pollock observed in the Shumagin Islands (Fig 7). Pollock 17-24 cm FL, indicative of age-2s, accounted for 2.2% by numbers and 1.1% by biomass. Pollock ≥ 30 cm FL accounted for 35.1% and 84.9% of the numbers and biomass, respectively. This survey showed high numbers of fish with lengths characteristic of age-1 pollock (10-16 cm FL), but not as many as in 2018 when they were particularly numerous (99% of the catch by numbers).

A total of 30.6 million pollock weighing 4,889 t were estimated to be in the Shumagin Islands at the time of the survey. The 2020 biomass was 28.1% of that observed in 2018 (17,389 t) and 7.1% of the historic mean of 68.4 thousand tons (Table 6; Figs. 8 and 9). The 2020 survey

biomass estimate is the smallest in the Shumagin Islands survey time series (Table 6; Figs. 8 and 9). The relative estimation error of the 2020 biomass estimate based on the 1-D geostatistical analysis was 12.2%.

The no-selectivity correction analysis (Analysis 2) for 2020 generated an overall increase of 7.94% by numbers (to 33.0 million) and an increase of 23.1% by numbers (to 6,017 t) for pollock in the Shumagin Islands area compared to the primary analysis. The non-selectivity analysis decreased the number of small pollock and increased the number of adults relative to the primary analysis, and as age-1 pollock were numerous in 2020, the overall impact of this change was noticeable. The "historic-mimic" analysis (Analysis 3) for 2020 generated an overall increase of 25% by numbers (to 38 million) and an increase of 35% by biomass (to 6,578 t) for pollock in the Shumagin Islands area as compared to the primary analysis as more of the observed backscatter was assigned to pollock and escapement was not accounted for (Fig. 10).

## Shelikof Strait

Acoustic backscatter was measured along 1,425 km (769.5 nmi) of transects spaced mainly 13.9 km (7.5 nmi) apart, with spacing varying 11.3 km to 27.8 km (6.1 to 15 nmi) in the survey area (Fig. 11). Due to the emergence of the global COVID-19 pandemic, management determined that the survey should be completed as quickly as possible, so once backscatter amounts decreased near the Semidi Islands (where backscatter amounts have historically decreased) transect spacing was doubled to 27.8 km (15 nmi) for the final two transects. Bottom depths in the survey area ranged from 39 m to 326 m.

Surface water temperatures in Shelikof Strait averaged 3.2 °C overall (Fig. 12), and ranged from 1.7 °C to 4.4 °C as measured by the ship's flow-through instrumentation. Surface water temperatures at haul locations averaged 2.6 °C (Table 7). This was 1.6 °C cooler than the average of 4.2 °C observed during 2019 and 1.1 °C lower than the historic mean of the prior 36 surveys conducted in this area since 1981 (3.7 °C). Mean temperature between the surface and

deepest trawl depth at haul locations varied by around 2.8 °C across all hauls (Fig. 13). The mean water temperature at fishing depths was 5.4 °C (Table 7).

Trawl Samples

Biological data and specimens were collected in the Shelikof Strait area from 23 LFS1421 hauls and 11 AWT hauls (Tables 7, 8, and 9; Fig. 11) targeting backscatter attributed to pollock. The lengths of an average of 315 randomly selected pollock were measured from each LFS haul in Shelikof, with an average of 42 individuals more extensively sampled for at least one of the following: body weight, maturity, and age (Table 10). A total of 524 otoliths to estimate pollock ages were collected from Shelikof Strait (Table 10).

In the Shelikof Strait area, pollock and eulachon were the most abundant species by weight in the LFS1421 hauls, contributing 91.5% and 7.8% of the catch by weight, respectively (Table 9). Eulachon and pollock were the most abundant species by numbers with 46.2% and 38% of total catch numbers, respectively.

Pollock observed in the Shelikof Strait were generally in pre-spawning (females) or spawning (males) maturity stages. The maturity composition of males > 40 cm FL (n = 312) was 0% immature, 0% developing, 4% pre-spawning, 90% spawning, and 6% spent (Fig. 14a). The maturity composition of females > 40 cm FL (n = 258) was 6% immature, 0% developing, 88% pre-spawning, 1% spawning, and 5% spent (Fig. 14a). The length at which 50% of female pollock > 20 cm FL were determined to be reproductively mature (i.e., pre-spawning, spawning, or spent) is 39.4 cm FL (Fig. 14b). The average GSI from 212 pre-spawning females was 0.15 $\pm$ 0.02 (Fig. 14c, mean $\pm$ standard deviation), which was very similar to the 2019 estimate and the historical mean (0.13 $\pm$ 0.03). Most females were in the pre-spawning stage of maturity and substantially fewer were spawning or spent, which suggests that the timing of the 2020 Shelikof Strait survey relative to the spawning period was appropriate.

Distribution and Abundance

Adult pollock were detected throughout Shelikof Strait, with most distributed along the west side from Cape Nukshak to Cape Kekurnoi and in the center of the sea valley south of Cape Kekurnoi

(Fig. 15), as is typical for most previous Shelikof surveys, most adult pollock (defined as 75% of the biomass) were detected between depths of 155-255 m (Fig. 16a). Most juvenile pollock were detected between depths of 75-235 m (Fig. 16b). Most adult pollock were observed within 75 m of the bottom, with most juveniles found within 165 m and ranging up to 195 m (includes 95% of the biomass) off the bottom (Fig. 16c and d), computed from bottom-referenced analysis. Adult pollock depth distributions in 2020 were shallower than those in 2019, and deeper than in the prior 4 years (Fig. 16a and c), with about 8% of the biomass observed within 10 m of the seafloor, and 64% percent of biomass within 50 m of the seafloor (Fig. 16c).

Age-1 pollock accounted for 1.8 % of the numbers and $\leq$ 0.1% of the biomass of all pollock observed in Shelikof Strait (Figs. 17 and 18). Age-2 pollock, the 2018 year class, accounted for 8.3% by numbers and 1.3% by biomass of all pollock. Age-3 pollock accounted for 35.1% and 12.9% of the numbers and biomass, respectively. Pollock of most ages had shorter lengths when compared to the same age group from previous winter acoustic-trawl surveys (Fig. 21).

A total of 985.0 million pollock weighing 459,399 t were estimated to be in Shelikof Strait at the time of the survey. The 2020 biomass was 35.9% of that observed in 2019 (1,281,094 t) and 63.5% of the historic mean of 722.89 thousand tons (Table 11; Fig. 22). Survey biomass estimates in 2017, 2018, and 2019 were the largest since the mid-1980s, while the 2020 biomass estimate is on par with the estimates from the early 2000s (Table 11; Figs. 19, 20 and 22). The relative estimation error of the 2020 biomass estimate based on the 1-D geostatistical analysis was 2.9%.

The continued strength of the 2012 year class in Shelikof Strait was visible in the population size composition time series for both numbers and biomass of pollock beginning in 2013 (Tables 12-15; Fig. 19). Older pollock (ca. 40 cm FL to 55 cm FL) and age-3 pollock from the 2017 year class contributed the majority of the biomass in Shelikof Strait (Figs. 17, 18, and 19; Tables 13 and 15). This survey did not encounter high numbers of age-1 pollock, unlike 2019 when they were particularly numerous as compared to previous years (Figs. 18 and 19; Table 14).

McKelvey (1996) showed that there was a strong relationship between the estimated number of age-1 pollock from the Shelikof Strait AT survey and year-class strength for GOA pollock. The McKelvey index is based on data that did not include a correction for escapement of age-1 pollock. Thus, the 2020 no-selectivity based estimate (Analysis 2) was used to classify the strength of the 2019 year class (age-1 pollock observed in 2020) in the context of the McKelvey index. This estimate was 9.7 million age-1 pollock, which is considered a low or weak year class based on the McKelvey index. The no-selectivity correction analysis for 2020 generated an overall increase of 2% by numbers (to 1,005 million) and an increase of 2.9% by weight (to 472,813 t) for all pollock in the Shelikof Strait area compared to the primary analysis (Fig. 23). The non-selectivity analysis decreased the number of small pollock and increased the number of adults relative to the primary analysis, but, as there were few age-1 pollock in 2020, the overall impact of this change was negligible (Fig. 23). The "historic-mimic" analysis (Analysis 5) for 2020 generated an overall increase of 3.3% by numbers (to 1,018 million) and an increase of 2.7% by biomass (to 472,009 t) for pollock in Shelikof Strait area as compared to the primary analysis (Fig. 23).

## ACKNOWLEDGMENTS

The authors would like to thank the officers and crew of the NOAA ship *Oscar Dyson* for their dedication and contribution to the successful completion of this work. Thanks also to AFSC and University of Washington scientists for their invaluable assistance with fish processing, data collection, and data analysis.

## CITATIONS


Bodholt, H., 2002. The effect of water temperature and salinity on echo sounder measurements. ICES Symposium on Acoustics in Fisheries, Montpellier 10–14 June 2002.

Bodholt, H., and H. Solli. 1992. Split beam techniques used in Simrad EK500 to measure target strength, p. 16-31. *In* World Fisheries Congress, May 1992, Athens, Greece.

Demer, D. A., Berger, L., Bernasconi, M., Bethke, E., Boswell, K., Chu, D., Domokos, R., et al. 2015. Calibration of acoustic instruments. ICES Coop. Res. Rep. 326, 133 pp.

Demer, D. A., and S. G. Conti. 2005. New target-strength model indicates more krill in the Southern Ocean. ICES J. Mar. Sci. 62: 25-32.

De Robertis, A., R. Levine, and C. D. Wilson. 2018. Can a bottom-moored echo sounder array provide a survey-comparable index of abundance? Can. J. Fish. Aquat. Sci. 75: 629-640. dx.doi.org/10.1139/cjfas-2017-0013.

De Robertis, A., D. R. McKelvey, and P. H. Ressler. 2010. Development and application of an empirical multifrequency method for backscatter classification. Can. J. Fish. Aquat. Sci. 67:1459-1474.

De Robertis, A., and K. Taylor. 2014. *In situ* target strength measurements of the scyphomedusa *Chrysaora melanaster*. Fish. Res. 153:18-23.

De Robertis, A., K. Taylor, K. Williams, and C. D. Wilson. 2017a. Species and size selectivity of two midwater trawls used in an acoustic survey of the Alaska Arctic. Deep-Sea Res. Part II 135:40–50.

De Robertis, A., K. Taylor, C.D. Wilson, and E. V. Farley. 2017b. Abundance and distribution of Arctic cod (*Boreogadus saida*) and other pelagic fishes over the U.S. continental shelf of the northern Bering and Chukchi seas. Deep-Sea Res. II. 135: 51-65.3

De Robertis, A., and K. Williams. 2008. Weight-length relationships in fisheries studies: the standard allometric model should be applied with caution. Trans. Am. Fish. Soc. 137: 707-719.

Foote, K.G. 1987. Fish target strengths for use in echo integration surveys. J. Acoust. Soc. Am. 82: 981-987.

Foote, K. G., and J. Traynor. 1988. Comparison of walleye pollock target-strength estimates determined from *in situ* measurements and calculations based on swimbladder form. J. Acoust. Soc. Am. 83: 9-17.

Foote, K. G., H. P. Knudsen, G. Vestnes, and E. J. Simmonds. 1987. Calibration of acoustic instruments for fish density estimation: a practical guide. ICES Coop. Res. Rep. 144, 69 p.

Gauthier, S., and J. K. Horne. 2004. Acoustic characteristics of forage fish species in the Gulf of Alaska and Bering Sea. Can. J. Fish. Aquat. Sci. 61: 1839-1850.

Guttormsen, M. A., and C. D. Wilson. 2009. *In situ* measurements of capelin (*Mallotus villosus*) target strength in the North Pacific Ocean. ICES J. Mar. Sci. 66: 258-263.

Honkalehto, T., N. Williamson, D. Jones, A. McCarthy, and D. McKelvey. 2008. Results of the echo integration-trawl survey of walleye pollock (*Theragra chalcogramma*) on the U.S. and Russian Bering Sea Shelf in June and July 2007. U.S. Dep. Commer., NOAA Tech. Memo. NMFS-AFSC-190, 53 p.

Jech, J. M., K. G. Foote, D. Chu, and L. C. Hufnagle. 2005. Comparing two 38-kHz scientific echosounders. ICES J. Mar. Sci. 62: 1168-1179.

Jones, D. T., A. De Robertis, and N. J. Williamson. 2011. Statistical combination of multifrequency sounder-detected bottom lines reduces bottom integrations. U.S. Dep. Commer., NOAA Tech. Memo. NMFS-AFSC-219, 13 p.

Jones, D., Wilson, C. D., De Robertis, A., Weber, T.C., and Butler, J. L. 2012. Evaluation of Rockfish Abundance in Untrawlable Habitat: Combining Acoustics with Alternate Sampling Tools. Fishery Bulletin, U.S. 110: 332-343.

Jones, D. T., N. E. Lauffenburger, K. Williams, and A. De Robertis. 2019. Results of the acoustic trawl survey of walleye pollock (*Gadus chalcogrammus*) in the Gulf of Alaska, June August 2017 (DY2017-06), AFSC Processed Rep. 2019- 08, 110 p. Alaska Fish. Sci. Cent., NOAA, Natl. Mar. Fish. Serv., 7600 Sand Point Way NE Seattle, WA 98115.

Kang, D., T. Mukai, K. Iida, D. Hwang, and J.-G. Myoung. 2005. The influence of tilt angle on the acoustic target strength of the Japanese common squid (*Todarodes pacificus*). ICES J. Mar. Sci. 62: 779-789.

MacLennan, D. N., P. G. Fernandes, and J. Dalen. 2002. A consistent approach to definitions and symbols in fisheries acoustics. ICES J. Mar. Sci. 59: 365-369.

McCarthy, A. L., S. Stienessen, and D. Jones. 2018. Results of the acoustic-trawl surveys of walleye pollock (*Gadus chalcogrammus*) in the Gulf of Alaska, February-March 2017 (DY2017-01, DY2017-02, and DY2017-03). AFSC Processed Rep. 2018-04, 126 p. Alaska Fish. Sci. Cent., NOAA, Natl. Mar. Fish. Serv., 7600 Sand Point Way NE, Seattle WA 98115.

McKelvey, D. R. 1996. Juvenile walleye pollock, *Theragra chalcogramma*, distribution and abundance in Shelikof Strait—what can we learn from acoustic surveys, p. 25-34. *In* Ecology of juvenile walleye pollock, *Theragra chalcogramma*, U.S. Dep. Commer., NOAA Tech. Rep. NMFS- 126.

National Marine Fisheries Service (NMFS) 2014. NOAA protocols for fisheries acoustics surveys and related sampling (Alaska Fisheries Science Center), 26 p. Prepared by Midwater Assessment and Conservation Engineering Program, Alaska Fish. Sci. Center, Natl. Mar. Fish. Serv., NOAA

Petitgas, P. 1993. Geostatistics for fish stock assessments: a review and an acoustic application. ICES J. Mar. Sci. 50: 285-298.

R Core Team. 2019. R: A language and environment for statistical computing. R Foundation for Statistical Computing, Vienna, Austria. URL https://www.R-project.org/.

Rivoirard, J., J. Simmonds, K. G. Foote, P. Fernandez, and N. Bez. 2000. Geostatistics for estimating fish abundance. Blackwell Science Ltd., Osney Mead, Oxford OX2 0EL, England. 206 p.

Rogers, L.A., and A.B. Dougherty. 2019. Effects of climate and demography on reproductive phenology of a harvested marine fish population. Global Change Biol. 25(2): 708-720. https://doi.org/10.1111/gcb.14483.

Simrad. 2018. EK80 scientific echo sounder software reference manual. 848 p. Simrad AS, Strandpromenenaden 50, 3183 Horten, Norway.

Stanley, R. D., R. Kiesser, K. Cooke, A. M. Surry, and B. Mose, 2000. Estimation of a widow rockfish (*Sebastes entomelas*) shoal off British Columbia, Canada as a joint exercise between stock assessment staff and the fishing industry. ICES J. Mar. Sci. 57:1035-1049.

Towler, R., and K. Williams. 2010. An inexpensive millimeter-accuracy electronic length measuring board. Fish. Res. 106:107-111.

Traynor J. 1996. Target-strength measurements of walleye pollock *(Theragra chalcogramma*) and Pacific whiting *(Merluccius productus*). ICES J. Mar. Sci. 53:253-258.

Walline, P. D. 2007. Geostatistical simulations of eastern Bering Sea walleye pollock spatial distributions, to estimate sampling precision. ICES J. Mar. Sci. 64:559-569.

Williams, K., A. E. Punt, C. D. Wilson, and J. K. Horne. 2011. Length-selective retention of walleye pollock, *Theragra chalcogramma*, by midwater trawls. ICES J. Mar. Sci. 68: 119-129.

Williams, K. 2007. Evaluation of the macroscopic staging method for determining maturity of female walleye pollock *Theragra chalcogramma* in Shelikof Strait, Alaska. Alaska Fish. Res. Bull., 12: 252-263.

Williamson, N. J., and J. J. Traynor. 1996. Application of a one-dimensional geostatistical procedure to fisheries acoustic surveys of Alaskan pollock. ICES J. Mar. Sci. 53: 423-428.

Wilson, C.D. 1994. Echo integration-trawl survey of pollock in Shelikof Strait Alaska in 1994, p. 1-39. *In* Stock Assessment and Fishery Evaluation Report for the 1994 Gulf of Alaska Groundfish Fishery, November 1994, Supplement. Prepared by the Gulf of Alaska Groundfish Plan Team, North Pacific Fishery Management Council, P.O. Box 103136, Anchorage, AK 99510.

Table 1. -- Simrad EK80 38 kHz acoustic system description and settings used during the winter 2020 Gulf of Alaska acoustic-trawl surveys of walleye pollock. These include environmental parameters and results from standard sphere acoustic system calibrations conducted in association with the survey and final values used to calculate biomass and abundance data. The system settings column contains February 12 EK80 calibration utility results. Other columns are a combination of on-axis and EK80 calibration utility results (see Methods and Results and Discussion sections of text for details).

| | Winter 2020 system settings | 12 Feb Uganik Bay Alaska | 16 Mar Kalsin Bay Alaska | Final analysis parameters |
|---|---|---|---|---|
| Echosounder | Simrad EK80 | -- | -- | Simrad EK80 |
| Transducer | ES38-7 s/n 324 | -- | -- | ES38-7 s/n 324 |
| Frequency (kHz) | 38 | -- | -- | 38 |
| Transducer depth (m) | 9.15 | -- | -- | 9.15 |
| Pulse length (ms) | 1.024 | -- | -- | 1.024 |
| Transmitted power (W) | 2000 | -- | -- | 2000 |
| Angle sensitivity along | 18.00 | -- | -- | 18.00 |
| Angle sensitivity athwart | 18.00 | -- | -- | 18.00 |
| 2-way beam angle (dB re 1 steradian) | -20.70 | -- | -- | -20.52 |
| Gain (dB) | 27.18 | 27.13 | 27.17 | 27.15 |
| $s_A$ correction (dB) | -0.04 | -0.05 | -0.05 | -0.05 |
| Integration gain (dB) | 27.14 | 27.08 | 27.12 | 27.10 |
| 3 dB beamwidth along | 6.35 | 6.35 | 6.40 | 6.38 |
| 3 dB beamwidth athwart | 6.44 | 6.44 | 6.46 | 6.45 |
| Angle offset along | -0.04 | -0.04 | -0.04 | -0.04 |
| Angle offset athwart | 0.06 | 0.06 | 0.06 | 0.06 |
| Post-processing $S_v$ threshold (dB re 1 $m^{-1}$) | -70 | NA | NA | -70 |
| Standard sphere TS (dB re 1 $m^2$) | NA | -42.15 | -42.13 | NA |
| Sphere range from transducer (m) | NA | 20.27 | 20.78 | NA |
| Absorption coefficient (dB/m) | 0.0099 | 0.0099 | 0.0098 | 0.0099 |
| Soundspeed (m/s) | 1466.0 | 1460.5 | 1460.5 | 1466.0 |
| Water temp at transducer (°C) | NA | 3.8 | 3.3 | NA |

Note: Gain and beam pattern terms are defined in the Operator Manual for Simrad ER60 Scientific echosounder application, which is available from Simrad Strandpromenaden 50, Box 111, N-3191 Horten, Norway. -- symbol indicates the same values for the system settings and final analysis are also applicable for the various calibrations. NA indicates 'not applicable'.

Table 2. -- Target strength (TS) to size relationships from the literature used to allocate 38 kHz acoustic backscatter to most species in this report. The symbols in the equations are as follows: r is the bell radius in cm and L is length in cm for all groups except pelagic crustaceans, in which case L is in mm.

| Group | TS (dB re 1 $m^2$) | Length type | TS derived for which species | Reference |
|---|---|---|---|---|
| walleye pollock | $TS = 20 \log_{10} L\text{-}66$ | L = fork length | *Gadus chalcogrammus* | Foote & Traynor 1988, Traynor 1996 |
| pacific herring | $TS = 20 \log_{10} L\text{-}2.3 \log_{10}(1 + depth/10) - 65.4$ | L = fork length | *Clupea harengus* | Ona 2003 |
| fish with swim bladders | $TS = 20 \log_{10} L - 67.4$ | L = total length | Physoclist fishes | Foote 1987 |
| fish without swim bladders | $TS = 20 \log_{10} L - 83.2$ | L = total length | *Pleurogrammus monopterygius* | Gauthier & Horne 2004 |
| jellyfish | $TS = 10 \log_{10}(pir^2) - 86.8$ | r = bell radius | *Chrysaora melanaster* | De Robertis & Taylor 2014 |
| squid | $TS = 20 \log_{10} L - 75.4$ | L = mantle length | *Todarodes pacificus* | Kang et al. 2005 |
| eulachon | $TS = 20 \log_{10} L - 84.5$ | L = total length | *Thaleichthys pacificus* | Gauthier & Horne 2004 |
| pelagic crustaceans[1] | $TS = A * (\log_{10}(BkL)/(BkL))^c + D((kL)^6) + E((kL)^5) + F((kL)^4) + G((kL)^3) + H((kL)^2) + I(kL) + J + 20 \log_{10}(L/L_0)$ | L = total length | *Euphausia superba* | Demer & Conti 2005 |

[1] A = -930.429983; B = 3.21027896; C = 1.74003785; D = 1.36133896 x $10^{-8}$; E = -2.26958555 x $10^{-6}$; F=1.50291244 x $10^{-4}$; G = -4.86306872 x $10^{-3}$; H = 0.0738748423.
If L < 15 mm, TS = -105 dB; and if L > 65 mm, TS = -73 dB.
k = 2*pi*fc, where f = 38,000 (frequency in Hz) and c = 1470 (sound speed in m/s).

Table 3. -- Trawl stations and catch data summary from the winter 2020 acoustic-trawl survey of walleye pollock in the Shumagin Islands regions.

| Haul | Area | Gear | Date | Time | Duration | Start Position | | Depth (m) | | Temp (°C) | | walleye pollock | | Other |
|---|---|---|---|---|---|---|---|---|---|---|---|---|---|---|
| No. | | Type[a] | (GMT) | (GMT) | (mins) | Lat. (N) | Long. (W) | Headrope[b] | Bottom | Headrope | Surface[c] | (kg) | Number | (kg) |
| 1 | Shumagin Islands | LFS1421 | 15-Feb | 11:33 | 18.0 | 55.3958 | -159.8337 | 63 | 94 | 3.7 | 3.4 | 5.9 | 35 | 0.9 |
| 2 | Shumagin Islands | LFS1421 | 16-Feb | 01:29 | 42.7 | 55.5733 | -159.9909 | 143 | 170 | 5.0 | 3.3 | 16.0 | 136 | 26.1 |
| 3 | Shumagin Islands | LFS1421 | 16-Feb | 12:04 | 12.1 | 55.1644 | -160.3055 | 124 | 208 | 3.7 | 3.5 | 372.4 | 1,777 | 2.2 |
| 4 | Shumagin Islands | LFS1421 | 16-Feb | 23:04 | 10.8 | 55.5830 | -160.1831 | 140 | 181 | 5.2 | 3.4 | 61.0 | 3,039 | 10.7 |
| 5 | Shumagin Islands | LFS1421 | 18-Feb | 15:41 | 55.6 | 55.4636 | -160.4805 | 100* | 149 | - | 3.3 | 249.9 | 320 | 1.2 |

[a]LFS1421 = LFS1421 midwater trawl

[b]Headrope depth obtained from SBE temperature logger. In hauls without SBE temperature logger records, footrope depth was obtained from scientist notes when possible.

[c]Average temperature measured from an SBE temperature logger

[*]Depth obtained from FS70 logger due to SBE failure

Table 4. -- Catch by species and numbers of length and weight measurements taken from 5 LFS1421 hauls during the 2020 acoustic-trawl survey of walleye pollock in Shumagin Islands.

| | | Catch | | | | Measurements | |
|---|---|---|---|---|---|---|---|
| Species name | Scientific name | Weight (kg) | % | Number | % | Length | Weight |
| walleye pollock | *Gadus chalcogrammus* | 705.2 | 94.5 | 5,307 | 62.0 | 1,079 | 314 |
| eulachon | *Thaleichthys pacificus* | 23.4 | 3.1 | 2,196 | 25.6 | 138 | 57 |
| chinook salmon | *Oncorhynchus tshawytscha* | 6.2 | 0.8 | 3 | <0.1 | 3 | 2 |
| Pacific herring | *Clupea pallasii* | 4.4 | 0.6 | 427 | 5.0 | 75 | 31 |
| euphausiid unid. | Euphausiacea (order) | 1.6 | 0.2 | <0.1 | <0.1 | - | - |
| flathead sole | *Hippoglossoides elassodon* | 1.4 | 0.2 | 5 | <0.1 | 5 | 5 |
| capelin | *Mallotus villosus* | 0.9 | 0.1 | 176 | 2.1 | 114 | 30 |
| smooth lumpsucker | *Aptocyclus ventricosus* | 0.9 | 0.1 | 1 | <0.1 | 1 | 1 |
| Aequorea sp. | *Aequorea sp.* | 0.7 | <0.1 | 73 | 0.9 | 17 | 17 |
| northern rock sole | *Lepidopsetta polyxystra* | 0.3 | <0.1 | 1 | <0.1 | 1 | 1 |
| southern rock sole | *Lepidopsetta bilineata* | 0.3 | <0.1 | 1 | <0.1 | 1 | 1 |
| smelt unid. | Osmeridae (family) | 0.3 | <0.1 | 255 | 3.0 | 27 | - |
| Pacific sandfish | *Trichodon trichodon* | 0.3 | <0.1 | 1 | <0.1 | 1 | 1 |
| Pandalus sp. | *Pandalus sp.* | 0.1 | <0.1 | 74 | 0.9 | 27 | - |
| isopod unid. | Isopoda (order) | 0.1 | <0.1 | 8 | <0.1 | 4 | - |
| Alaskan pink shrimp | *Pandalus eous* | <0.1 | <0.1 | 27 | 0.3 | 12 | - |
| squid unid. | Cephalopoda (class) | <0.1 | <0.1 | 7 | <0.1 | 1 | 1 |
| ribbed sculpin | *Triglops pingeli* | <0.1 | <0.1 | 1 | <0.1 | 1 | 1 |
| prickleback unid. | Stichaeidae (family) | <0.1 | <0.1 | 1 | <0.1 | 1 | - |
| sculpin unid. | Cottidae (family) | <0.1 | <0.1 | 1 | <0.1 | 1 | 1 |
| fish unid. | Actinopterygii (class) | <0.1 | <0.1 | 1 | <0.1 | - | - |
| Total | | 746.3 | | 8,566 | | 1,509 | 463 |

Table 5. -- Numbers of walleye pollock measured and biological samples collected during the winter 2020 acoustic-trawl survey of Shumagin Islands.

| Haul no. | Region name | Catch lengths | Weights | Maturities | Otoliths | Ovary weights | Ovaries collected |
|---|---|---|---|---|---|---|---|
| 1 | Shumagin Islands | 35 | 35 | 35 | 35 | - | 8 |
| 2 | Shumagin Islands | 55 | 55 | 39 | 44 | 9 | 14 |
| 3 | Shumagin Islands | 467 | 69 | 49 | 44 | 2 | 9 |
| 4 | Shumagin Islands | 202 | 69 | 50 | 40 | 3 | 11 |
| 5 | Shumagin Islands | 320 | 86 | 82 | 52 | 17 | 11 |
| Total | | 1,079 | 314 | 255 | 215 | 31 | 53 |

Table 6. -- Estimates of walleye pollock biomass (thousands of metric tons) and relative estimation error for the Shumagin Islands, Sanak Trough, Morzhovoi Bay, and Pavlof Bay region. Estimates for 2009- 2020 reflect selectivity corrections for escapement of juveniles. Blank values indicate no survey or estimation error was completed within a given region and year.

| Year | Shumagin Islands | | Sanak Trough | | Morzhovoi Bay | | Pavlof Bay | |
|---|---|---|---|---|---|---|---|---|
| | Biomass | Est. error | Biomass | Est. error | Biomass | Est. error | Biomass | Est. error |
| 1994 | 112.0[1] | | | | | | | |
| 1995 | 290.1 | | | | | | | |
| 1996 | 117.7[2] | | | | | | | |
| 1997 | | | | | | | | |
| 1998 | | | | | | | | |
| 1999 | | | | | | | | |
| 2000 | | | | | | | | |
| 2001 | 119.6 | | | | | | | |
| 2002 | 135.6 | 27.1% | | | | | | |
| 2003 | 67.7 | 17.2% | 80.5 | 21.6% | | | | |
| 2004 | | | | | | | | |
| 2005 | 52.0 | 11.4% | 65.5 | 7.4% | | | | |
| 2006 | 37.3 | 10.1% | 127.2 | 10.4% | 11.7 | 15.1% | | |
| 2007 | 20.0 | 8.6% | 60.3 | 5.7% | 2.5 | 15.1% | | |
| 2008 | 30.6 | 9.8% | 19.8 | 6.7% | | | | |
| 2009 | 55.4 | 10.8% | 31.4 | 17.4% | | | | |
| 2010 | 18.2 | 11.6% | 27.0 | 11.6% | 1.8 | | 0.2 | |
| 2011 | | | | | | | | |
| 2012 | 15.5 | 5.2% | 24.3 | 15.6% | | | | |
| 2013 | 63.0 | 17.3% | 13.3 | 5.1% | 2.1 | 11.6% | | |
| 2014 | 35.5 | 18.2% | 7.3 | 9.0% | | | | |
| 2015 | 61.3 | 17.1% | 17.9 | 10.0% | | | | |
| 2016 | 20.4 | 7.2% | 3.6 | 6.9% | 11.5 | 12.0% | 2.1 | 14.7% |
| 2017 | 29.8 | 9.8% | 0.8 | 19.6% | 3.9 | 6.5% | 2.1 | 9.5% |
| 2018 | 17.4 | 8.3% | 1.3 | 12.2% | 3.8 | 23.0% | 4.6 | 19.9% |
| 2019 | | | | | | | | |
| 2020 | 4.9 | 12.2% | | | | | | |

[1]Survey conducted after peak spawning had occurred.

[2]Partial survey.

Table 7. -- Trawl stations and catch data summary from the winter 2020 acoustic-trawl survey of walleye pollock in the Shelikof Strait.

| Haul | Area | Gear | Date | Time | Duration | Start Position | | Depth (m) | | Temp (°C) | | walleye pollock | | Other |
|---|---|---|---|---|---|---|---|---|---|---|---|---|---|---|
| No. | | Type[a] | (GMT) | (GMT) | (mins) | Lat. (N) | Long. (W) | Headrope[b] | Bottom | Headrope | Surface[c] | (kg) | Number | (kg) |
| 1 | Shelikof Strait | AWT | 6-Mar | 15:38 | 18.0 | 58.2278 | -153.2995 | 165 | 206 | 5.3 | 3.6 | 304.7 | 568 | 41.5 |
| 2 | Shelikof Strait | LFS1421 | 6-Mar | 19:24 | 20.0 | 58.2244 | -153.3142 | 181 | 212 | 5.5 | 2.8 | 286.8 | 502 | 29.0 |
| 3 | Shelikof Strait | AWT | 7-Mar | 01:30 | 5.1 | 58.1894 | -154.0671 | 194 | 277 | 5.4 | 2.8 | 333.4 | 527 | 119.6 |
| 4 | Shelikof Strait | LFS1421 | 7-Mar | 03:58 | 15.0 | 58.1911 | -154.0648 | 214 | 274 | 5.6 | 2.8 | 587.5 | 947 | 35.3 |
| 5 | Shelikof Strait | AWT | 7-Mar | 09:18 | 5.2 | 57.9424 | -153.7991 | 145 | 197 | 5.4 | 3.1 | 115.9 | 369 | 59.3 |
| 6 | Shelikof Strait | LFS1421 | 7-Mar | 12:03 | 7.1 | 57.9376 | -153.8079 | 151 | 198 | 5.5 | 3.3 | 106.8 | 393 | 56.0 |
| 7 | Shelikof Strait | LFS1421 | 7-Mar | 15:45 | 4.7 | 58.0950 | -154.1653 | 225 | 286 | 5.5 | 2.5 | 964.1 | 1,491 | 20.6 |
| 8 | Shelikof Strait | AWT | 7-Mar | 19:13 | 5.2 | 58.1018 | -154.1551 | 211 | 291 | 5.3 | 2.6 | 1,651.6 | 2,314 | 6.4 |
| 9 | Shelikof Strait | LFS1421 | 8-Mar | 00:46 | 9.0 | 57.8831 | -154.0084 | 160 | 204 | 5.5 | 3.3 | 341.4 | 1,160 | 260.6 |
| 10 | Shelikof Strait | AWT | 8-Mar | 03:14 | 9.7 | 57.8755 | -154.0050 | 159 | 211 | 5.5 | 3.3 | 421.4 | 1,652 | 937.4 |
| 11 | Shelikof Strait | AWT | 8-Mar | 07:50 | 5.3 | 57.9355 | -154.5470 | 175 | 266 | 5.3 | 2.2 | 509.6 | 699 | 37.1 |
| 12 | Shelikof Strait | LFS1421 | 8-Mar | 10:12 | 6.9 | 57.9309 | -154.5634 | 165 | 268 | 5.2 | 2.3 | 811.0 | 1,527 | 51.0 |
| 13 | Shelikof Strait | LFS1421 | 8-Mar | 16:12 | 16.6 | 57.7670 | -154.5338 | 184 | 213 | 5.7 | 3.1 | 591.2 | 2,076 | 324.2 |
| 14 | Shelikof Strait | LFS1421 | 8-Mar | 21:18 | 3.5 | 57.7876 | -154.9759 | 216 | 318 | 5.8 | 2.3 | 1,451.9 | 1,887 | 3.1 |
| 15 | Shelikof Strait | LFS1421 | 9-Mar | 01:23 | 4.0 | 57.6211 | -154.8637 | 73 | 227 | 3.5 | - | 1,120.4 | 5,145 | 0.0 |
| 16 | Shelikof Strait | LFS1421 | 9-Mar | 03:18 | 5.3 | 57.6098 | -154.8956 | 185 | 225 | 5.8 | 3.1 | 434.7 | 1,053 | 106.1 |
| 17 | Shelikof Strait | LFS1421 | 10-Mar | 16:42 | 8.1 | 58.0066 | -154.3525 | 223 | 268 | 5.5 | 0.9 | 683.2 | 999 | 41.0 |
| 18 | Shelikof Strait | AWT | 11-Mar | 05:36 | 2.2 | 57.9925 | -154.3648 | 223 | 279 | 5.6 | 1.4 | 949.0 | 1,526 | 18.2 |
| 19 | Shelikof Strait | LFS1421 | 11-Mar | 08:24 | 3.5 | 57.9903 | -154.3694 | 230 | 283 | 5.6 | 2.2 | 451.7 | 642 | 142.8 |
| 20 | Shelikof Strait | LFS1421 | 11-Mar | 11:11 | 14.0 | 57.9930 | -154.3636 | 222 | 278 | 5.4 | 2.5 | 829.8 | 1,600 | 45.2 |
| 21 | Shelikof Strait | AWT | 11-Mar | 13:59 | 10.2 | 57.9875 | -154.3757 | 228 | 288 | 5.6 | 2.2 | 288.5 | 1,153 | 18.1 |
| 22 | Shelikof Strait | AWT | 11-Mar | 19:38 | 11.1 | 57.9200 | -154.5307 | 220 | 274 | 5.8 | 1.8 | 582.5 | 3,791 | 129.0 |
| 23 | Shelikof Strait | LFS1421 | 11-Mar | 22:27 | 11.4 | 57.9209 | -154.5330 | 226 | 276 | 5.7 | 2.2 | 701.5 | 3,441 | 43.4 |
| 24 | Shelikof Strait | LFS1421 | 12-Mar | 00:31 | 10.0 | 57.9194 | -154.5693 | - | 276 | - | 2.5 | 1,205.3 | 4,829 | 49.7 |
| 25 | Shelikof Strait | AWT | 12-Mar | 03:21 | 9.1 | 57.9140 | -154.5870 | - | 273 | - | 2.3 | 1,182.4 | 4,005 | 31.6 |
| 26 | Shelikof Strait | LFS1421 | 12-Mar | 06:39 | 15.0 | 57.8620 | -154.8127 | - | 276 | - | 1.2 | 1,949.7 | 3,484 | 159.8 |
| 27 | Shelikof Strait | AWT | 12-Mar | 09:55 | 6.0 | 57.8701 | -154.8119 | 208 | 277 | 5.5 | 1.3 | 644.7 | 1,506 | 16.2 |
| 28 | Shelikof Strait | LFS1421 | 12-Mar | 16:49 | 15.2 | 57.4121 | -155.2074 | 211 | 243 | 5.4 | 2.8 | 981.3 | 1,686 | 210.5 |
| 29 | Shelikof Strait | LFS1421 | 13-Mar | 02:49 | 10.1 | 57.1953 | -155.4676 | 218 | 262 | 5.5 | 3.0 | 229.1 | 498 | 28.1 |
| 30 | Shelikof Strait | LFS1421 | 13-Mar | 09:37 | 5.0 | 57.1424 | -155.7204 | 234 | 278 | 5.4 | 3.1 | 1,160.6 | 1,526 | 12.5 |
| 31 | Shelikof Strait | LFS1421 | 13-Mar | 17:55 | 8.2 | 56.7847 | -155.3113 | 92 | 200 | 3.5 | 3.3 | 1,164.9 | 5,917 | 0.1 |
| 32 | Shelikof Strait | LFS1421 | 13-Mar | 22:06 | 3.6 | 56.9057 | -155.9049 | 231 | 293 | 5.5 | 3.1 | 769.8 | 1,096 | 9.0 |
| 33 | Shelikof Strait | LFS1421 | 14-Mar | 07:57 | 8.6 | 56.6467 | -155.9382 | 224 | 282 | 4.3 | 3.0 | 683.2 | 1,363 | 4.1 |

| Haul | Area | Gear | Date | Time | Duration | Start Position | | Depth (m) | | Temp (°C) | | walleye pollock | | Other |
|---|---|---|---|---|---|---|---|---|---|---|---|---|---|---|
| No. | | Type[a] | (GMT) | (GMT) | (mins) | Lat. (N) | Long. (W) | Headrope[b] | Bottom | Headrope | Surface[c] | (kg) | Number | (kg) |
| 34 | Shelikof Strait | LFS1421 | 14-Mar | 22:59 | 20.0 | 56.3241 | -156.3307 | 215 | 262 | 5.8 | 3.0 | 326.9 | 1,047 | 25.2 |

[a]AWT = Aleutian Wing Trawl, LFS1421 = LFS1421 midwater trawl

[b]Headrope depth obtained from SBE temperature logger. In hauls without SBE temperature logger records, footrope depth was obtained from scientist notes when possible. Missing data indicated with – means SBE failed during haul.

[c]Average temperature measured from an SBE temperature logger

Table 8. -- Catch by species and numbers of length and weight measurements taken from 11 AWT hauls during the 2020 acoustic-trawl survey of walleye pollock in Shelikof Strait.

| | | Catch | | | | Measurements | |
|---|---|---|---|---|---|---|---|
| Species name | Scientific name | Weight (kg) | % | Number | % | Length | Weight |
| walleye pollock | *Gadus chalcogrammus* | 6,983.7 | 83.2 | 18,110 | 25.5 | 3,105 | - |
| eulachon | *Thaleichthys pacificus* | 1,336.2 | 15.9 | 48,040 | 67.7 | 404 | 10 |
| northern smoothtongue | *Leuroglossus schmidti* | 28.6 | 0.3 | 2,440 | 3.4 | 102 | - |
| chinook salmon | *Oncorhynchus tshawytscha* | 24.8 | 0.3 | 22 | <0.1 | 19 | - |
| Pacific cod | *Gadus macrocephalus* | 4.8 | <0.1 | 2 | <0.1 | 2 | - |
| arrowtooth flounder | *Atheresthes stomias* | 4.0 | <0.1 | 14 | <0.1 | 4 | - |
| Pacific herring | *Clupea pallasii* | 2.7 | <0.1 | 34 | <0.1 | 24 | - |
| shrimp unid. | Malacostraca (class) | 1.8 | <0.1 | 665 | 0.9 | 35 | - |
| Stenobrachius sp. | *Stenobrachius sp.* | 1.8 | <0.1 | 373 | 0.5 | 72 | - |
| salmon unid. | Oncorhynchus (genus) | 1.6 | <0.1 | 6 | <0.1 | 6 | - |
| magistrate armhook squid | *Berryteuthis magister* | 1.6 | <0.1 | 3 | <0.1 | 2 | - |
| smelt unid. | Osmeridae (family) | 1.4 | <0.1 | 910 | 1.3 | 56 | - |
| Chrysaora melanaster | *Chrysaora melanaster* | 1.1 | <0.1 | 2 | <0.1 | - | - |
| Pacific ocean perch | *Sebastes alutus* | 0.8 | <0.1 | 1 | <0.1 | 1 | - |
| flathead sole | *Hippoglossoides elassodon* | 0.8 | <0.1 | 3 | <0.1 | 1 | - |
| jellyfish unid. | Scyphozoa (class) | 0.6 | <0.1 | 1 | <0.1 | - | - |
| squid unid. | Cephalopoda (class) | 0.5 | <0.1 | 34 | <0.1 | 3 | - |
| capelin | *Mallotus villosus* | 0.3 | <0.1 | 66 | <0.1 | 39 | - |
| fish larvae unid. | Actinopterygii (class) | 0.3 | <0.1 | 211 | 0.3 | 12 | - |
| sablefish | *Anoplopoma fimbria* | 0.2 | <0.1 | 1 | <0.1 | 1 | - |
| Phacellophora sp. | *Phacellophora sp.* | 0.2 | <0.1 | 2 | <0.1 | 1 | - |
| lanternfish unid. | Myctophidae (family) | <0.1 | <0.1 | 26 | <0.1 | - | - |
| Pacific glass shrimp | *Pasiphaea pacifica* | <0.1 | <0.1 | 7 | <0.1 | 3 | - |
| isopod unid. | Isopoda (order) | <0.1 | <0.1 | 8 | <0.1 | - | - |
| Alaskan pink shrimp | *Pandalus eous* | <0.1 | <0.1 | 4 | <0.1 | 2 | - |
| Pacific lamprey | *Lampetra tridentata* | <0.1 | <0.1 | 1 | <0.1 | 1 | - |
| Mysidae | *Mysidae* | <0.1 | <0.1 | <0.1 | <0.1 | - | - |
| crangonid shrimp unid. | Crangonidae (family) | <0.1 | <0.1 | 2 | <0.1 | 1 | - |
| Total | | 8,398.1 | | 70,988 | | 3,896 | 10 |

Table 9. -- Catch by species and numbers of length and weight measurements taken from 23 LFS1421 hauls during the 2020 acoustic-trawl survey of walleye pollock in Shelikof Strait.

| | | Catch | | | | Measurements | |
|---|---|---|---|---|---|---|---|
| Species name | Scientific name | Weight (kg) | % | Number | % | Length | Weight |
| walleye pollock | *Gadus chalcogrammus* | 17,832.8 | 91.5 | 44,309 | 38.0 | 7,255 | 1,196 |
| eulachon | *Thaleichthys pacificus* | 1,516.4 | 7.8 | 53,856 | 46.2 | 798 | 183 |
| northern smoothtongue | *Leuroglossus schmidti* | 53.1 | 0.3 | 6,957 | 6.0 | 402 | 149 |
| chinook salmon | *Oncorhynchus tshawytscha* | 30.1 | 0.2 | 28 | <0.1 | 28 | 24 |
| Stenobrachius sp. | *Stenobrachius sp.* | 9.0 | <0.1 | 1,661 | 1.4 | 189 | 82 |
| smooth lumpsucker | *Aptocyclus ventricosus* | 6.7 | <0.1 | 7 | <0.1 | 1 | 1 |
| Pacific glass shrimp | *Pasiphaea pacifica* | 6.0 | <0.1 | 2,873 | 2.5 | 114 | - |
| arrowtooth flounder | *Atheresthes stomias* | 4.7 | <0.1 | 24 | <0.1 | 23 | 11 |
| Pacific herring | *Clupea pallasii* | 4.3 | <0.1 | 111 | <0.1 | 51 | 47 |
| magistrate armhook squid | *Berryteuthis magister* | 4.1 | <0.1 | 9 | <0.1 | 9 | 3 |
| capelin | *Mallotus villosus* | 3.8 | <0.1 | 689 | 0.6 | 104 | 50 |
| smelt unid. | Osmeridae (family) | 3.7 | <0.1 | 2,810 | 2.4 | 143 | 1 |
| Chrysaora melanaster | *Chrysaora melanaster* | 3.3 | <0.1 | 7 | <0.1 | 7 | 5 |
| fish larvae unid. | Actinopterygii (class) | 2.9 | <0.1 | 1,811 | 1.6 | 88 | - |
| shrimp unid. | Malacostraca (class) | 2.2 | <0.1 | 548 | 0.5 | 11 | - |
| squid unid. | Cephalopoda (class) | 1.7 | <0.1 | 44 | <0.1 | 11 | 3 |
| flathead sole | *Hippoglossoides elassodon* | 1.5 | <0.1 | 5 | <0.1 | 5 | 3 |
| Alaskan pink shrimp | *Pandalus eous* | 1.2 | <0.1 | 596 | 0.5 | 67 | 1 |
| Aurelia sp. | *Aurelia sp.* | 1.0 | <0.1 | 2 | <0.1 | 2 | 2 |
| Pacific ocean perch | *Sebastes alutus* | 0.8 | <0.1 | 1 | <0.1 | 1 | 1 |
| sidestripe shrimp | *Pandalopsis dispar* | 0.4 | <0.1 | 72 | <0.1 | 16 | - |
| lanternfish unid. | Myctophidae (family) | 0.2 | <0.1 | 119 | 0.1 | 43 | 12 |
| Pacific lamprey | *Lampetra tridentata* | 0.1 | <0.1 | 4 | <0.1 | 4 | 1 |
| isopod unid. | Isopoda (order) | <0.1 | <0.1 | 55 | <0.1 | - | - |
| eelpout unid. | Zoarcidae (family) | <0.1 | <0.1 | 6 | <0.1 | 1 | 1 |
| Mysidae | *Mysidae* | <0.1 | <0.1 | 17 | <0.1 | - | - |
| jellyfish unid. | Scyphozoa (class) | <0.1 | <0.1 | 1 | <0.1 | - | - |
| crangonid shrimp unid. | Crangonidae (family) | <0.1 | <0.1 | 4 | <0.1 | 1 | - |
| euphausiid unid. | Euphausiacea (order) | <0.1 | <0.1 | 7 | <0.1 | - | - |
| prickleback unid. | Stichaeidae (family) | <0.1 | <0.1 | 6 | <0.1 | 1 | - |
| Total | | 19,490.2 | | 116,639 | | 9,375 | 1,776 |

Table 10. -- Numbers of walleye pollock measured and biological samples collected during the winter 2020 acoustic-trawl survey of Shelikof Strait.

| Haul no. | Region name | Catch lengths | Weights | Maturities | Otoliths | Ovary weights | Ovaries collected |
|---|---|---|---|---|---|---|---|
| 1 | Shelikof Strait | 297 | - | - | - | - | - |
| 2 | Shelikof Strait | 502 | 50 | 49 | 30 | 21 | 11 |
| 3 | Shelikof Strait | 299 | - | - | - | - | - |
| 4 | Shelikof Strait | 438 | 85 | 81 | 40 | 16 | 4 |
| 5 | Shelikof Strait | 199 | - | - | - | - | - |
| 6 | Shelikof Strait | 280 | 83 | 76 | 30 | 11 | 7 |
| 7 | Shelikof Strait | 461 | 50 | 47 | 30 | 15 | 8 |
| 8 | Shelikof Strait | 290 | - | - | - | - | - |
| 9 | Shelikof Strait | 276 | 61 | 59 | 36 | 14 | - |
| 10 | Shelikof Strait | 228 | - | - | - | - | - |
| 11 | Shelikof Strait | 207 | - | - | - | - | - |
| 12 | Shelikof Strait | 350 | 89 | 89 | 29 | 5 | 8 |
| 13 | Shelikof Strait | 388 | 81 | 78 | 30 | 15 | 10 |
| 14 | Shelikof Strait | 404 | 74 | 74 | 30 | 9 | 7 |
| 15 | Shelikof Strait | 249 | 41 | 41 | 25 | - | - |
| 16 | Shelikof Strait | 250 | 50 | 50 | 30 | - | - |
| 17 | Shelikof Strait | 365 | 70 | 69 | - | 7 | - |
| 18 | Shelikof Strait | 207 | - | - | - | - | - |
| 19 | Shelikof Strait | 194 | 24 | 24 | - | 11 | - |
| 20 | Shelikof Strait | 263 | - | - | - | - | - |
| 21 | Shelikof Strait | 311 | - | - | - | - | - |
| 22 | Shelikof Strait | 297 | - | - | - | - | - |
| 23 | Shelikof Strait | 247 | - | - | - | - | - |
| 24 | Shelikof Strait | 367 | - | - | - | - | - |
| 25 | Shelikof Strait | 487 | - | - | - | - | - |
| 26 | Shelikof Strait | 222 | 28 | 28 | - | 10 | - |
| 27 | Shelikof Strait | 283 | - | - | - | - | - |
| 28 | Shelikof Strait | 285 | 75 | 68 | 29 | 6 | 8 |
| 29 | Shelikof Strait | 280 | 44 | 43 | 35 | 5 | - |
| 30 | Shelikof Strait | 210 | 50 | 49 | 30 | 23 | 8 |
| 31 | Shelikof Strait | 370 | 86 | 86 | 31 | 23 | 2 |
| 32 | Shelikof Strait | 297 | 70 | 69 | 30 | 4 | 4 |
| 33 | Shelikof Strait | 301 | 29 | 29 | 29 | 18 | 1 |
| 34 | Shelikof Strait | 256 | 56 | 56 | 30 | 19 | 4 |
| Total | | 10,360 | 1,196 | 1,165 | 524 | 232 | 82 |

Table 11. -- Estimates of walleye pollock biomass (thousands of metric tons) and relative estimation error for the Shelikof Strait, Chirikof shelf break, and Marmot Bay regions. Estimates for 2008-2020 reflect selectivity corrections for escapement of juveniles. Blank values indicate no survey or estimation error was completed within a given region and year.

| Year | Shelikof Strait | | Chirikof Shelfbreak | | Marmot Region | |
|---|---|---|---|---|---|---|
| | Biomass | Est. error | Biomass | Est. error | Biomass | Est. error |
| 1981 | 2,785.7 | | | | | |
| 1982 | | | | | | |
| 1983 | 2,278.1 | | | | | |
| 1984 | 1,757.1 | | | | | |
| 1985 | 1,175.2 | | | | | |
| 1986 | 585.7 | | | | | |
| 1987 | | | | | | |
| 1988 | 301.7 | | | | | |
| 1989 | 290.5 | | | | 2.4 | |
| 1990 | 374.7 | | | | | |
| 1991 | 380.3 | | | | | |
| 1992 | 713.4 | 3.6% | | | | |
| 1993 | 435.8 | 4.6% | | | | |
| 1994 | 492.6 | 4.5% | | | | |
| 1995 | 763.6 | 4.5% | | | | |
| 1996 | 777.2 | 3.7% | | | | |
| 1997 | 583.0 | 3.7% | | | | |
| 1998 | 504.8 | 3.8% | | | | |
| 1999 | | | | | | |
| 2000 | 448.6 | 4.6% | | | | |
| 2001 | 432.7 | 4.5% | | | | |
| 2002 | 256.7 | 6.9% | 82.1 | 12.2% | | |
| 2003 | 317.3 | 5.2% | 31.0 | 20.7% | | |
| 2004 | 330.8 | 9.2% | 30.0 | 20.4% | | |
| 2005 | 356.1 | 4.1% | 77.0 | 20.7% | | |
| 2006 | 293.6 | 4.0% | 69.0 | 11.0% | | |
| 2007 | 180.9 | 5.8% | 37.0 | 6.7% | 3.6 | 5.0% |
| 2008 | 197.7 | 5.6% | 22.0 | 9.6% | | |
| 2009 | 257.2 | 5.9% | 0.4 | 32.3% | 19.9 | |
| 2010 | 421.4 | 2.6% | 9.4 | 15.0% | 5.6 | |
| 2011 | | | | | | |
| 2012 | 327.6 | 7.9% | 21.2 | 16.4% | | |
| 2013 | 796.4 | 5.3% | 63.2 | 31.4% | 19.9 | 4.1% |
| 2014 | 829.0 | 4.7% | | | 14.5 | 9.4% |
| 2015 | 859.0 | 4.3% | 11.7 | 14.2% | 22.5 | 3.1% |
| 2016 | 666.8 | 6.5% | | | 24.9 | 8.8%[1] |
| 2017 | 1,465.1 | 4.3% | 2.5 | 24.0% | 13.1 | 7.9% |
| 2018 | 1,321.2 | 3.9% | | | 13.5 | 7.5%[1] |
| 2019 | 1,281.1 | 6.6% | 9.9 | 17.7% | 6.3 | 7.9% |
| 2020 | 459.4 | 2.9% | | | | |

[1]During these years, outer Marmot was surveyed in a zig-zag pattern, rather than parallel transects. Inner Marmot was surveyed with parallel transects. Relative estimation error was determined by combining estimation of error for biomass within the inner bay (1-D) and outer bay (2-D).

Table 12. -- Numbers-at-length estimates (millions of fish) from acoustic-trawl surveys of walleye pollock in Shelikof Strait. Numbers from 2008-2020 reflect selectivity corrections for escapement of juveniles. Non-selectivity corrected estimates (prior to 2008) are presented in Appendix V.

| Length | 2008 | 2009 | 2010 | 2012 | 2013 | 2014 | 2015 | 2016 | 2017 | 2018 | 2019 | 2020 |
|---|---|---|---|---|---|---|---|---|---|---|---|---|
| 5 | 0 | 0 | 0 | 0 | 0 | 0 | 0 | 0 | 0 | 0 | 0 | 0 |
| 6 | 0 | 0 | 0 | 0 | 0 | 0 | 0 | 0 | 0 | 0 | 0 | 0 |
| 7 | 0 | 0 | 0 | 0 | 0 | 0 | 0 | 0 | 0 | 0 | 0 | 0 |
| 8 | 0 | 0 | 4.5 | 0 | 0 | 15.4 | <1 | 0 | 0 | 0 | 14.9 | 0 |
| 9 | 26.2 | 9.3 | 10.4 | <1 | 454.9 | 44.6 | 0 | 0 | 1.3 | 77.1 | 115.7 | 0 |
| 10 | 69.3 | 80.4 | 51.3 | 10.3 | 750.9 | 275.7 | 7.6 | 0 | 57.4 | 556.5 | 1799.9 | <1 |
| 11 | 304.7 | 239.8 | 70.8 | 36.4 | 3789.1 | 433.0 | 5.5 | 0 | 134.1 | 756.8 | 3103.3 | <1 |
| 12 | 570.8 | 310.0 | 75.9 | 71.8 | 3096.5 | 382.4 | 4.7 | 0 | 308.5 | 375.4 | 1906.8 | 2.8 |
| 13 | 461.6 | 128.6 | 43.5 | 78.1 | 834.6 | 190.2 | 4.5 | 0 | 185.9 | 40.7 | 341.1 | 4.7 |
| 14 | 262.2 | 42.8 | 11.4 | 35.8 | 255.7 | 44.4 | 2.6 | 0 | 40.2 | 9.4 | 78.6 | 5.2 |
| 15 | 72.4 | 2.1 | 1.6 | 12.6 | 70.9 | 10.7 | <1 | 0 | 16.8 | 2.4 | 0 | 2.0 |
| 16 | 9.2 | 1.2 | <1 | 3.3 | 22.1 | 5.0 | <1 | 0 | <1 | 1.2 | <1 | 1.2 |
| 17 | 1.8 | 0 | <1 | 0 | 6.9 | 40.5 | <1 | 0 | 0 | 0 | 5.8 | <1 |
| 18 | <1 | 5.2 | <1 | 0 | <1 | 104.7 | <1 | 0 | 0 | <1 | 37.4 | <1 |
| 19 | 4.4 | 6.6 | 9.2 | 9.4 | <1 | 461.0 | <1 | 0 | 0 | 3.6 | 172.2 | <1 |
| 20 | 3.6 | 70.7 | 15.4 | 54.4 | 1.4 | 995.0 | 1.6 | 0 | <1 | 5.6 | 432.7 | 9.2 |
| 21 | 18.0 | 165.6 | 34.4 | 151.3 | 3.0 | 942.7 | 8.6 | 0 | 0 | 16.3 | 437.5 | 19.8 |
| 22 | 34.6 | 322.4 | 62.4 | 189.6 | 9.1 | 501.0 | 16.2 | <1 | 0 | 26.3 | 291.5 | 24.0 |
| 23 | 76.8 | 275.2 | 86.1 | 195.8 | 8.1 | 308.6 | 14.8 | 0 | <1 | 27.9 | 166.1 | 17.0 |
| 24 | 108.2 | 173.4 | 49.5 | 132.7 | 11.8 | 115.5 | 18.3 | <1 | <1 | 23.2 | 76.1 | 11.7 |
| 25 | 69.9 | 75.0 | 26.7 | 65.8 | 15.3 | 46.3 | 15.5 | <1 | <1 | 19.0 | 40.5 | 19.0 |
| 26 | 32.7 | 18.7 | 16.3 | 33.2 | 21.4 | 16.1 | 33.8 | <1 | 0 | 7.8 | 14.8 | 23.3 |
| 27 | 27.7 | 9.2 | 7.8 | 10.8 | 9.3 | 4.2 | 86.0 | <1 | 0 | 7.9 | 4.2 | 44.4 |
| 28 | 18.0 | 12.5 | 9.2 | 6.3 | 9.4 | 3.7 | 172.0 | <1 | <1 | 4.1 | 6.2 | 53.4 |
| 29 | 12.4 | 5.0 | 28.6 | <1 | 7.5 | <1 | 274.3 | <1 | 0 | 0 | 16.0 | 77.4 |
| 30 | 9.6 | 6.2 | 56.6 | 4.4 | 22.2 | <1 | 296.4 | 1.9 | 0 | 1.2 | 19.9 | 53.3 |
| 31 | 25.1 | 8.5 | 91.5 | <1 | 33.9 | <1 | 244.2 | 3.2 | 0 | <1 | 24.5 | 43.5 |
| 32 | 35.2 | 12.2 | 109.6 | 4.8 | 39.3 | 2.0 | 193.6 | 10.7 | 0 | <1 | 31.8 | 23.1 |
| 33 | 39.1 | 23.7 | 91.4 | 3.2 | 66.6 | 3.6 | 128.9 | 22.0 | <1 | <1 | 17.9 | 16.7 |
| 34 | 29.1 | 23.0 | 66.8 | 3.0 | 74.9 | 2.3 | 68.3 | 50.7 | 1.1 | 0 | 14.1 | 16.8 |
| 35 | 28.9 | 19.1 | 32.2 | 4.3 | 112.3 | 3.0 | 50.0 | 91.1 | <1 | 0 | 6.7 | 9.5 |
| 36 | 15.3 | 16.2 | 25.8 | 4.4 | 102.8 | 3.8 | 26.6 | 139.3 | 4.8 | 0 | 2.1 | 14.2 |
| 37 | 17.2 | 8.4 | 14.0 | 2.9 | 103.1 | 5.1 | 19.3 | 209.6 | 9.0 | 1.2 | 5.1 | 10.2 |
| 38 | 6.7 | 11.5 | 10.6 | 2.5 | 56.5 | 7.6 | 13.4 | 274.3 | 56.3 | 1.8 | 2.1 | 5.6 |
| 39 | 3.0 | 15.2 | 7.7 | 2.2 | 39.8 | 13.2 | 10.9 | 271.5 | 130.6 | 10.2 | 1.6 | 4.4 |
| 40 | 7.6 | 9.3 | 8.5 | 4.0 | 21.5 | 24.4 | 8.0 | 204.9 | 352.4 | 45.3 | 1.5 | 3.3 |
| 41 | 6.7 | 13.4 | 8.5 | 5.5 | 13.7 | 37.5 | 5.0 | 138.2 | 530.2 | 101.3 | 5.0 | 2.3 |
| 42 | 3.9 | 15.6 | 9.8 | 9.0 | 10.3 | 51.8 | 5.8 | 76.3 | 578.5 | 202.3 | 34.3 | 7.8 |
| 43 | 3.6 | 14.2 | 10.2 | 15.8 | 8.2 | 55.8 | 9.5 | 40.2 | 544.0 | 305.4 | 102.9 | 15.1 |
| 44 | 2.9 | 13.9 | 10.9 | 13.6 | 9.9 | 52.1 | 13.0 | 22.2 | 326.5 | 371.2 | 177.4 | 34.3 |
| 45 | 3.9 | 11.6 | 14.1 | 17.6 | 4.4 | 37.2 | 20.2 | 13.0 | 169.8 | 351.5 | 245.3 | 67.1 |
| 46 | 2.4 | 8.6 | 13.2 | 20.0 | 5.7 | 25.2 | 30.6 | 10.1 | 80.9 | 258.9 | 244.9 | 78.3 |
| 47 | 1.3 | 5.3 | 11.2 | 20.0 | 8.7 | 14.8 | 33.1 | 7.0 | 46.4 | 191.2 | 221.6 | 74.7 |
| 48 | <1 | 4.5 | 11.3 | 22.0 | 12.3 | 13.0 | 38.8 | 7.4 | 24.0 | 117.6 | 169.1 | 62.0 |
| 49 | 1.2 | 2.6 | 10.5 | 19.6 | 14.2 | 11.6 | 33.8 | 8.8 | 8.9 | 62.6 | 122.9 | 40.9 |

| | | | | | | | | | | | | |
|---|---|---|---|---|---|---|---|---|---|---|---|---|
| 50 | <1 | 2.8 | 12.0 | 19.6 | 13.9 | 15.3 | 26.5 | 6.4 | 6.8 | 30.7 | 68.2 | 33.0 |
| 51 | <1 | 2.5 | 10.5 | 16.5 | 23.0 | 16.2 | 25.6 | 4.3 | 3.5 | 29.3 | 35.2 | 20.4 |
| 52 | 1.2 | 3.4 | 9.1 | 12.2 | 18.1 | 31.5 | 21.2 | 5.4 | 2.6 | 9.8 | 25.3 | 13.2 |
| 53 | 1.0 | 2.0 | 6.0 | 10.6 | 21.2 | 28.3 | 24.1 | 2.7 | <1 | 9.5 | 10.4 | 5.6 |
| 54 | 1.8 | 2.3 | 7.2 | 9.7 | 28.6 | 33.4 | 23.0 | 2.8 | 2.8 | 3.7 | 5.3 | 4.9 |
| 55 | 1.6 | 1.6 | 7.9 | 7.4 | 21.6 | 28.7 | 28.4 | 2.3 | 4.5 | 6.8 | 4.7 | 2.9 |
| 56 | 3.4 | 2.4 | 5.9 | 6.8 | 26.9 | 36.0 | 25.5 | 2.7 | 4.5 | 1.8 | <1 | 1.4 |
| 57 | <1 | 1.6 | 4.9 | 6.9 | 18.9 | 24.7 | 23.2 | 2.7 | <1 | <1 | <1 | <1 |
| 58 | 2.1 | 1.2 | 6.2 | 5.2 | 17.2 | 19.3 | 20.2 | 1.2 | 2.0 | 0 | <1 | <1 |
| 59 | 2.5 | 1.2 | 5.6 | 3.1 | 16.5 | 12.5 | 15.4 | <1 | <1 | 0 | <1 | <1 |
| 60 | 1.6 | 1.2 | 3.3 | 3.5 | 18.6 | 9.6 | 14.3 | 1.3 | <1 | <1 | <1 | <1 |
| 61 | 2.4 | 1.2 | 5.2 | 1.5 | 7.9 | 9.0 | 8.3 | <1 | <1 | 0 | <1 | <1 |
| 62 | 1.0 | 1.0 | 3.8 | <1 | 8.8 | 6.8 | 6.9 | <1 | <1 | <1 | 0 | <1 |
| 63 | 1.2 | <1 | 3.3 | 1.2 | 11.1 | 1.2 | 3.8 | <1 | <1 | 0 | 0 | <1 |
| 64 | 1.3 | <1 | 3.8 | <1 | 2.7 | 2.9 | 1.6 | 0 | 0 | 0 | 0 | 0 |
| 65 | <1 | <1 | 3.3 | <1 | 1.7 | 1.2 | 2.1 | 0 | 0 | 0 | 0 | 0 |
| 66 | <1 | <1 | 2.5 | <1 | 2.5 | 1.0 | <1 | 0 | 0 | 0 | 0 | 0 |
| 67 | <1 | <1 | 2.4 | <1 | <1 | <1 | <1 | 0 | 0 | 0 | 0 | 0 |
| 68 | <1 | <1 | 1.3 | <1 | <1 | <1 | <1 | 0 | 0 | 0 | 0 | 0 |
| 69 | <1 | <1 | <1 | 0 | 0 | 0 | <1 | 0 | 0 | 0 | 0 | 0 |
| 70 | 0 | <1 | <1 | <1 | <1 | <1 | 0 | 0 | 0 | 0 | 0 | 0 |
| 71 | 0 | <1 | <1 | 0 | <1 | 0 | 0 | 0 | 0 | 0 | 0 | 0 |
| 72 | 0 | 0 | <1 | 0 | 0 | 0 | 0 | 0 | 0 | 0 | 0 | 0 |
| 73 | 0 | 0 | 0 | 0 | <1 | 0 | 0 | 0 | 0 | 0 | 0 | 0 |
| 74 | 0 | 0 | 0 | 0 | <1 | <1 | 0 | 0 | 0 | 0 | 0 | 0 |
| 75 | 0 | 0 | 0 | 0 | 0 | 0 | 0 | 0 | 0 | 0 | 0 | 0 |
| 76 | 0 | <1 | 0 | 0 | 0 | 0 | 0 | 0 | 0 | 0 | 0 | 0 |
| Total | 2451.9 | 2225.5 | 1338.7 | 1385.4 | 10401.5 | 5584.3 | 2188.2 | 1636.9 | 3638.7 | 4076.3 | 10664.6 | 985.0 |

Table 13. -- Biomass-at-length estimates (thousands of metric tons) from acoustic-trawl surveys of walleye pollock in the Shelikof Strait area. Biomass from 2008-2020 reflects selectivity corrections for escapement of juveniles. Non-selectivity corrected estimates (prior to 2008) are presented in Appendix V.

| Length | 2008 | 2009 | 2010 | 2012 | 2013 | 2014 | 2015 | 2016 | 2017 | 2018 | 2019 | 2020 |
|---|---|---|---|---|---|---|---|---|---|---|---|---|
| 5 | 0 | 0 | 0 | 0 | 0 | 0 | 0 | 0 | 0 | 0 | 0 | 0 |
| 6 | 0 | 0 | 0 | 0 | 0 | 0 | 0 | 0 | 0 | 0 | 0 | 0 |
| 7 | 0 | 0 | 0 | 0 | 0 | 0 | 0 | 0 | 0 | 0 | 0 | 0 |
| 8 | 0 | 0 | <1 | 0 | 0 | <1 | <1 | 0 | 0 | 0 | <1 | 0 |
| 9 | <1 | <1 | <1 | <1 | 1.7 | <1 | 0 | 0 | <1 | <1 | <1 | 0 |
| 10 | <1 | <1 | <1 | <1 | 4.6 | 1.7 | <1 | 0 | <1 | 3.6 | 11.5 | <1 |
| 11 | 2.9 | 2.0 | <1 | <1 | 29.5 | 4.3 | <1 | 0 | 1.0 | 6.2 | 25.5 | <1 |
| 12 | 6.3 | 3.3 | <1 | <1 | 29.4 | 4.0 | <1 | 0 | 3.0 | 3.9 | 18.9 | <1 |
| 13 | 7.0 | 1.7 | <1 | 1.1 | 10.1 | 2.5 | <1 | 0 | 2.3 | <1 | 4.3 | <1 |
| 14 | 4.6 | <1 | <1 | <1 | 3.8 | <1 | <1 | 0 | <1 | <1 | 1.1 | <1 |
| 15 | 1.6 | <1 | <1 | <1 | 1.3 | <1 | <1 | 0 | <1 | <1 | 0 | <1 |
| 16 | <1 | <1 | <1 | <1 | <1 | <1 | <1 | 0 | <1 | <1 | <1 | <1 |
| 17 | <1 | 0 | <1 | 0 | <1 | 1.3 | <1 | 0 | 0 | 0 | <1 | <1 |
| 18 | <1 | <1 | <1 | 0 | <1 | 3.9 | <1 | 0 | 0 | <1 | 1.4 | <1 |
| 19 | <1 | <1 | <1 | <1 | <1 | 20.3 | <1 | 0 | 0 | <1 | 7.5 | <1 |
| 20 | <1 | 3.8 | <1 | 3.1 | <1 | 49.4 | <1 | 0 | <1 | <1 | 22.0 | <1 |
| 21 | 1.2 | 10.4 | 2.1 | 9.4 | <1 | 54.5 | <1 | 0 | 0 | 1.1 | 25.3 | 1.2 |
| 22 | 2.7 | 22.9 | 4.3 | 13.5 | <1 | 34.2 | 1.1 | <1 | 0 | 1.9 | 19.1 | 1.7 |
| 23 | 6.3 | 21.9 | 6.8 | 16.0 | <1 | 23.3 | 1.2 | 0 | <1 | 2.3 | 12.7 | 1.3 |
| 24 | 10.3 | 15.7 | 4.6 | 12.0 | 1.1 | 10.1 | 1.6 | <1 | <1 | 2.1 | 6.7 | 1.1 |
| 25 | 7.7 | 7.5 | 2.7 | 6.5 | 1.5 | 4.6 | 1.7 | <1 | <1 | 2.0 | 4.1 | 1.9 |
| 26 | 4.2 | 2.3 | 1.9 | 3.9 | 2.5 | 1.9 | 4.0 | <1 | 0 | <1 | 1.7 | 2.7 |
| 27 | 3.8 | 1.3 | 1.1 | 1.5 | 1.2 | <1 | 11.3 | <1 | 0 | 1.1 | <1 | 5.8 |
| 28 | 2.9 | 2.0 | 1.4 | <1 | 1.4 | <1 | 25.4 | <1 | <1 | <1 | <1 | 7.8 |
| 29 | 2.3 | <1 | 4.9 | <1 | 1.3 | <1 | 44.2 | <1 | 0 | 0 | 2.5 | 12.6 |
| 30 | 1.9 | 1.2 | 10.8 | <1 | 4.3 | <1 | 53.6 | <1 | 0 | <1 | 3.8 | 9.7 |
| 31 | 5.8 | 1.8 | 19.1 | <1 | 7.3 | <1 | 49.3 | <1 | 0 | <1 | 4.7 | 8.7 |
| 32 | 9.0 | 2.8 | 25.0 | 1.1 | 9.3 | <1 | 43.2 | 2.3 | 0 | <1 | 7.2 | 5.1 |
| 33 | 11.2 | 5.9 | 23.0 | <1 | 17.6 | <1 | 32.4 | 5.3 | <1 | <1 | 4.5 | 4.2 |
| 34 | 9.1 | 6.3 | 18.4 | <1 | 21.8 | <1 | 18.5 | 13.4 | <1 | 0 | 4.0 | 4.6 |
| 35 | 9.9 | 5.8 | 9.7 | 1.3 | 36.4 | <1 | 14.9 | 26.5 | <1 | 0 | 2.2 | 2.9 |
| 36 | 5.6 | 5.4 | 8.8 | 1.5 | 35.4 | 1.3 | 8.9 | 44.2 | 1.5 | 0 | <1 | 4.7 |
| 37 | 7.0 | 3.2 | 5.2 | 1.1 | 40.1 | 1.9 | 7.0 | 72.4 | 3.1 | <1 | 2.1 | 3.7 |
| 38 | 3.0 | 4.7 | 4.3 | <1 | 24.0 | 3.0 | 5.5 | 102.8 | 20.6 | <1 | <1 | 2.2 |
| 39 | 1.5 | 6.9 | 3.6 | <1 | 17.8 | 5.7 | 4.8 | 108.5 | 51.3 | 4.1 | <1 | 1.9 |
| 40 | 4.1 | 4.5 | 4.2 | 1.9 | 13.0 | 11.6 | 4.0 | 88.3 | 150.1 | 20.0 | <1 | 1.6 |
| 41 | 4.0 | 7.3 | 4.7 | 2.9 | 7.5 | 19.2 | 2.7 | 64.0 | 243.8 | 47.6 | 2.5 | 1.1 |
| 42 | 2.4 | 8.9 | 5.8 | 5.0 | 6.0 | 28.6 | 3.3 | 37.5 | 283.7 | 99.7 | 18.8 | 4.2 |
| 43 | 2.5 | 8.8 | 6.5 | 9.6 | 5.1 | 33.0 | 5.7 | 21.6 | 280.7 | 164.4 | 59.6 | 8.9 |
| 44 | 2.1 | 9.6 | 7.5 | 8.7 | 6.7 | 33.3 | 8.4 | 12.7 | 181.0 | 215.3 | 108.3 | 21.8 |
| 45 | 3.0 | 8.6 | 10.8 | 12.4 | 3.2 | 25.6 | 14.5 | 7.8 | 100.0 | 214.3 | 159.7 | 44.8 |
| 46 | 2.1 | 6.7 | 10.9 | 15.1 | 4.5 | 18.4 | 23.6 | 6.5 | 52.3 | 168.7 | 170.0 | 54.3 |
| 47 | 1.2 | 4.6 | 9.7 | 16.0 | 7.4 | 11.6 | 27.2 | 4.7 | 32.2 | 132.0 | 165.7 | 58.4 |
| 48 | <1 | 4.2 | 10.5 | 18.4 | 11.1 | 11.0 | 33.9 | 5.6 | 18.0 | 89.1 | 136.1 | 51.8 |
| 49 | 1.2 | 2.7 | 10.7 | 18.5 | 13.8 | 10.5 | 31.6 | 7.2 | 7.7 | 49.8 | 108.4 | 37.5 |

| | | | | | | | | | | | | |
|---|---|---|---|---|---|---|---|---|---|---|---|---|
| 50 | <1 | 3.1 | 12.7 | 20.0 | 15.1 | 14.8 | 27.0 | 5.4 | 6.2 | 24.8 | 63.8 | 31.2 |
| 51 | <1 | 2.8 | 12.2 | 17.8 | 25.8 | 17.4 | 27.4 | 3.7 | 3.1 | 28.4 | 35.7 | 21.4 |
| 52 | 1.5 | 4.5 | 11.3 | 14.1 | 22.1 | 36.6 | 23.9 | 5.1 | 2.6 | 9.4 | 25.9 | 14.3 |
| 53 | 1.4 | 3.0 | 8.0 | 12.5 | 27.7 | 35.9 | 29.3 | 2.8 | <1 | 9.7 | 12.3 | 6.9 |
| 54 | 2.5 | 3.5 | 9.9 | 12.2 | 39.7 | 42.9 | 29.5 | 3.0 | 3.0 | 4.0 | 6.2 | 6.2 |
| 55 | 2.6 | 2.6 | 11.7 | 10.2 | 30.0 | 39.5 | 37.6 | 2.5 | 5.2 | 7.7 | 6.3 | 4.2 |
| 56 | 5.5 | 4.0 | 9.3 | 10.1 | 41.2 | 52.3 | 36.6 | 2.9 | 5.4 | 2.2 | <1 | 2.0 |
| 57 | 1.7 | 2.8 | 8.6 | 10.1 | 30.2 | 38.0 | 34.6 | 3.0 | <1 | <1 | 1.3 | 1.1 |
| 58 | 3.8 | 2.3 | 11.0 | 9.1 | 29.8 | 31.2 | 32.3 | 1.5 | 2.7 | 0 | <1 | <1 |
| 59 | 4.6 | 2.5 | 10.3 | 5.4 | 29.5 | 20.6 | 25.2 | 1.1 | 1.1 | 0 | <1 | <1 |
| 60 | 3.2 | 2.7 | 6.4 | 6.3 | 35.7 | 18.4 | 25.0 | 1.6 | <1 | <1 | <1 | <1 |
| 61 | 5.1 | 2.5 | 10.5 | 2.8 | 15.8 | 16.2 | 15.4 | <1 | <1 | 0 | <1 | 1.4 |
| 62 | 2.4 | 2.3 | 7.9 | 1.6 | 18.6 | 13.6 | 13.2 | 1.0 | <1 | <1 | 0 | <1 |
| 63 | 2.8 | 2.1 | 7.4 | 2.5 | 24.6 | 2.5 | 7.2 | <1 | <1 | 0 | 0 | <1 |
| 64 | 3.2 | 1.6 | 8.8 | 2.0 | 6.4 | 6.2 | 3.4 | 0 | 0 | 0 | 0 | 0 |
| 65 | 1.2 | <1 | 8.4 | 1.3 | 4.2 | 2.8 | 4.7 | 0 | 0 | 0 | 0 | 0 |
| 66 | 1.7 | 2.4 | 6.4 | <1 | 6.5 | 2.4 | 1.9 | 0 | 0 | 0 | 0 | 0 |
| 67 | 1.2 | 1.3 | 6.7 | <1 | <1 | <1 | <1 | 0 | 0 | 0 | 0 | 0 |
| 68 | <1 | 1.2 | 3.7 | <1 | 1.5 | <1 | <1 | 0 | 0 | 0 | 0 | 0 |
| 69 | <1 | <1 | 1.5 | 0 | 0 | 0 | <1 | 0 | 0 | 0 | 0 | 0 |
| 70 | 0 | <1 | 2.9 | <1 | 1.7 | <1 | 0 | 0 | 0 | 0 | 0 | 0 |
| 71 | 0 | <1 | 1.8 | 0 | 3.1 | 0 | 0 | 0 | 0 | 0 | 0 | 0 |
| 72 | 0 | 0 | 1.6 | 0 | 0 | 0 | 0 | 0 | 0 | 0 | 0 | 0 |
| 73 | 0 | 0 | 0 | 0 | 1.3 | 0 | 0 | 0 | 0 | 0 | 0 | 0 |
| 74 | 0 | 0 | 0 | 0 | <1 | <1 | 0 | 0 | 0 | 0 | 0 | 0 |
| 75 | 0 | 0 | 0 | 0 | 0 | 0 | 0 | 0 | 0 | 0 | 0 | 0 |
| 76 | 0 | <1 | 0 | 0 | 0 | 0 | 0 | 0 | 0 | 0 | 0 | 0 |
| Total | 197.7 | 257.2 | 421.4 | 327.6 | 796.4 | 829.0 | 859.0 | 666.8 | 1465.1 | 1321.2 | 1281.1 | 459.4 |

Table 14. -- Numbers-at-age estimates (millions of fish) from acoustic-trawl surveys of walleye pollock in the Shelikof Strait area. Numbers from 2008-2020 reflect selectivity corrections for escapement of juveniles. Non-selectivity corrected estimates (prior to 2008) are presented in Appendix V.

| Age | 2008 | 2009 | 2010 | 2012 | 2013 | 2014 | 2015 | 2016 | 2017 | 2018 | 2019 | 2020 |
|---|---|---|---|---|---|---|---|---|---|---|---|---|
| 1 | 1778.2 | 814.1 | 270.5 | 248.3 | 9282.1 | 1397.8 | 25.6 | 0 | 745.0 | 1819.4 | 7361.3 | 17.6 |
| 2 | 359.2 | 1127.2 | 299.1 | 848.7 | 116.7 | 3544.0 | 97.7 | 1.9 | 0 | 142.6 | 1671.7 | 81.4 |
| 3 | 230.2 | 105.8 | 538.7 | 28.5 | 659.3 | 15.8 | 1565.2 | 78.2 | 9.2 | 1.6 | 155.5 | 345.3 |
| 4 | 49.0 | 95.8 | 82.9 | 79.8 | 50.0 | 269.5 | 71.4 | 1451.8 | 126.4 | 9.9 | 6.1 | 72.2 |
| 5 | 11.2 | 57.8 | 76.3 | 107.1 | 62.6 | 81.2 | 172.4 | 43.4 | 2576.4 | 165.9 | 6.6 | 15.5 |
| 6 | 2.0 | 9.5 | 27.7 | 42.1 | 102.5 | 61.0 | 71.6 | 33.5 | 126.0 | 1804.6 | 261.7 | 27.0 |
| 7 | 3.7 | 2.7 | 11.2 | 25.0 | 58.0 | 106.6 | 60.7 | 15.5 | 32.0 | 85.7 | 1127.5 | 68.5 |
| 8 | 9.8 | <1 | 5.1 | 3.7 | 42.7 | 54.6 | 70.9 | 3.6 | 8.9 | 46.7 | 53.9 | 192.8 |
| 9 | 6.2 | 4.7 | 5.0 | <1 | 10.4 | 26.0 | 30.2 | 7.4 | <1 | 0 | 11.1 | 116.8 |
| 10 | 1.9 | 5.6 | 10.3 | <1 | 4.8 | 16.7 | 10.5 | 1.7 | <1 | 0 | 9.0 | 37.2 |
| 11 | <1 | 1.3 | 8.8 | <1 | 4.6 | 7.7 | 5.4 | 0 | 0 | 0 | <1 | 8.0 |
| 12 | 0 | <1 | 3.2 | <1 | <1 | <1 | 3.4 | 0 | 0 | 0 | <1 | 2.7 |
| 13 | 0 | 0 | 0 | 0 | 1.4 | 2.1 | <1 | 0 | 0 | 0 | 0 | 0 |
| 14 | 0 | 0 | 0 | 0 | 4.0 | 0 | <1 | 0 | 0 | 0 | 0 | 0 |
| 15 | 0 | 0 | 0 | 0 | 2.0 | <1 | 1.3 | 0 | 0 | 0 | 0 | 0 |
| 16 | 0 | 0 | 0 | 0 | 0 | 0 | <1 | 0 | 0 | 0 | 0 | 0 |
| 17 | 0 | 0 | 0 | 0 | 0 | 0 | 0 | 0 | 0 | 0 | 0 | 0 |
| 18 | 0 | 0 | 0 | 0 | 0 | 0 | 0 | 0 | 0 | 0 | 0 | 0 |
| Total | 2451.9 | 2225.5 | 1338.7 | 1384.6 | 10401.5 | 5584.3 | 2188.2 | 1636.9 | 3624.5 | 4076.3 | 10664.6 | 985.0 |

Table 15. -- Biomass-at-age estimates (thousands of metric tons) from acoustic-trawl surveys of walleye pollock in the Shelikof Strait area. Numbers from 2008-2020 reflect selectivity corrections for escapement of juveniles. Non-selectivity corrected estimates (prior to 2008) are presented in Appendix V.

| Age | 2008 | 2009 | 2010 | 2012 | 2013 | 2014 | 2015 | 2016 | 2017 | 2018 | 2019 | 2020 |
|---|---|---|---|---|---|---|---|---|---|---|---|---|
| 1 | 23.2 | 8.4 | 2.4 | 3.0 | 81.3 | 14.2 | <1 | 0 | 7.7 | 14.8 | 61.9 | <1 |
| 2 | 35.4 | 88.1 | 23.6 | 67.3 | 14.9 | 204.3 | 9.3 | <1 | 0 | 12.6 | 102.1 | 5.9 |
| 3 | 61.5 | 27.7 | 129.0 | 7.9 | 229.0 | 4.8 | 310.4 | 23.6 | 3.3 | <1 | 34.3 | 59.3 |
| 4 | 23.7 | 49.8 | 55.4 | 53.5 | 31.6 | 161.4 | 40.4 | 565.8 | 57.2 | 5.1 | 3.0 | 22.4 |
| 5 | 8.9 | 42.3 | 83.2 | 98.6 | 72.6 | 58.5 | 152.6 | 24.2 | 1287.5 | 89.4 | 4.2 | 7.5 |
| 6 | 2.8 | 10.1 | 35.5 | 53.5 | 140.7 | 78.3 | 75.2 | 25.2 | 70.4 | 1099.2 | 183.5 | 19.2 |
| 7 | 7.1 | 4.5 | 20.5 | 35.6 | 92.8 | 141.5 | 84.4 | 13.3 | 29.7 | 58.1 | 830.3 | 55.4 |
| 8 | 18.5 | 1.7 | 10.6 | 5.5 | 75.5 | 81.2 | 103.9 | 4.1 | 8.4 | 41.7 | 42.5 | 155.4 |
| 9 | 11.7 | 10.0 | 11.5 | 1.5 | 19.2 | 39.9 | 46.6 | 8.3 | <1 | 0 | 9.7 | 93.5 |
| 10 | 3.9 | 11.7 | 20.9 | <1 | 10.3 | 26.2 | 16.4 | 2.0 | <1 | 0 | 9.3 | 29.9 |
| 11 | <1 | 2.7 | 20.4 | <1 | 9.9 | 11.7 | 8.3 | 0 | 0 | 0 | <1 | 6.5 |
| 12 | 0 | <1 | 8.2 | <1 | 1.5 | 1.5 | 5.9 | 0 | 0 | 0 | <1 | 4.3 |
| 13 | 0 | 0 | 0 | 0 | 3.4 | 4.1 | 1.5 | 0 | 0 | 0 | 0 | 0 |
| 14 | 0 | 0 | 0 | 0 | 8.7 | 0 | <1 | 0 | 0 | 0 | 0 | 0 |
| 15 | 0 | 0 | 0 | 0 | 5.0 | 1.4 | 1.8 | 0 | 0 | 0 | 0 | 0 |
| 16 | 0 | 0 | 0 | 0 | 0 | 0 | 1.5 | 0 | 0 | 0 | 0 | 0 |
| 17 | 0 | 0 | 0 | 0 | 0 | 0 | 0 | 0 | 0 | 0 | 0 | 0 |
| 18 | 0 | 0 | 0 | 0 | 0 | 0 | 0 | 0 | 0 | 0 | 0 | 0 |
| Total | 197.7 | 257.2 | 421.4 | 327.6 | 796.4 | 829.0 | 859.0 | 666.8 | 1465.1 | 1321.2 | 1281.1 | 459.4 |

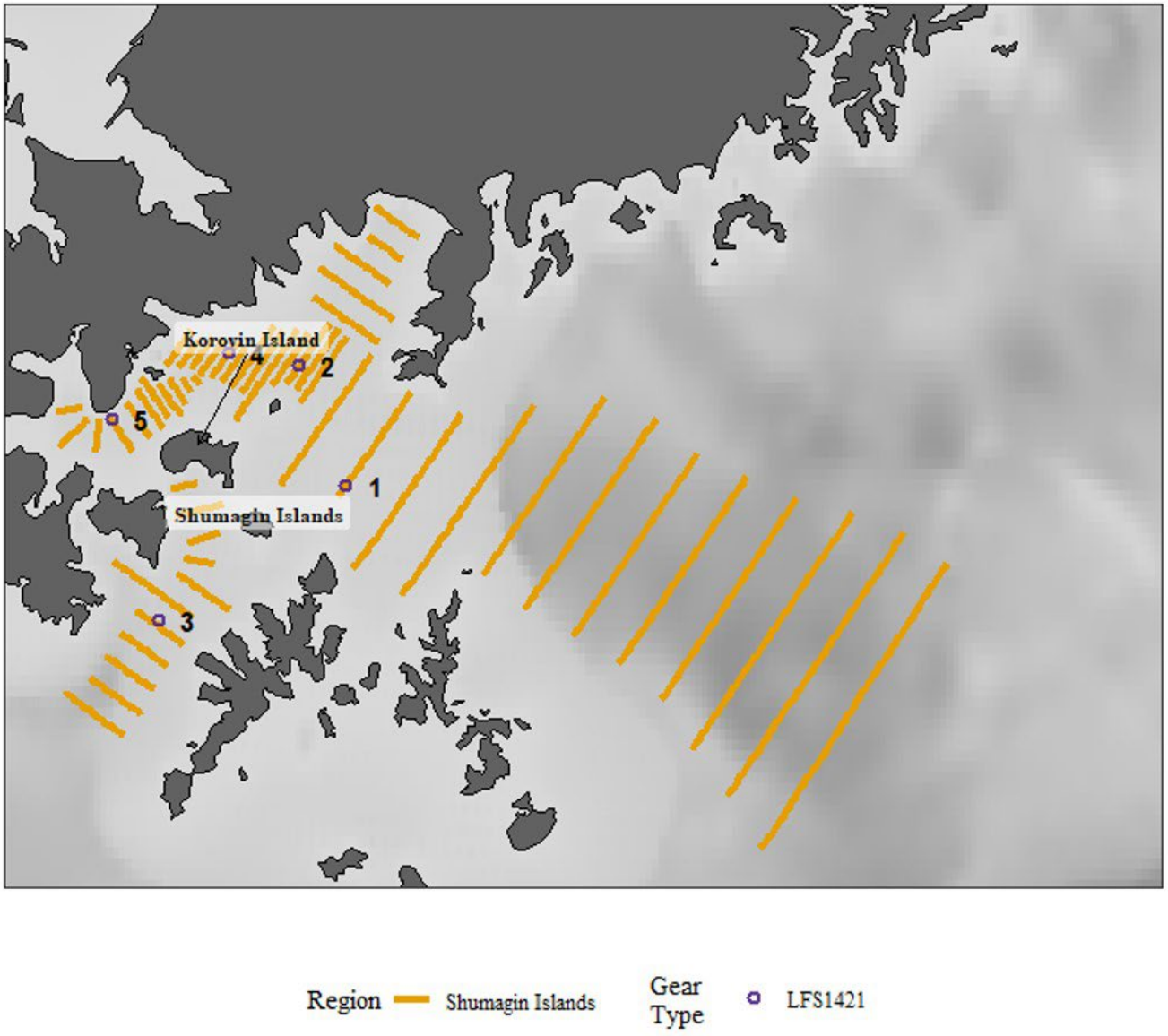


Figure 1. -- Transect lines and locations of trawl hauls during the winter 2020 acoustic-trawl survey of walleye pollock in the Shumagin Islands regions. Labels refer to areas referenced in text.

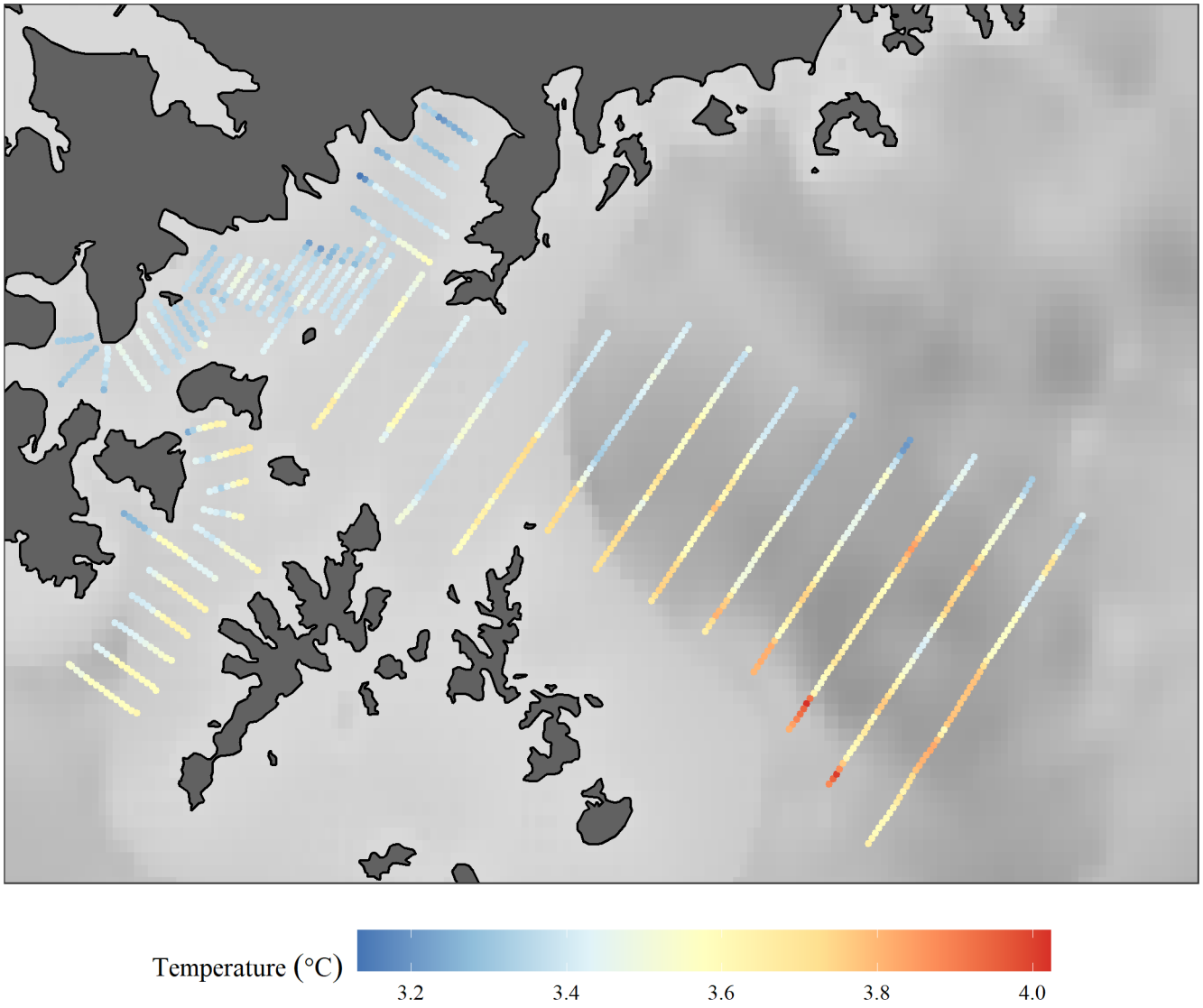


Figure 2. -- Surface water temperatures (°C) recorded at 5-second intervals during the winter 2020 acoustic-trawl survey of the Shumagin Islands regions.

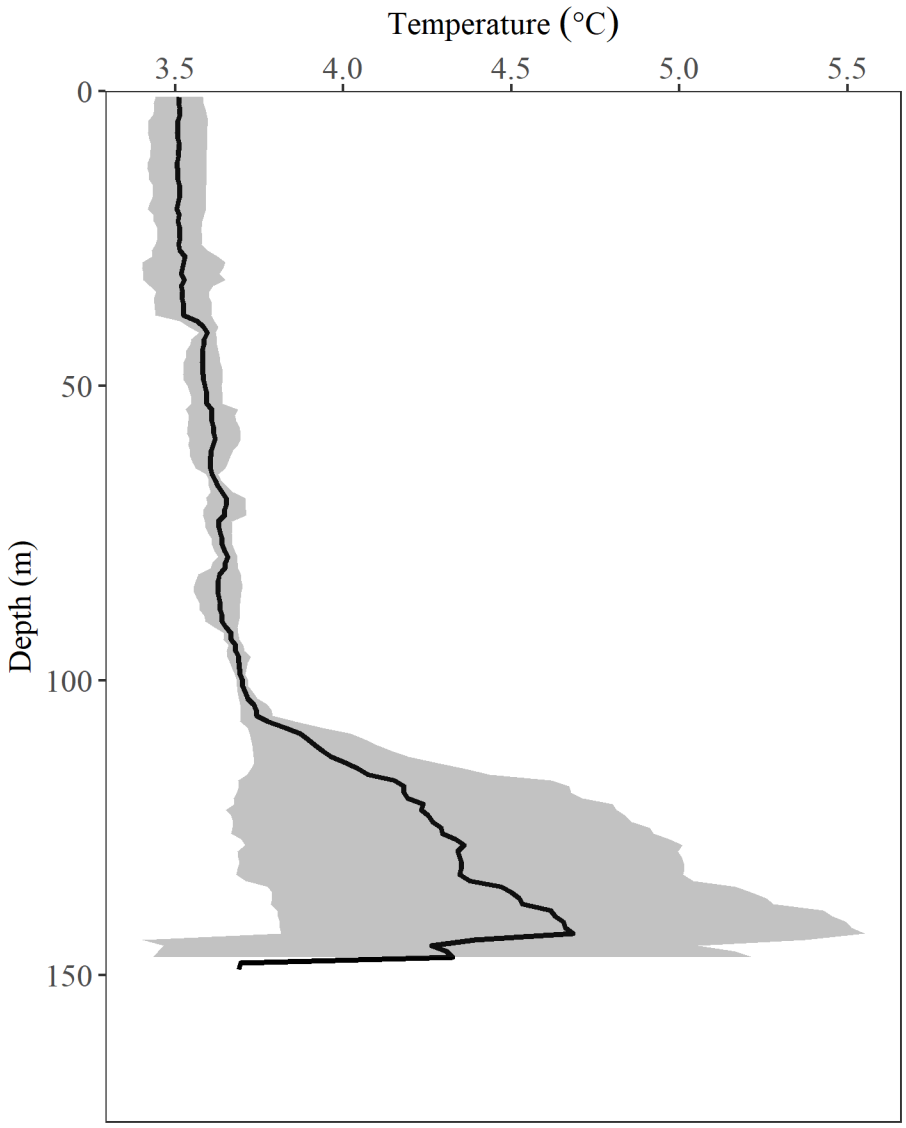


Figure 3. -- Mean water temperature (°C; solid line) by 1-m depth intervals measured at 4 trawl haul locations during the 2020 acoustic-trawl survey of walleye pollock in the Shumagin Islands area. The shaded area represents one standard deviation.

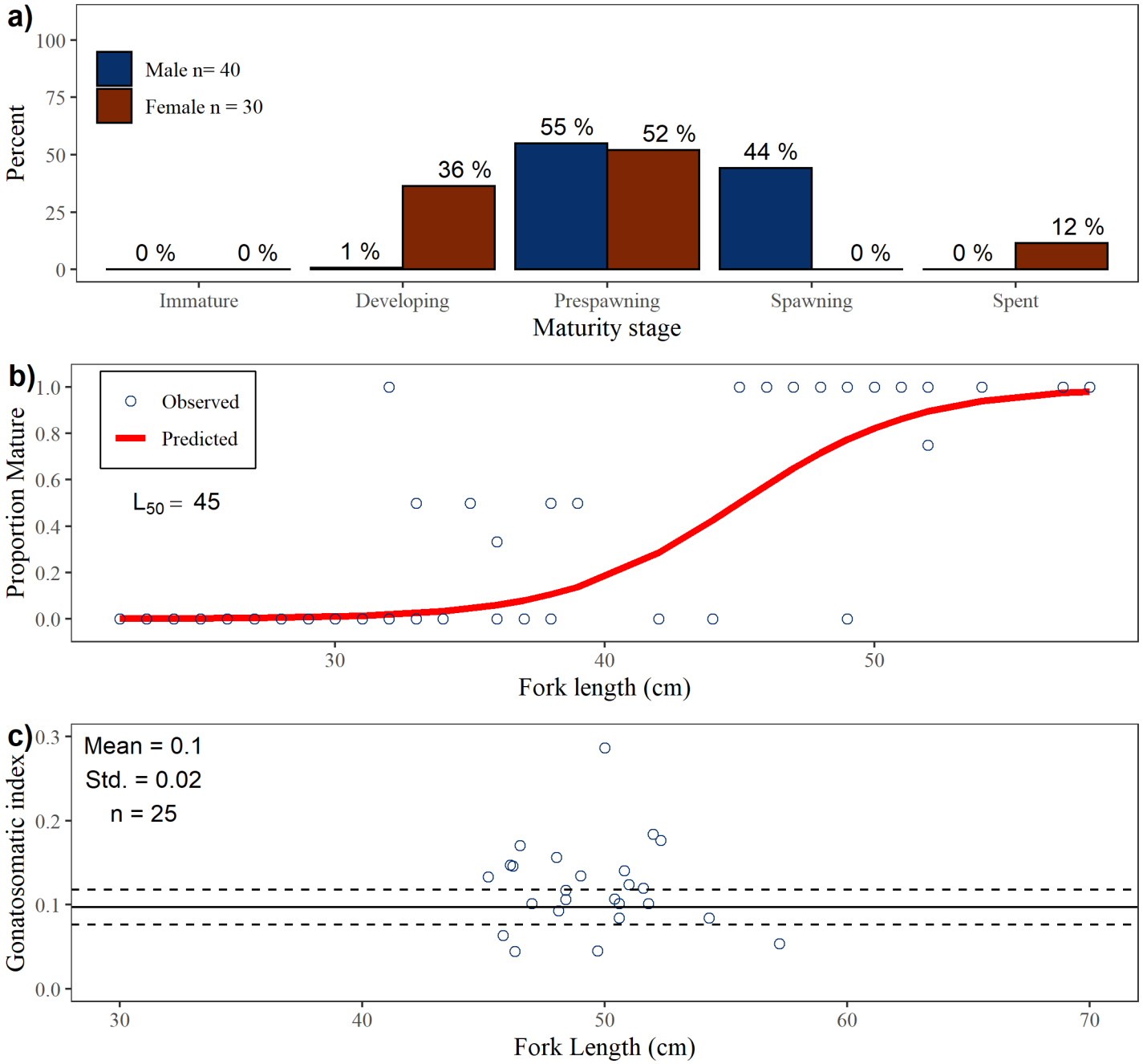


Figure 4. -- Walleye pollock maturity in the Shumagin Islands. a) Maturity composition for male and female walleye pollock greater than 40 cm FL within each stage; b) proportion mature (i.e. pre-spawning, spawning, or spent) by 1-cm size group for female walleye pollock; c) gonadosomatic index for females greater than 40 cm FL (with historic survey mean ± 1 std. dev.). All maturity quantities are weighted by local pollock abundance.

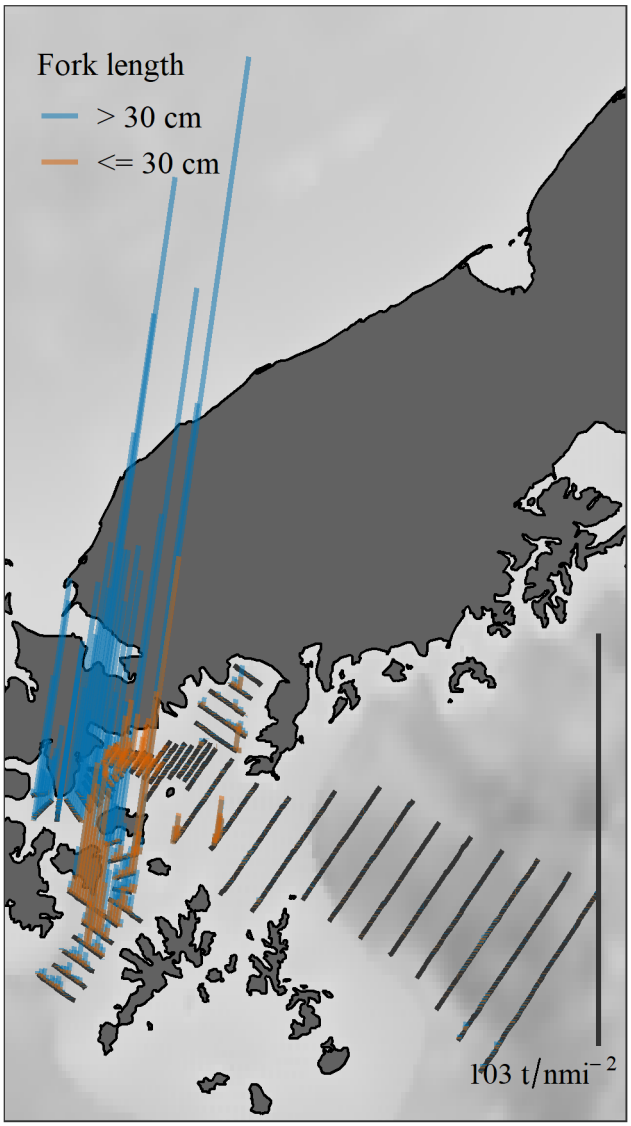


Figure 5. -- Biomass (t/nmi$^2$) attributed to walleye pollock (vertical lines) along tracklines surveyed during the winter 2020 acoustic-trawl survey of the Shumagin Islands regions. The tallest bar value is 206 t/nmi$^2$.

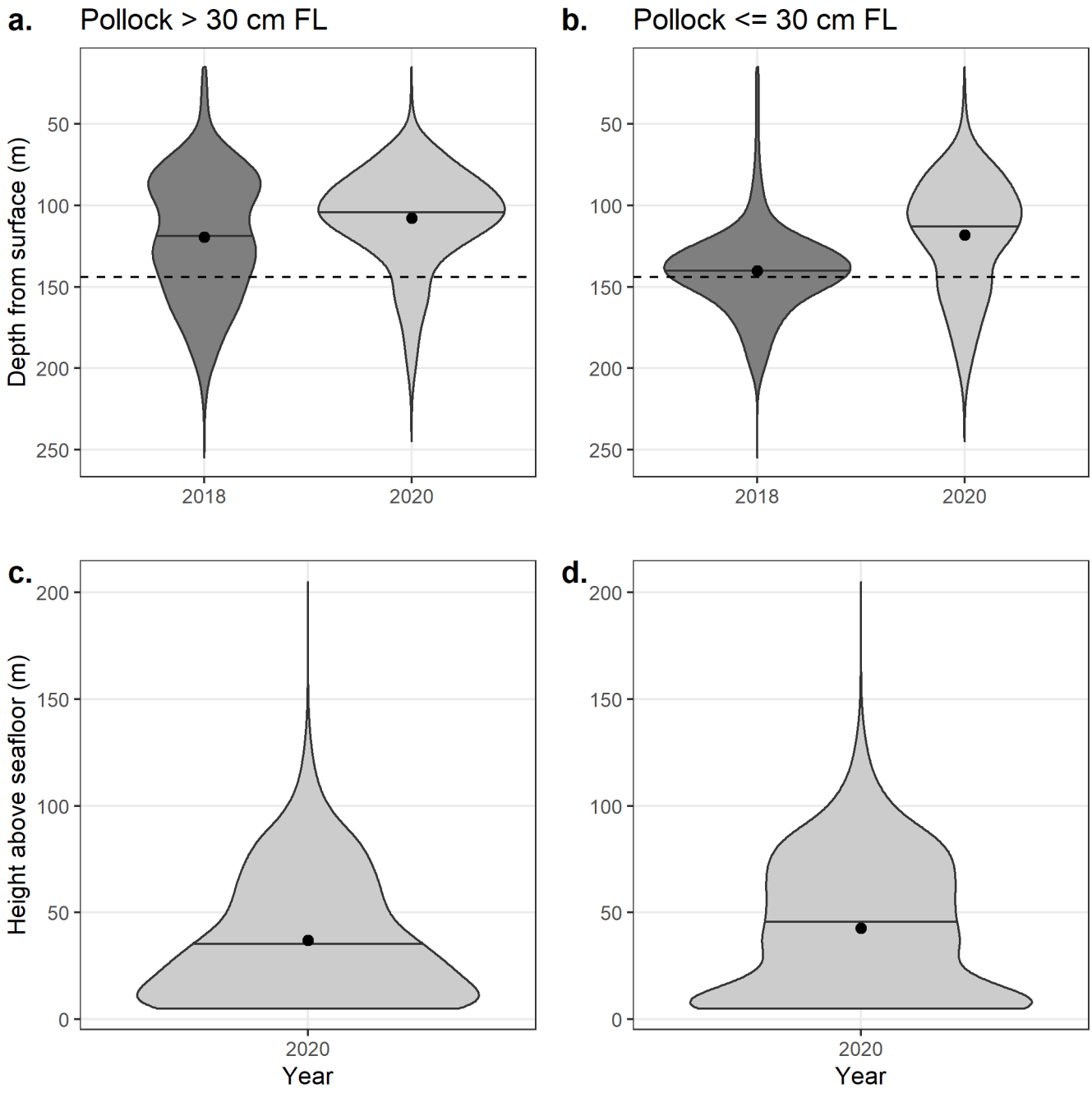


Figure 6. -- Estimated biomass distributions of adult pollock (> 30 cm FL) and juvenile pollock (≤ 30 cm FL) depth (a. and b.) and height (c. and d.) above the seafloor in the Shumagin Islands 2020 acoustic-trawl survey. Depth is referenced to the surface and height is referenced to the bottom. Data were averaged in 10 m depth bins. Mean bottom depth for 2020 is shown in a. and b. (dashed line). Plots show the probability density of pollock distribution, with median pollock depth noted by black horizontal lines, and the mean weighted pollock depth indicated by black points.

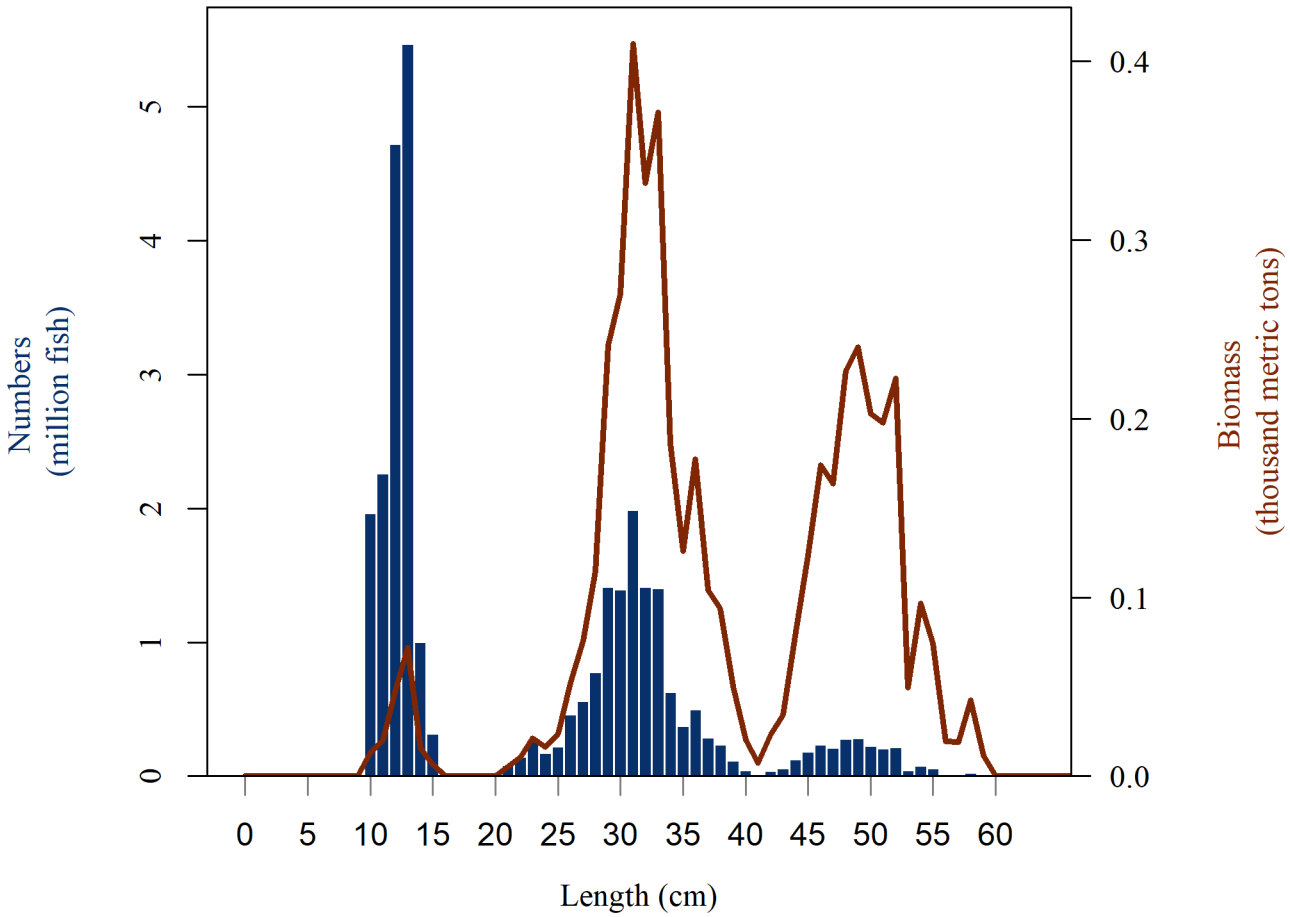


Figure 7. -- Length distribution of numbers of walleye pollock shown with blue bars (million fish) and biomass estimates in red line (thousand metric tons) for the 2020 acoustic-trawl survey of Shumagin Islands.

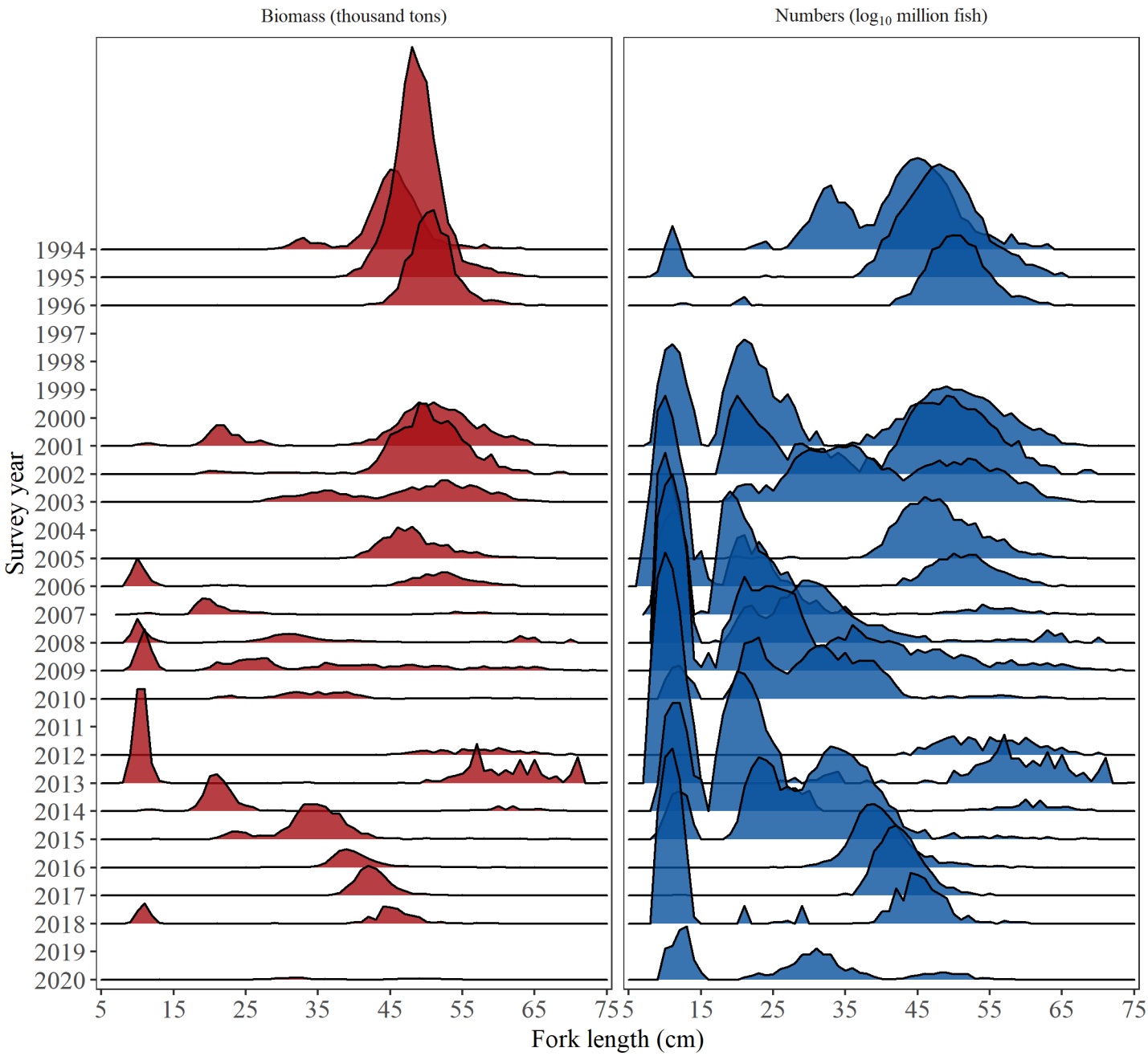


Figure 8. -- Time series of walleye pollock population size composition by weight (left panel, thousand metric tons) and numbers (right panel, $\log_{10}$(million fish)) from acoustic-trawl surveys of the Shumagin Islands area since 1994. Estimates for 2009-2020 include selectivity corrections for juvenile escapement (see text for explanation).

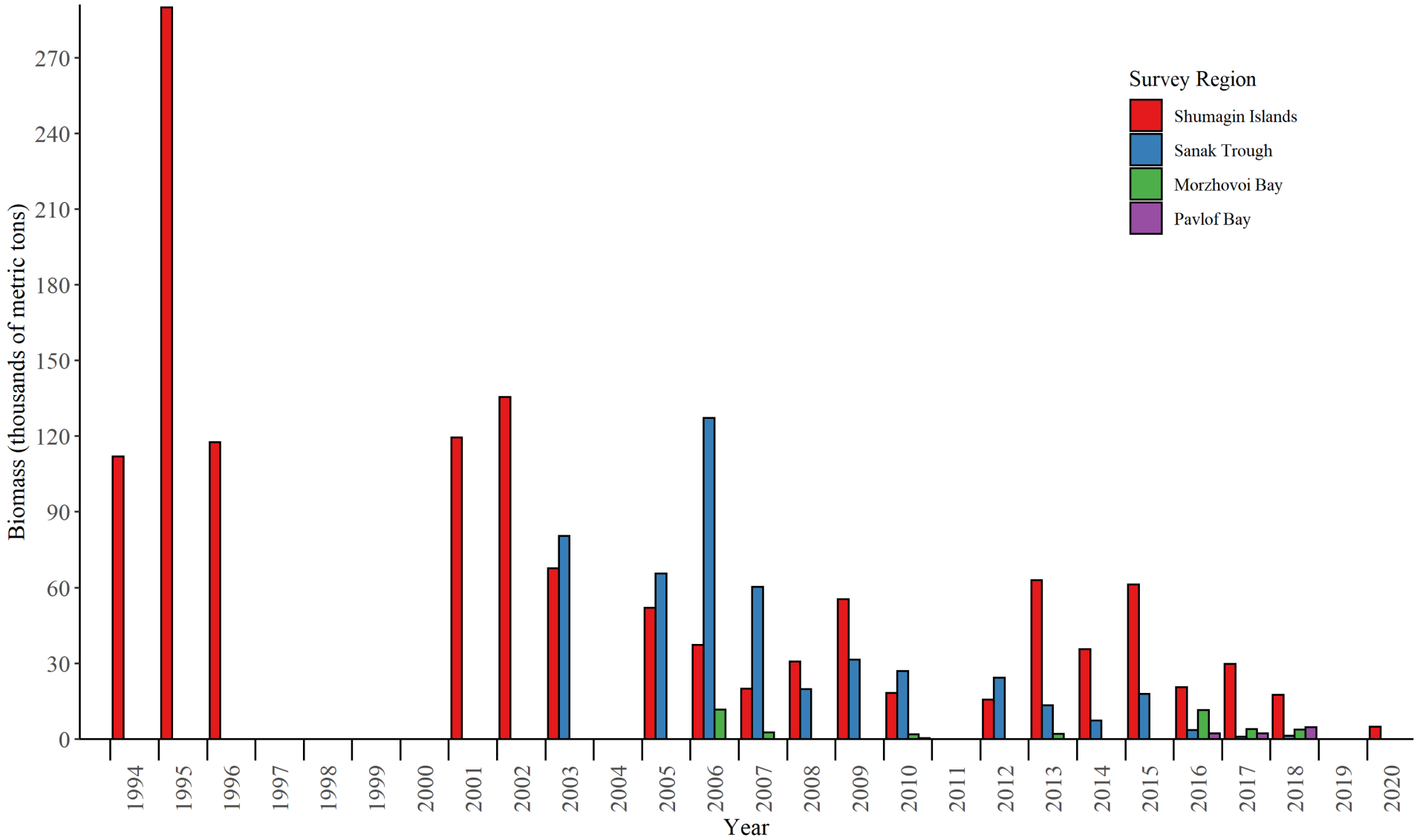


Figure 9. -- Summary of walleye pollock biomass estimates (thousands of metric tons) for the Shumagin Islands, Sanak Trough, Morzhovoi Bay, and Pavlof Bay areas based on acoustic-trawl surveys. Estimates for 2009-2020 include selectivity corrections for juvenile escapement (see text for explanation).

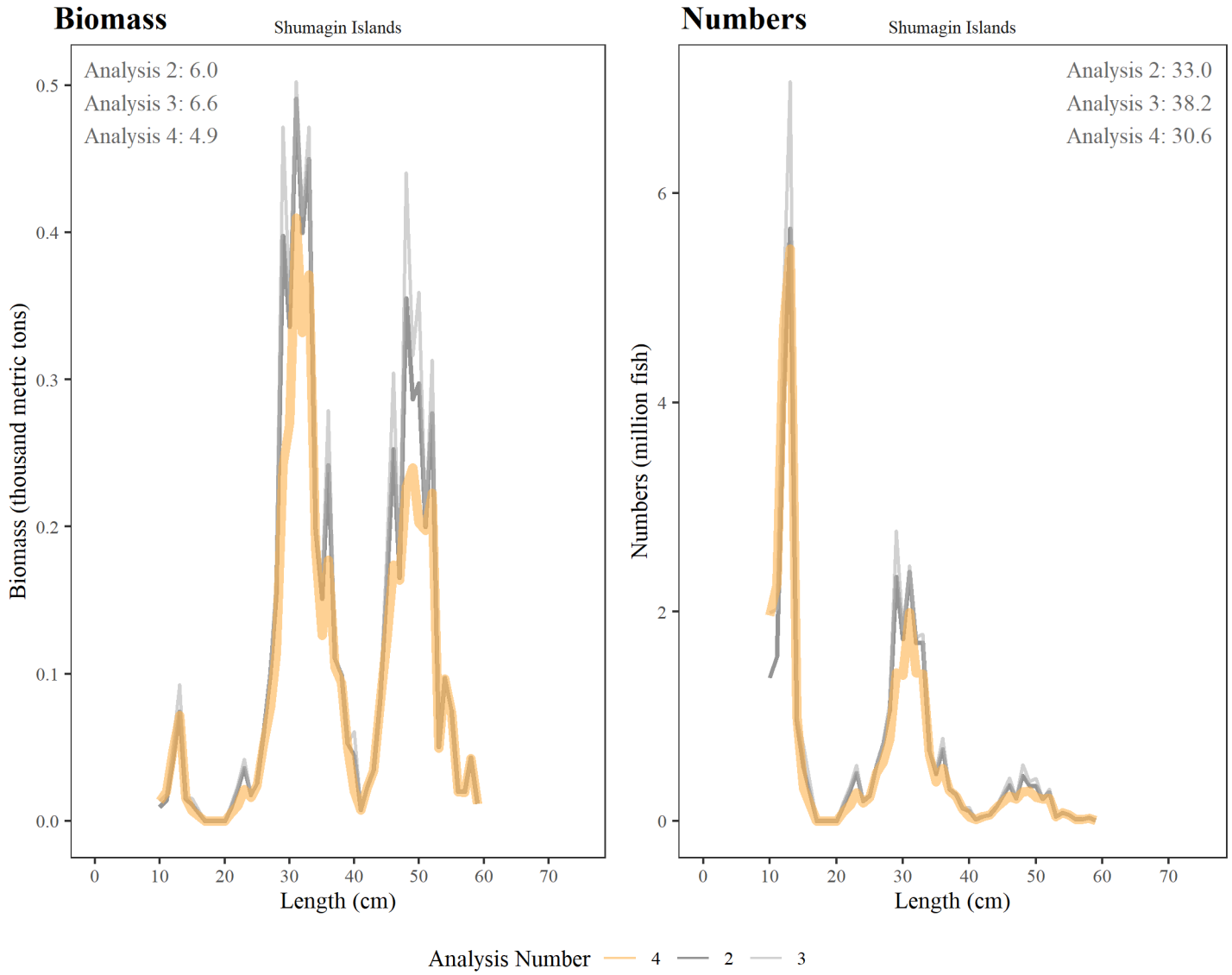


Figure 10. -- Numbers- and biomass- at length for the primary analysis (orange, Analysis 4) compared with alternate analyses (Analysis 2, Analysis 3, see text for explanation) for the 2020 Shumagins survey. The total numbers (million fish) and biomass (thousand metric tons) are also presented for each analysis.

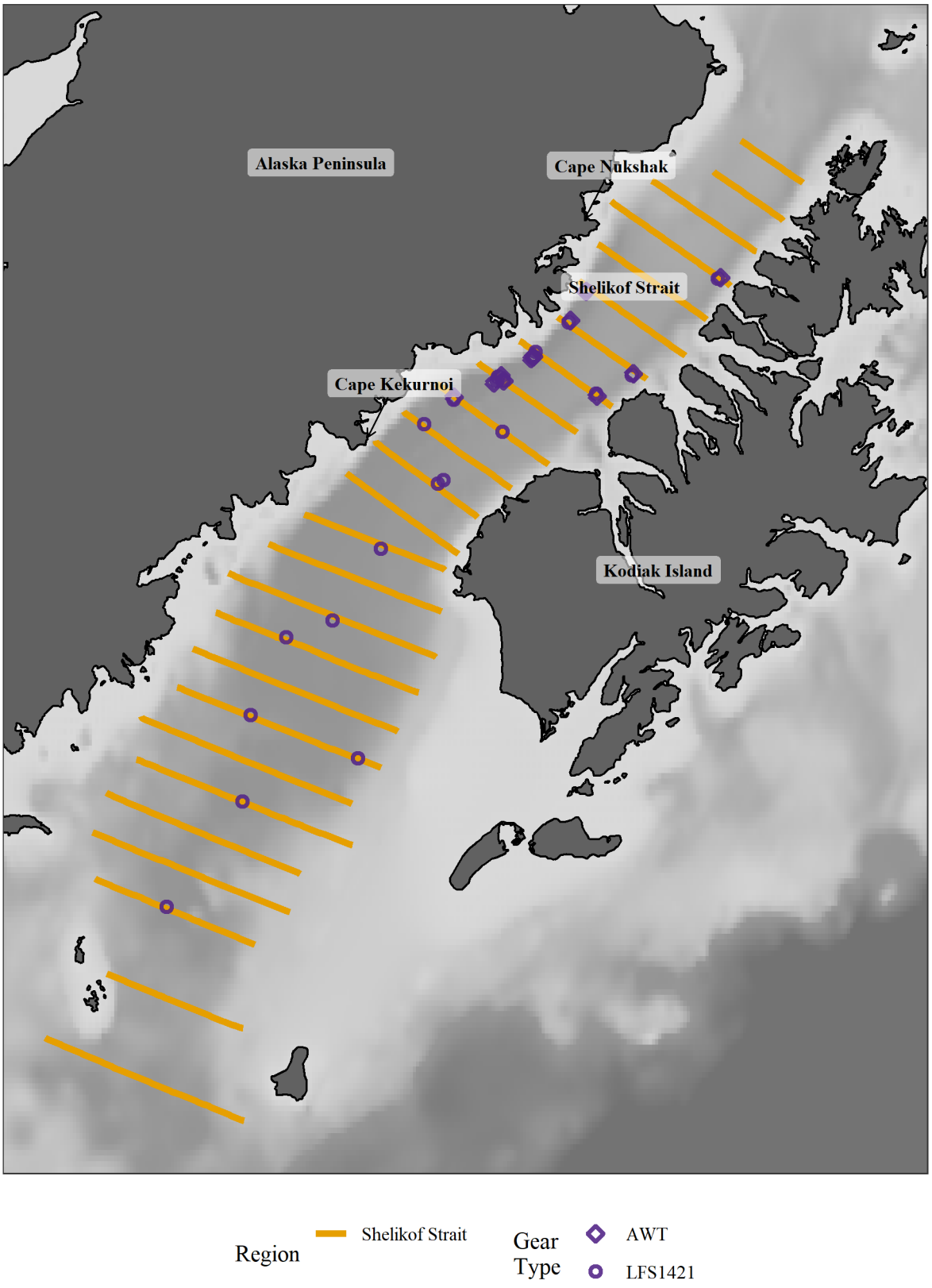


Figure 11. -- Transect lines and locations of trawl hauls during the winter 2020 acoustic-trawl survey of walleye pollock in the Shelikof Strait regions. Labels refer to areas referenced in text.

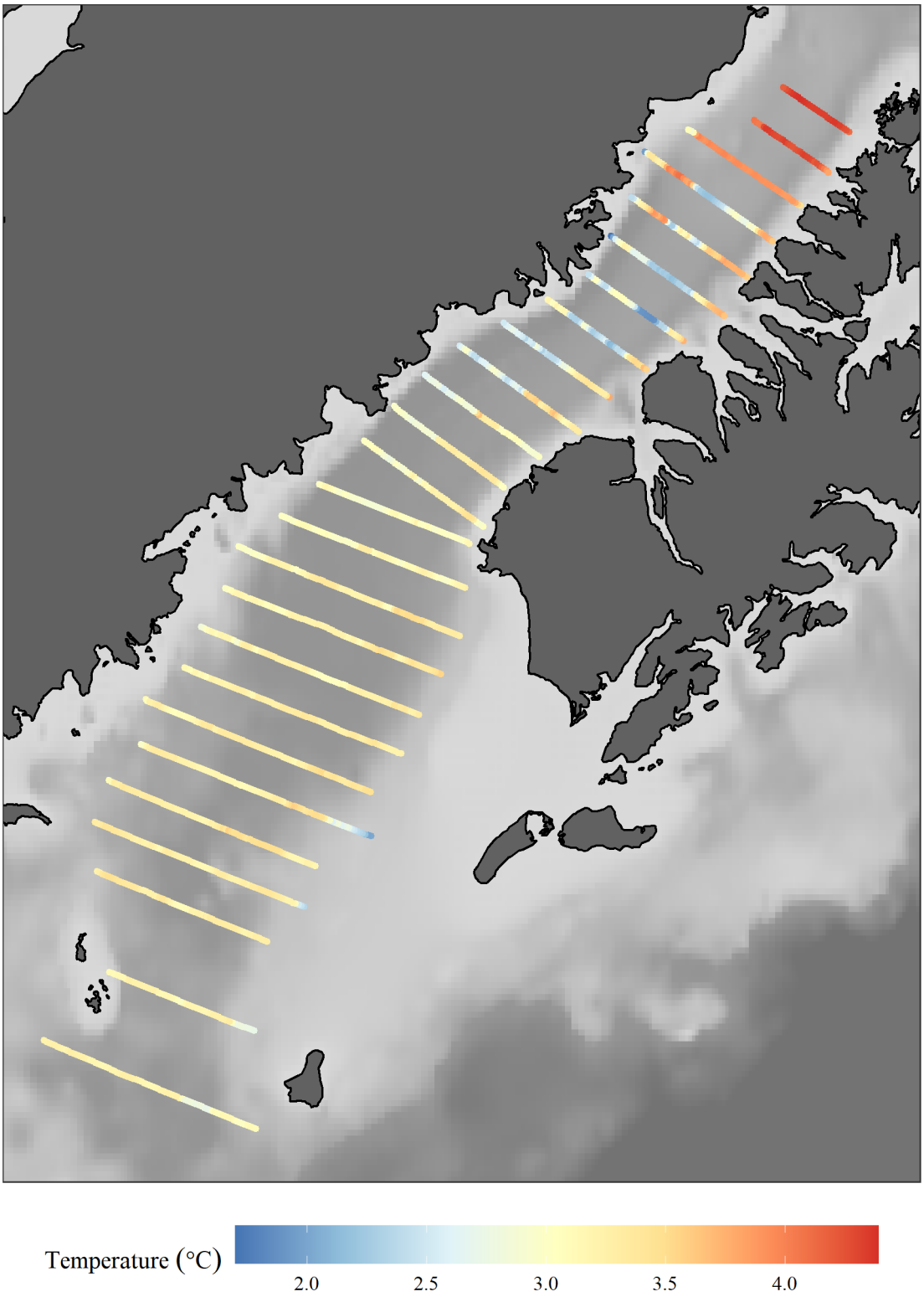


Figure 12. -- Surface water temperatures (°C) recorded at 5-second intervals during the winter 2020 acoustic-trawl survey of the Shelikof Strait regions.

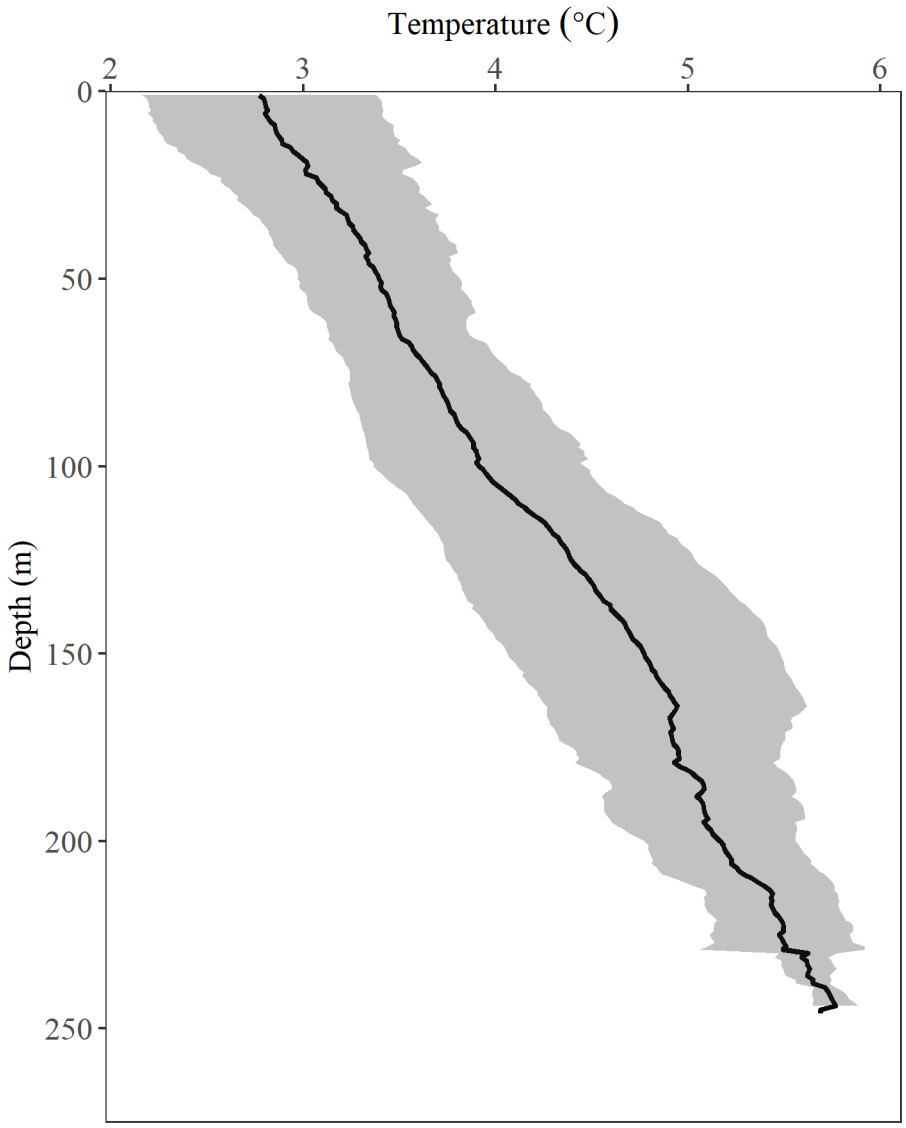


Figure 13. -- Mean water temperature (°C; solid line) by 1-m depth intervals measured at 31 trawl haul locations during the 2020 acoustic-trawl survey of walleye pollock in the Shelikof Strait area. The shaded area represents one standard deviation.

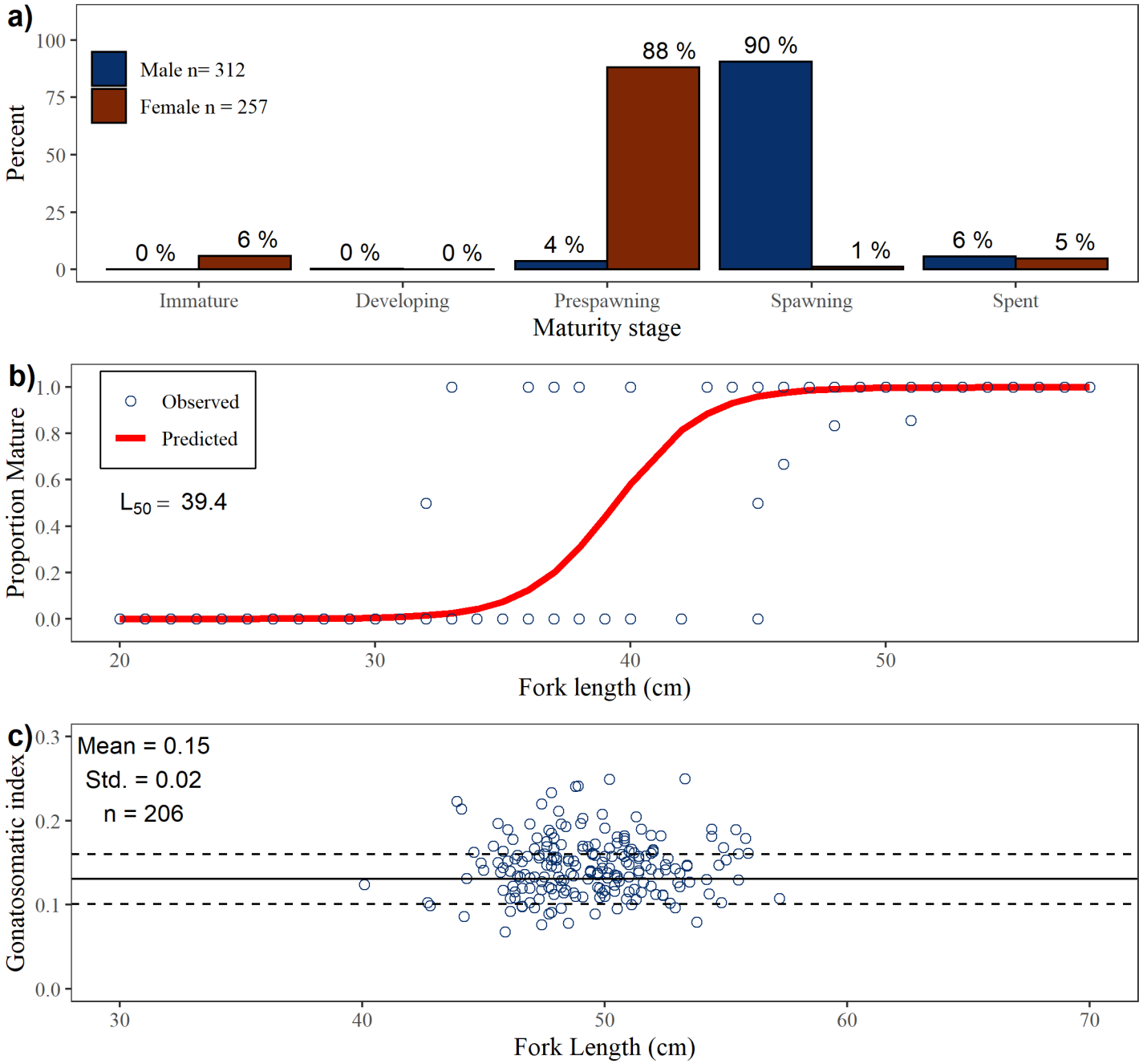


Figure 14. -- Walleye pollock maturity in the Shelikof Strait. a) Maturity composition for male and female walleye pollock greater than 40 cm FL within each stage; b) proportion mature (i.e. pre-spawning, spawning, or spent) by 1-cm size group for female walleye pollock; c) gonadosomatic index for females greater than 40 cm FL (with historic survey mean ± 1 std. dev.). All maturity quantities are weighted by local pollock abundance.

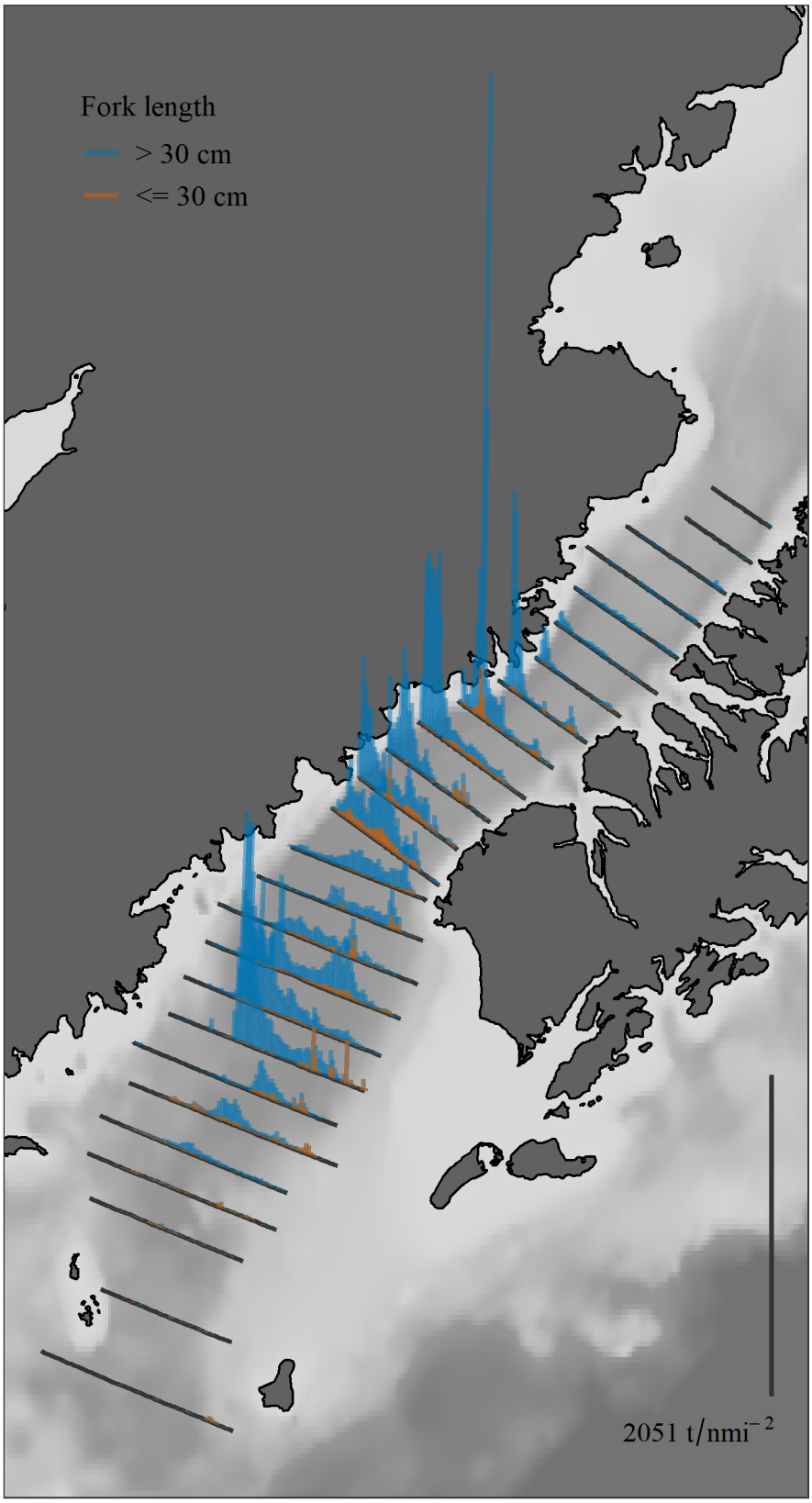


Figure 15. -- Biomass (t/nmi$^2$) attributed to walleye pollock (vertical lines) along tracklines surveyed during the winter 2020 acoustic-trawl survey of the Shelikof Strait regions. The tallest bar value is 4,103 t/nmi$^2$.

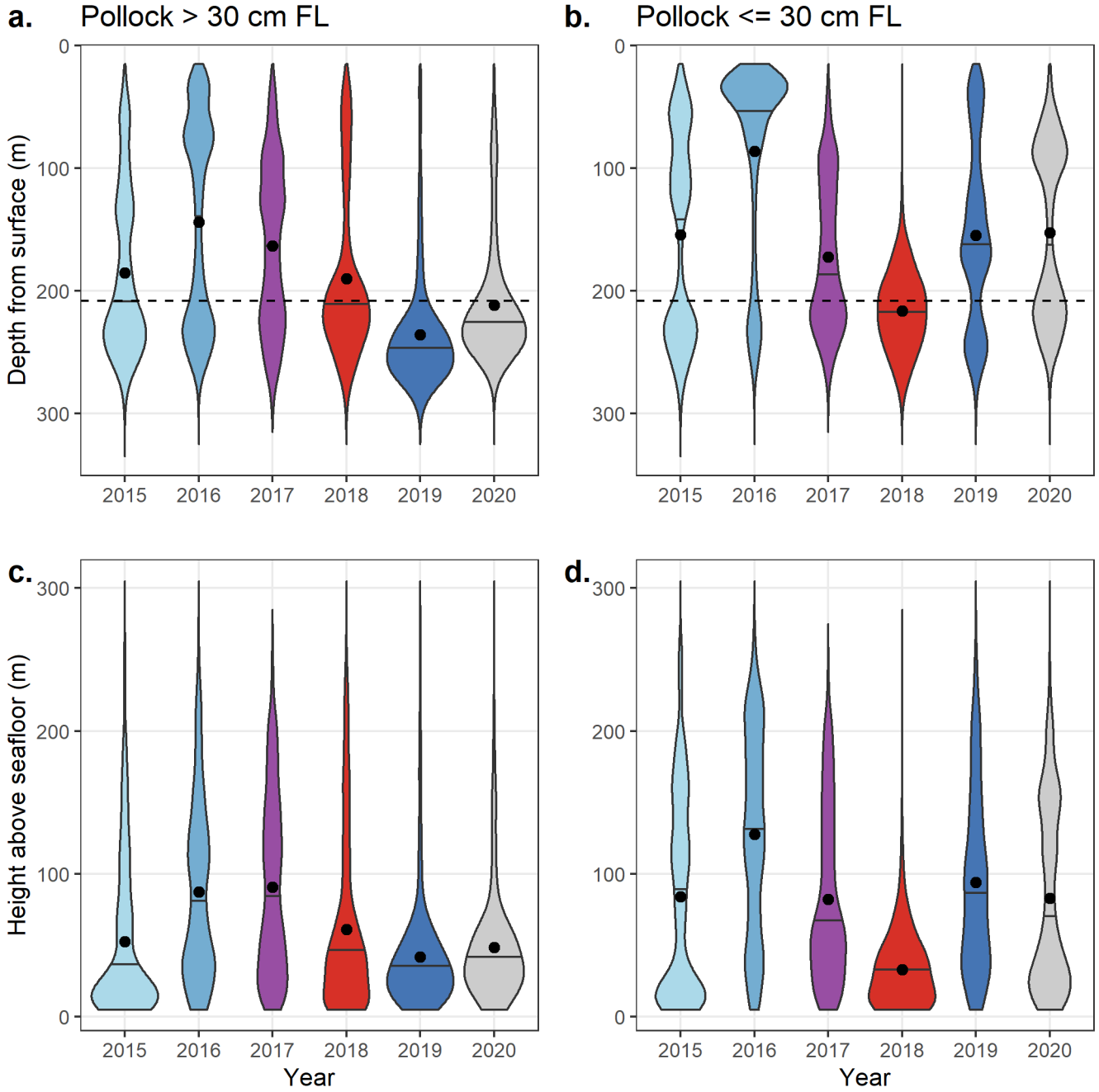


Figure 16. -- Estimated biomass distributions of adult pollock (> 30 cm FL) and juvenile pollock (<= 30 cm FL) depth (a. and b.) and height (c. and d.) above the seafloor in the Shelikof Strait 2020 acoustic-trawl survey. Results for the winter 2015-2019 acoustic-trawl surveys are included for comparison. Depth is referenced to the surface and height is referenced to the bottom. Data were averaged in 10 m depth bins. Mean bottom depth for 2020 is shown in a. and b. (dashed line). Plots show the probability density of pollock distribution, with median pollock depth noted by black horizontal lines, and the mean weighted pollock depth indicated by black points.

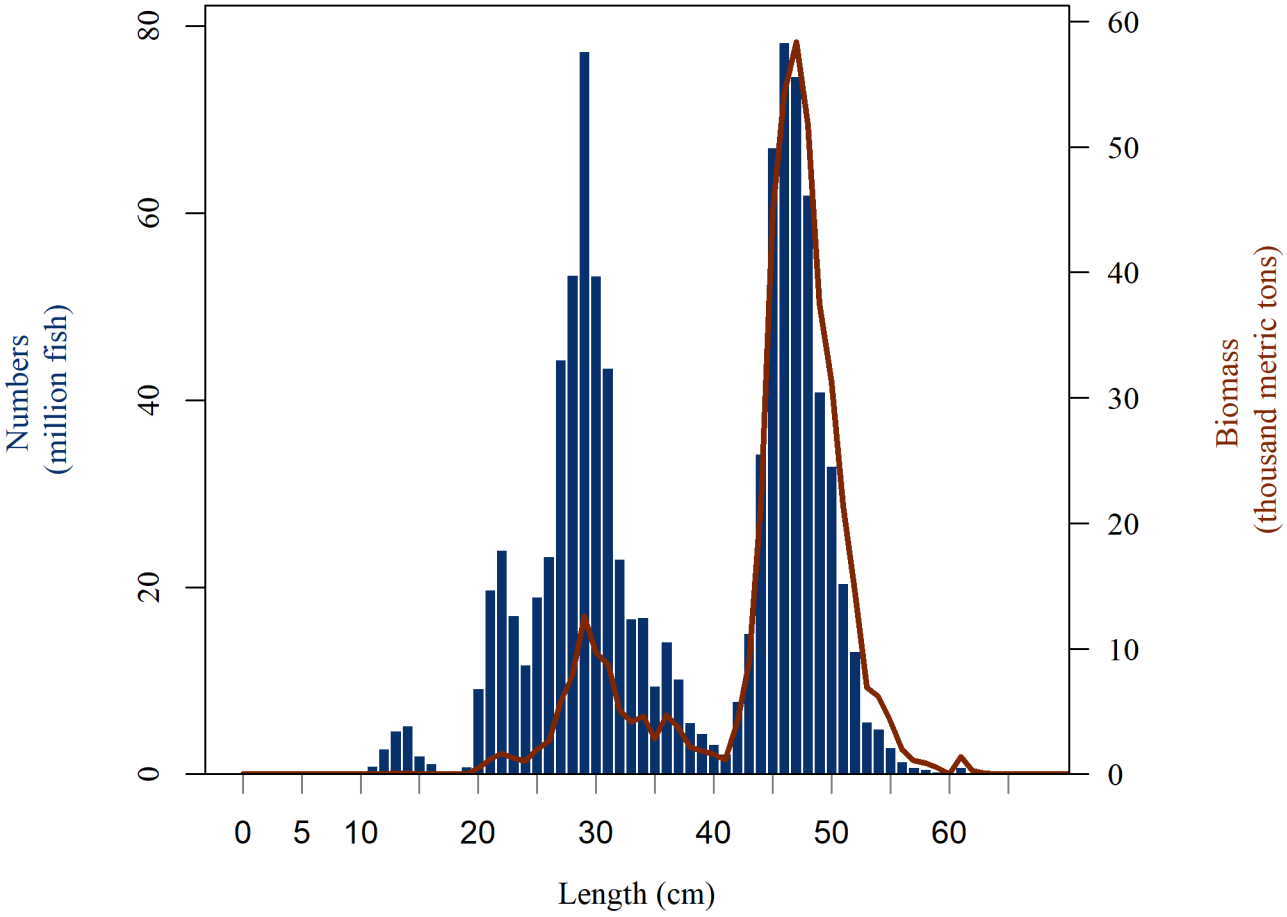


Figure 17. -- Number and biomass estimates of walleye pollock at length, shown with blue bars (million fish) and biomass estimates in red line (thousand metric tons) for the 2020 acoustic-trawl survey of Shelikof Strait.

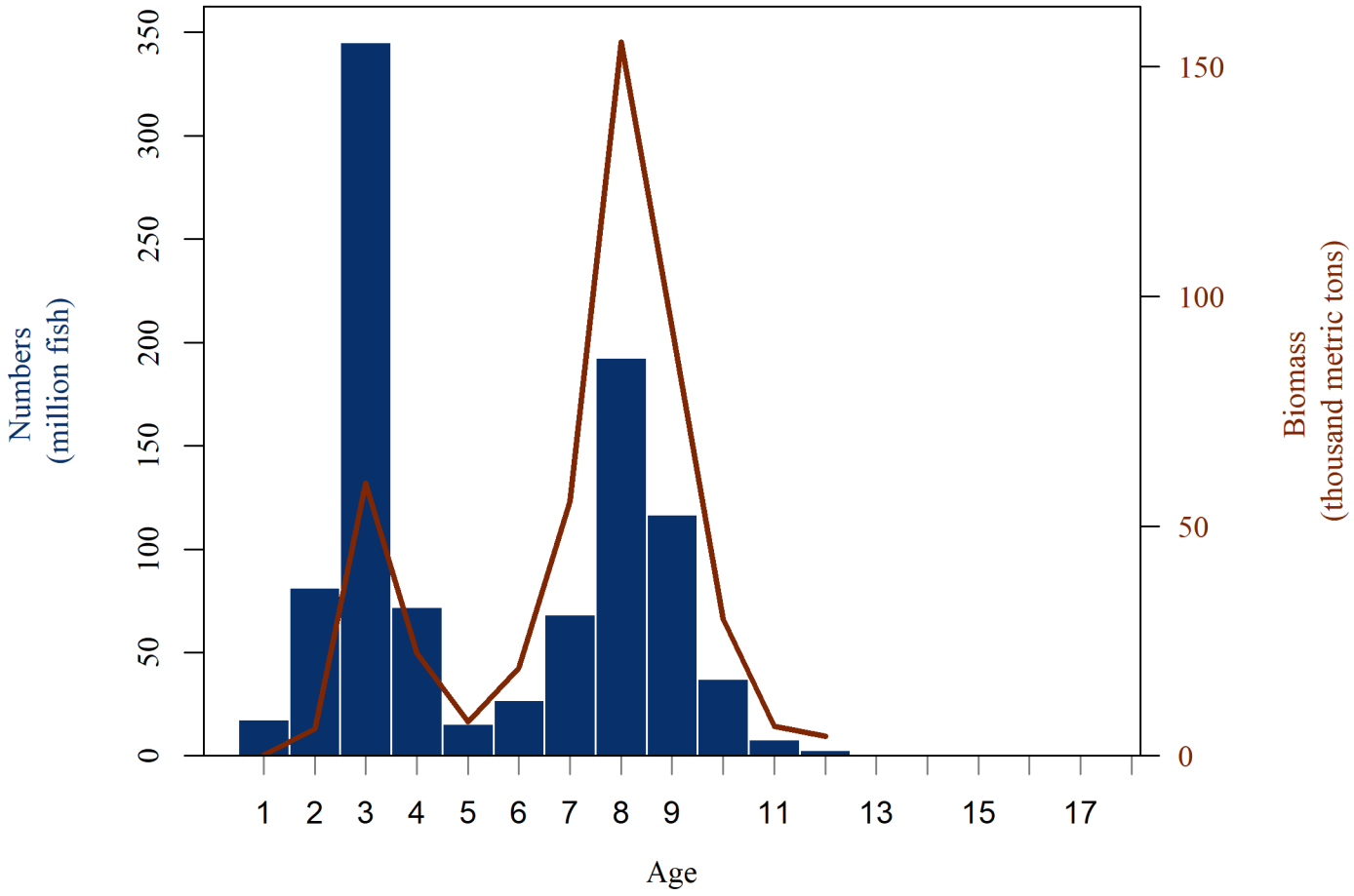


Figure 18. -- Numbers- and biomass- estimates of walleye pollock at age shown with blue bars (million fish) and biomass estimates in red line (thousand metric tons) for the 2020 acoustic-trawl survey of Shelikof Strait.

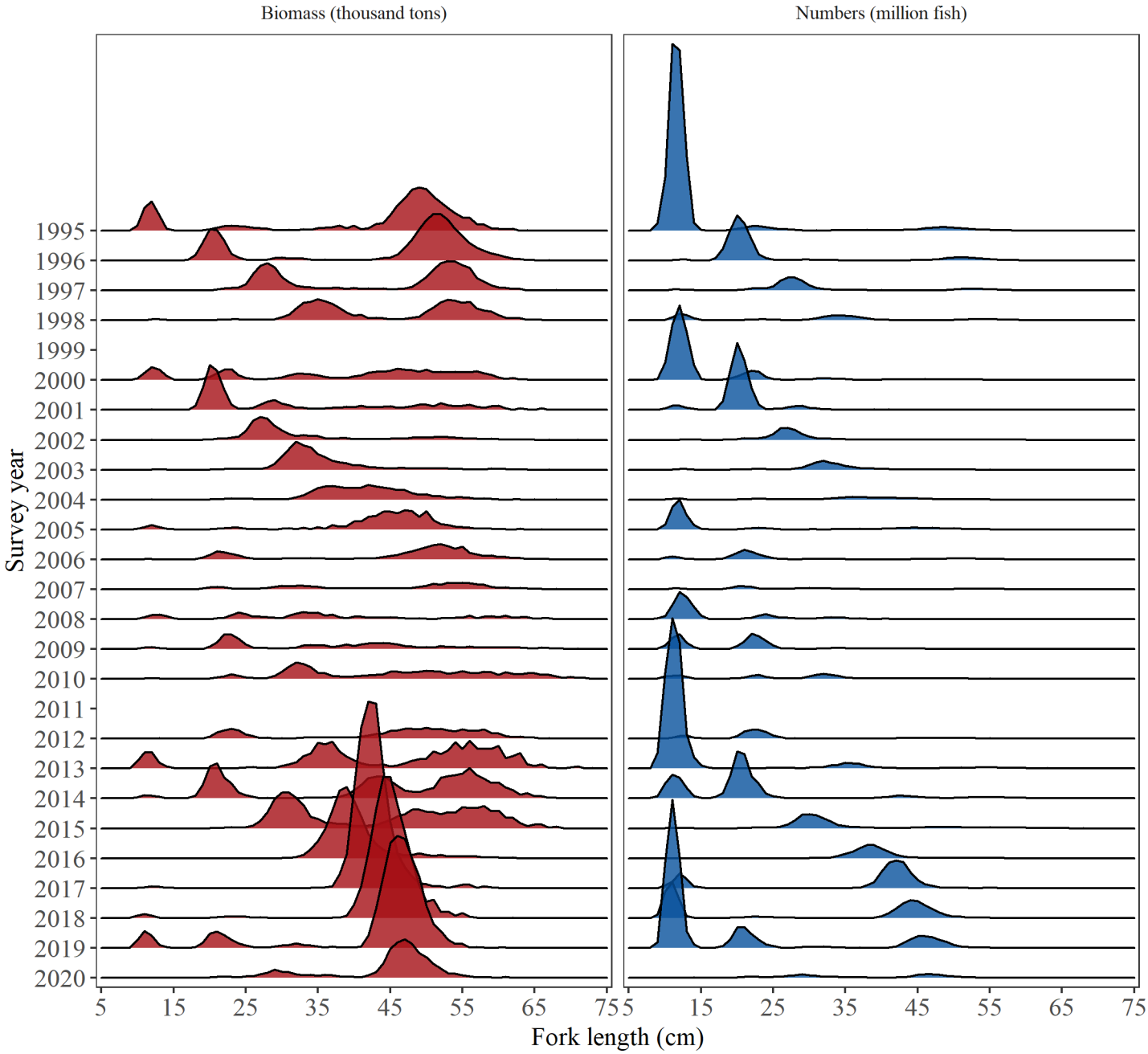


Figure 19. -- Time series of walleye pollock population size composition by weight (left panel, thousand metric tons) and numbers (right panel, million fish) from acoustic-trawl surveys of Shelikof Strait since 1995. Estimates for 2008-2020 include selectivity corrections for juvenile escapement (see text for explanation).

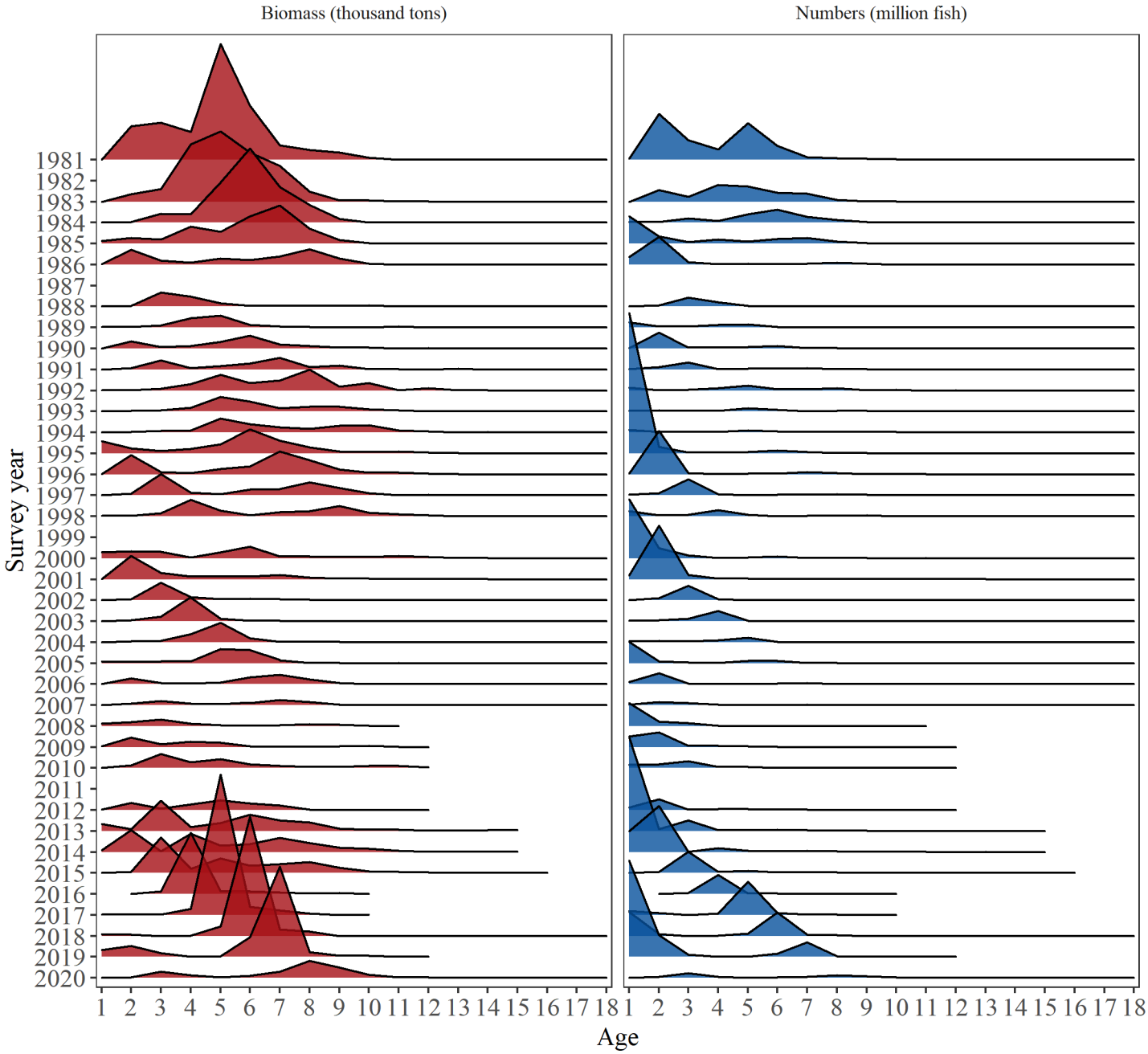


Figure 20. -- Time series of walleye pollock population size composition by weight (left panel, thousand tons) and numbers (right panel, million fish) from acoustic-trawl surveys of Shelikof Strait since 1981. Estimates for 2008-2020 include selectivity corrections for juvenile escapement (see text for explanation).

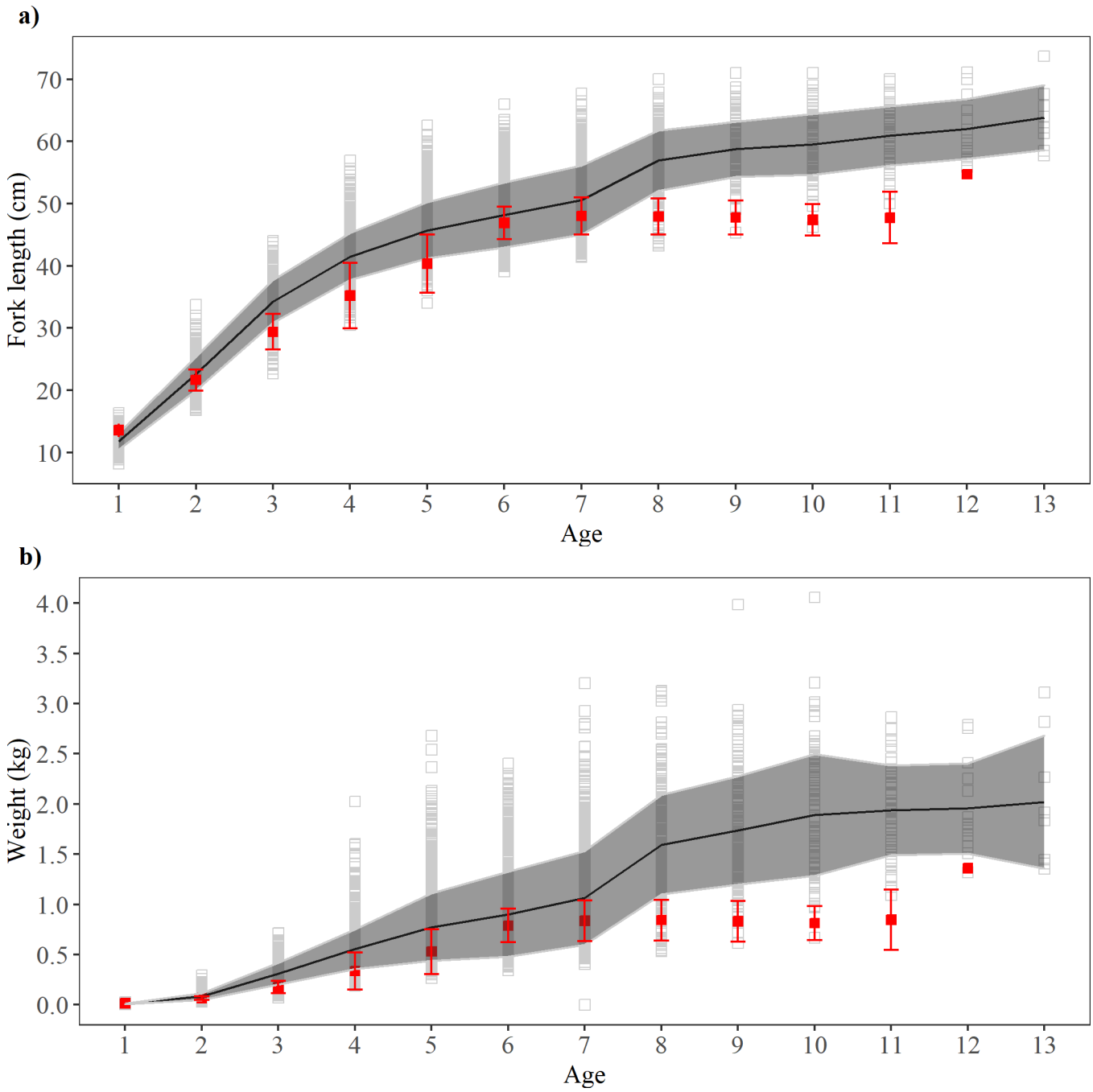


Figure 21. -- Walleye pollock a) length- and b) weight-at-age for Shelikof Strait. The 2020 survey symbols are red (mean +/- 1 s.d). Grey squares indicate the range of observations in previous surveys, and the black line and grey ribbon indicate mean length- or weight- at age in previous surveys +/- 1 s.d.

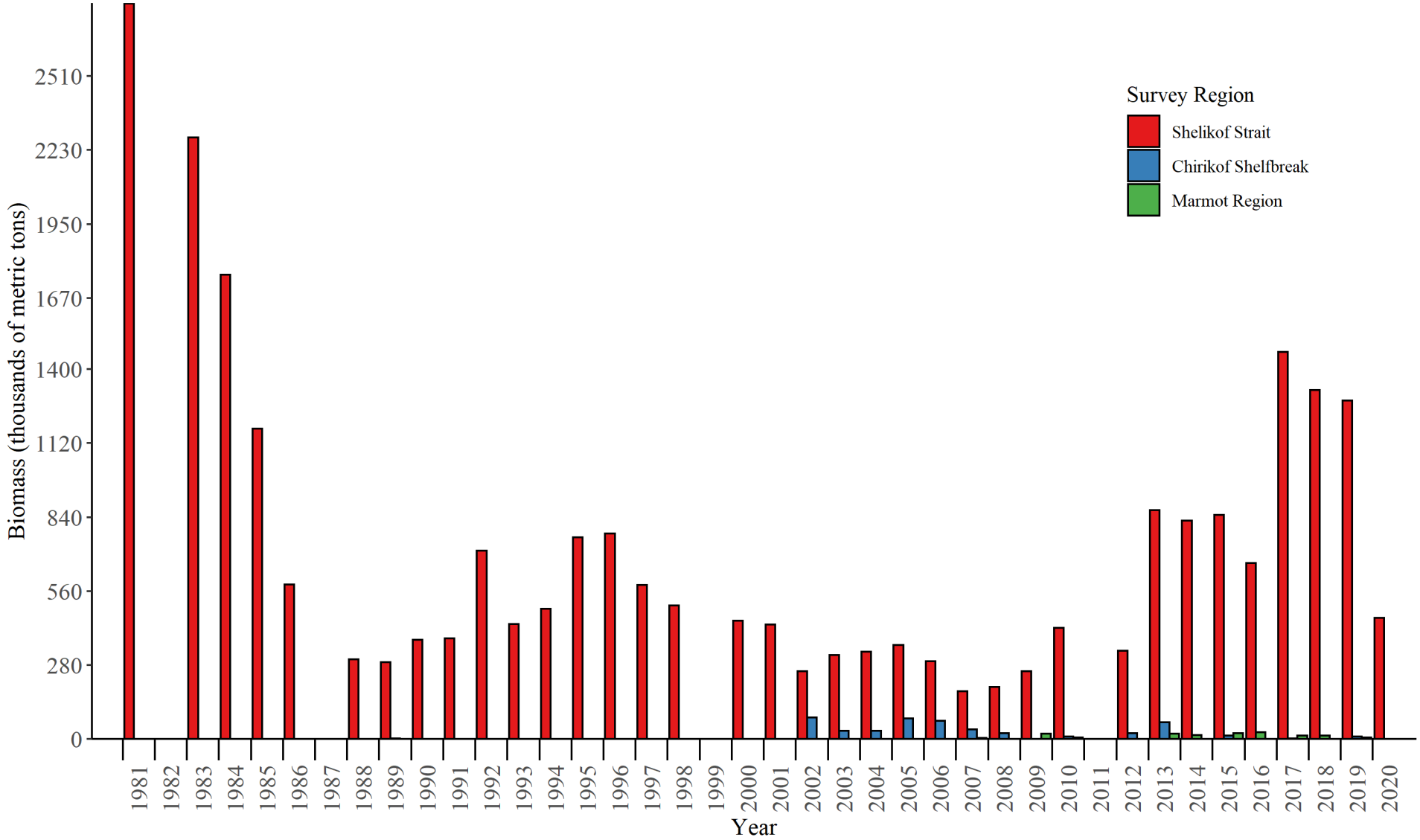


Figure 22. -- Summary of walleye pollock biomass estimates (thousands of metric tons) for the Shelikof Strait, Chirikof Shelfbreak, and Marmot Region areas based on acoustic-trawl surveys. Estimates for 2008-2020 include selectivity corrections for juvenile escapement (see text for explanation).

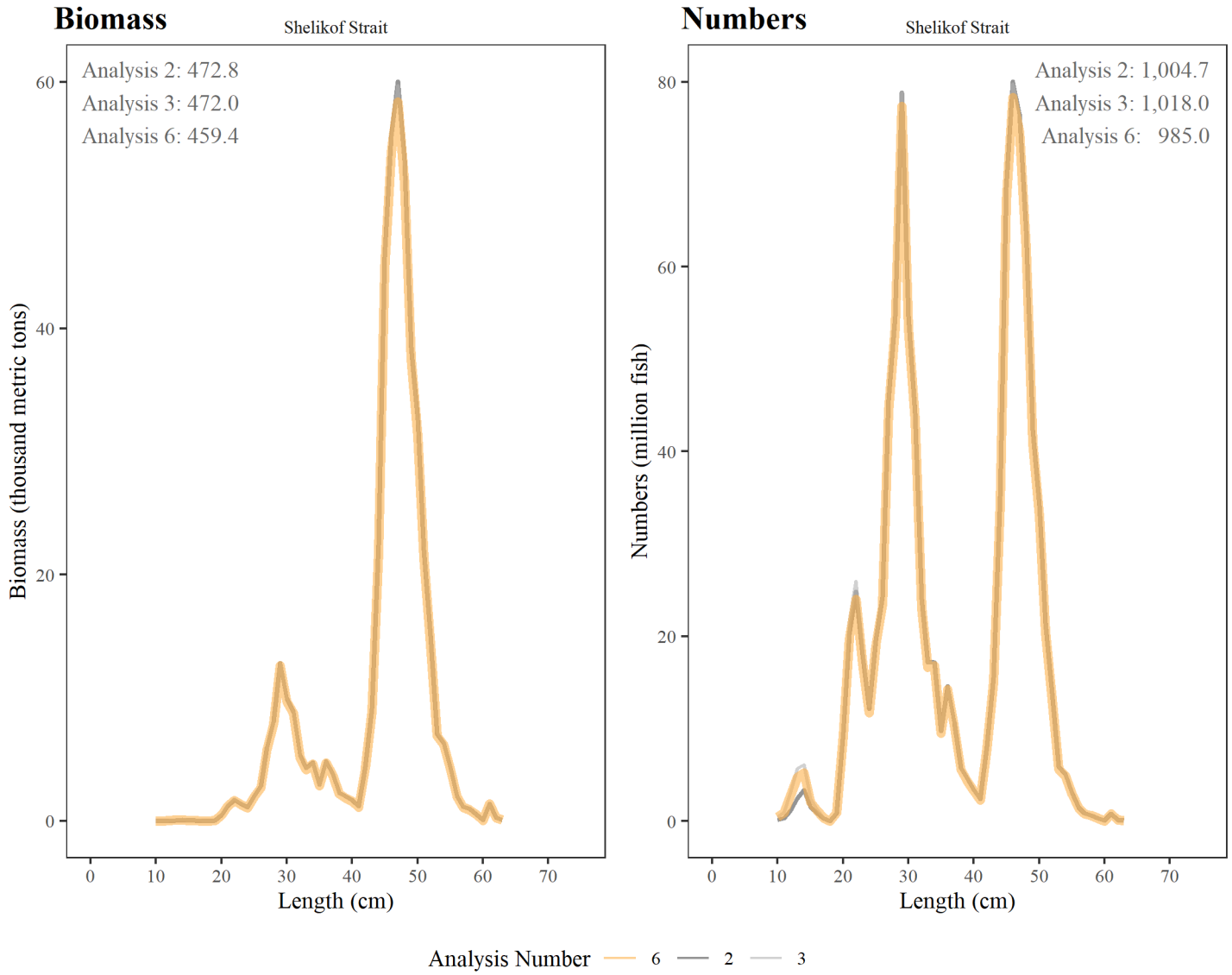


Figure 23. -- Numbers- and biomass- at length for the primary analysis (orange, Analysis 6) compared with alternate analyses (Analysis 2, Analysis 3, see text for explanation) for the 2020 Shelikof survey. The total numbers (million fish) and biomass (thousand metric tons) are also presented for each analysis.

## APPENDIX I. ITINERARY

DY2020-01

Shumagin Islands

| | |
|---|---|
| 11 Feb. | Depart Kodiak, AK. |
| 12 Feb. | Acoustic sphere calibration in Uganik Bay, AK. |
| 13-14 Feb. | Transit to Shumagin Islands area |
| 14-17 Feb. | Acoustic-trawl survey of Shumagin Islands. |
| 17 Feb. | Arrive Sand Point, AK. Crew swap. |
| 18 Feb. | Final trawl conducted at start of DY2020-02 survey |

DY2020-03

Shelikof Strait

| | |
|---|---|
| 3 Mar. | Depart Kodiak, AK. |
| 4-5 Mar. | Shelter from weather in Izhut Bay, transit through Whale Pass. |
| 6-9 Mar. | Acoustic-trawl survey of Shelikof Strait. |
| 9 Mar. | Return to Kodiak for medical emergency. |
| 10-15 Mar. | Resume acoustic-trawl survey of Shelikof Strait. |
| 16 Mar. | Acoustic sphere calibration in Kalsin Bay, AK. |
| 16 Mar. | Arrive Kodiak, AK. End cruise. |

## APPENDIX II. SCIENTIFIC PERSONNEL

DY2020-01

Shumagin Islands

| Name | Position | Organization |
|---|---|---|
| Taina Honkalehto | Chief Scientist | AFSC-RACE |
| Darin Jones | Fishery Biologist | AFSC-RACE |
| Scott Furnish | IT Specialist | AFSC-RACE |
| Matthew Phillips | Fishery Biologist | AIS |
| Mike Levine | Fishery Biologist | AFSC-RACE |
| Jerry Hoff | Fishery Biologist | AFSC-RACE |
| Ethan Beyer | Fishery Biologist | AIS |

DY2020-03

Shelikof Strait

| Name | Position | Organization |
|---|---|---|
| Darin Jones | Chief Scientist | AFSC-RACE |
| Scott Furnish | IT Spec. | AFSC-RACE |
| Matthew Phillips | Fishery Biologist | AIS |
| Ethan Beyer | Fishery Biologist | AIS |
| Kresimir Williams | Fishery Biologist | AFSC-RACE |
| Sarah Stienessen | Fishery Biologist | AFSC-RACE |
| Dave McGowan | Fishery Biologist | AFSC-RACE |
| Sandi Niedetcher | Fishery Biologist | AFSC-RACE |

AFSC- Alaska Fisheries Science Center, National Marine Fisheries Service, Seattle, WA

RACE- Resource Assessment and Conservation Engineering Division

AIS- AIS Scientific and Environmental Services, Inc.

## APPENDIX III. ABUNDANCE CALCULATIONS

The abundance of target species was calculated by combining the echosounder measurements with size and species distributions from trawl catches and target strength (TS) to length relationships from the literature (see De Robertis et al. 2017a for details). The echosounder measures volume backscattering strength, which is integrated vertically to produce the nautical area scattering coefficient, $s_A$ (units of $m^2$ $nmi^{-2}$; MacLennan et al. 2002). The backscatter from an individual fish of species *s* and at length *l* is referred to as its backscattering cross-section, $\sigma_{bs,s,l}$ ($m^2$), or in logarithmic terms as its target strength, $TS_{s,l}$ (dB re 1 $m^2$), where,

$$TS_{s,l} = 10 \log_{10} (\sigma_{bs,s,l}) \quad . \qquad \text{(Eq. i)}$$

The numbers of individuals of species *s* in length class *l* ($N_{s,l}$) captured in the nearest haul *h* were used to compute the proportion of acoustic backscatter associated with each species and length. First, the number of individuals in the catch was converted to a proportion ($P_{s,l,h}$)

$$P_{s,l,h} = \frac{N_{s,l,h}}{\sum_{s,l,h} N_{s,l,h}} \quad \text{, where } \sum_{s,l,h} P_{s,l,h} = 1 \qquad . \qquad \text{(Eq. ii)}$$

In analyses where trawl selectivity was considered, the selectivity-corrected numbers $N_{s_{corr},l,h}$ were used in place of $N_{s,l,h}$ in Eq. ii. This correction accounts for escapement in the trawl catch. The corrected catch is that expected for an unselective sampling device. Refer to the main text for a description of the selectivity corrections applied.

The mean backscattering cross section (an areal measure of acoustic scattering in $m^2$ – MacLennan et al., 2002) of species *s* of length class *l* is

$$\sigma_{bs_{s,l}} = 10^{(0.1 \cdot TS_{s,l})} \quad , \qquad \text{(Eq. iii)}$$

where TS is the target strength (dB re $m^2$) of species *s* at size *l* (Table 1).

The proportion of backscatter from species $s$ of length class $l$ in haul $h$ ($PB_{s,l,h}$) is computed from the proportion of individuals of species $s$ and length class $l$ estimated from haul $h$ ($P_{s,l,h}$) and their backscattering cross section,

$$PB_{s,l,h} = \frac{P_{s,l,h} \cdot \sigma_{bs_{s,l}}}{\sum_{s,l,h}(P_{s,l,h} \cdot \sigma_{bs_{s,l}})} \quad . \qquad \text{(Eq. iv)}$$

The measured nautical area backscattering coefficient ($s_A$) at interval $i$ was allocated to species $s$ and length $l$ as follows:

$$s_{A_{s,l,i}} = s_{A_i} \cdot PB_{s,l,h} \quad , \qquad \text{(Eq. v)}$$

where haul $h$ is the nearest haul within a stratum assigned to represent the species composition in a given 0.5 nmi along-track interval $i$. The nearest geographic haul was determined by using great-circle distance to find the nearest trawl location (defined as the location where the net is at depth and begins to catch fish) out of the pool of hauls assigned to the same stratum (see above for details) closest to the start of interval $i$.

The abundance of species of length $l$ in an area encompassing a series of transect intervals $i$ was estimated from the area represented by that interval ($A_i$, nmi$^2$), the mean areal backscatter attributed to species $s$ in a given length/size class $l$ ($s_{A_{s,l,i}}$, m$^2$ nmi$^{-2}$), and mean backscattering cross-section of species $s$ at that size ($\sigma_{bs_{s,l}}$ m$^2$) as follows:

$$\text{Numbers at length } l\text{: } N_{s,l} = \sum_i \left( \frac{s_{A,s,l,i}}{4\pi\sigma_{bs_{s,l,i}}} \cdot A_i \right) \quad , \qquad \text{(Eq. vi)}$$

$$\text{Biomass at length } l\text{: } B_{s,l} = \Sigma_i \, (W_{s,l} \times N_{s,l,i}) \quad , \qquad \text{(Eq. vii)}$$

where $W_{s,l}$ is the mean weight-at-length for species $s$ in each 1 cm length $l$ derived from length-weight regressions. In the case of pollock, when five or more individuals were measured within a length interval, the mean weight-at-length was used. Otherwise (i.e., for length classes of pollock

with <5 weight measurements, or other species), weight-at-length was estimated using a linear regression of the natural log-transformed length-weight data (De Robertis and Williams 2008).

The abundance at age was computed from $Q_{s,l,j}$, the proportion of *j*-aged individuals of species *s* in length class *l*, and the abundance of that species and age class in each surveyed interval follows

Numbers at age *j*: $N_{s,j} = \Sigma_i (Q_{s\,l,,j} \times N_{s,l})$ , (Eq. viii)

Biomass at age *j*: $B_{s,j} = \Sigma_i (Q_{s,l,,j} \times B_{s,l})$ . (Eq. ix)

## APPENDIX IV. SELECTIVITY CORRECTION

To account for the size- and species-dependent loss of organisms though the midwater trawl meshes ahead of the codend, or "mesh selection," length compositions were adjusted to that which would be expected from an unselective sampler. Species-specific selectivity relationships describing the probability of retaining a given sized individual were used for the most abundant species, and other species were pooled in broad taxonomic groups. Trawl selectivity $S_l$ for each cm length class ($l$) of all species or species group caught was estimated by analyzing the catch of the codend and that of small recapture nets mounted on the outside of the trawl during the current survey using methods similar to those presented in Williams et al. (2011). A generalized linear mixed effects model (GLMM) was fitted with a logistic link function and binomial error where variation between tows in selectivity was modeled with random effects. $S_l$ was then computed as:

$$S_l = \left(1 + e^{2\log 3(LR_{50} - l)/SR}\right)^{-1} \quad , \qquad \text{(Eq. x)}$$

where $LR_{50}$ is the length at which 50% of individuals were retained and $SR$ is the selection range (i.e., range in length between 25% and 75% retention values).

These trawl selectivity estimates were then applied to the codend catch composition to correct the sample for escapement from the trawl as

$$N_{sp\_corr,l} = \frac{N_{sp,}}{S_l} \quad , \qquad \text{(Eq. xi)}$$

where $N_{sp\_corr,l}$ is the number of fish within a species that would be captured in an unselective sampler in the sampled population and $N_{sp,l}$ is the number of fish within that species in the 1 cm length class $l$ in the trawl catch. In analyses with a selectivity correction applied, $N_{sp\_corr,l}$ was used in place of $N_{s,l}$ in the abundance calculations (see Appendix III, Eq. ii).

Selectivity curves for the most abundant taxa were estimated using the GLMM. Variance was estimated by multivariate normal resampling of selectivity parameters using the point estimates and variance-covariance matrix (n = 1,000). In the case of less abundant animals, the catch data were too sparse for this approach. For less abundant groups, data were combined across all hauls and a model was fit to the cumulative GLM result. Variance for this approach was estimated by bootstrap (random sub-sampling with replacement) of the input data by haul (n = 1,000). The criteria for deciding which of these approaches was used was based on whether a selectivity group had at least 10 hauls in which at least 20 individuals were encountered in the combined recapture nets. A simpler model, estimating the ratio of biomass retained in the codend without length dependence, was used for euphausiids because of their similar sizes and because reliable length estimates of retained individuals were not available, particularly from the codend where they were often damaged.

Selectivity curve estimates and their uncertainty are presented in Table A1 and Figure A1. For the GLMM, some hauls with strong outlier estimates of selectivity were further excluded. For all curves, a minimum retention of 0.25% was enforced to prevent overlarge extrapolation errors with model values approaching 0%.

Appendix Table A1. -- Selectivity curve estimates of length at 50% retention (*LR*50) and selection range (*SR*) from either the generalized linear mixed effects model (GLMM) or cumulative GLM for species and groups of species. Surveys used in estimating the selectivity are listed. All values are in centimeters.

| Selectivity Group | Survey Data Used | Model Used | Length at 50% Retention (*LR*50) | *LR*50 95% Range | Selection Range (*SR*) | *SR* 95% Range | Length Range in Haul and Recapture Nets |
|---|---|---|---|---|---|---|---|
| age 1+ pollock | DY2003 | GLMM | 13.73 | 6.63 – 16.24 | 6.28 | 5.06 – 11.67 | 10 – 63 |
| capelin | DY2001, DY2003 | cumulative GLM | 13.08 | 12.08 – 15.21 | 3.69 | 2.85 – 5.89 | 3 – 13 |
| eulachon | DY2001, DY2002, DY2003 | GLMM | 13.38 | 11.82 – 15.47 | 5.11 | 3.70 – 8.03 | 4 – 25 |
| fish larvae | DY2003 | cumulative GLM | 13.06 | -74.74 – 55.08 | 6.78 | -89.99 – 47.08 | 4 – 9 |
| gelatinous zooplankton | DY1906 | cumulative GLM | 15.2 | 10.28 – 18.65 | 11.34 | 5.01 – 16.31 | 1 – 62 |
| generic fish | DY2001, DY2002, DY2003 | cumulative GLM | 11.51 | 9.65 – 15.11 | 3.79 | 2.53 – 7.48 | 2 – 67 |
| herring | DY2001, DY2003 | cumulative GLM | 11.81 | 11.20 – 16.33 | 3.38 | 1.83 – 11.78 | 7 – 23 |
| myctophids | DY1906, DY2002, DY2003 | GLMM | 7.26 | 6.46 – 10.54 | 1.16 | 0.56 – 6.47 | 5 – 21 |
| non-krill crustaceans | DY1906, DY2002, DY2003 | GLMM | 8.34 | -4.41 – 24.12 | 1.71 | -7.29 – 14.55 | 5 – 11 |
| squid | DY1906, DY2001, DY2002, DY2003 | cumulative GLM | 6.69 | 5.46 – 9.27 | 2.26 | 1.60 – 3.34 | 1 – 32 |

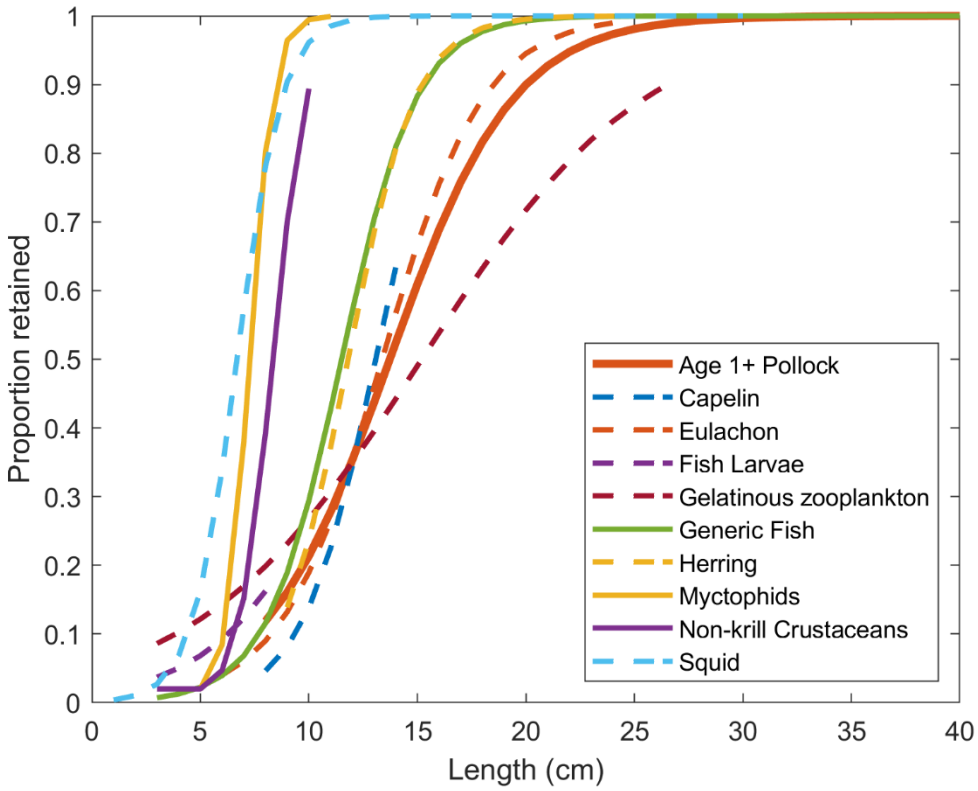


Appendix Figure A1. -- Selectivity functions estimated for the DY2003 survey using recapture nets. Selection function values are only plotted for length ranges encountered for each selectivity group.

December 2022

www.fisheries.noaa.gov

OFFICIAL BUSINESS

National Marine
Fisheries Service
Alaska Fisheries Science Center
7600 Sand Point Way N.E.
Seattle, WA 98115-6349